Pharmacokinetics and pharmacodynamics of antimalarial drugs in pregnant women

Frank L. Kloprogge

Green Templeton College

University of Oxford

A thesis submitted for the degree

Doctor of Philosophy

Michaelmas Term 2013

Pharmacokinetics and pharmacodynamics of antimalarial drugs in pregnant women

Frank L. Kloprogge
Green Templeton College
Submitted for the Degree Doctor of Philosophy
Michaelmas Term 2013

Abstract

Malaria is the most important parasitic disease in man and it kills approximately 2,000 people each day. Pregnant women are especially vulnerable to malaria with increased incidence and mortality rates. There are indications that pregnancy alters the pharmacokinetic properties of many antimalarial drugs. This is worrisome as lower drug exposures might result in lowered efficacy and lower drug exposures can also accelerate the development and spread of resistant parasites. The aim of this research was to study the pharmacokinetics and pharmacodynamics of the most commonly used drugs for the treatment of uncomplicated *Plasmodium falciparum* malaria during the second and third trimester of pregnancy using a pharmacometric approach.

This thesis presents a number of important findings that increase the current knowledge of antimalarial drug pharmacology and that may have an impact in terms of drug efficacy and resistance. (1) Lower lumefantrine plasma concentrations at day 7 were evident in pregnant women compared to that in non-pregnant patients. Subsequent *in-silico* simulations with the final pharmacokinetic-pharmacodynamic lumefantrine/desbutyl-lumefantrine model showed a decreased treatment failure rate after a proposed extended artemether-lumefantrine treatment. (2) Dihydroartemisinin exposure (after intravenous and oral administration of artesunate) was lower during pregnancy compared to that in women 3 months post-partum (same women without malaria). Consecutive *in-silico* simulations with the final model showed that the underexposure of dihydroartemisinin during pregnancy could be compensated by a 25% dose increase. (3) Artemether/dihydroartemisinin exposure in pregnant women was also lower compared to literature values in non-pregnant patients. This further supports the urgent need for a study in pregnant women with a non-pregnant control group. (4) Quinine pharmacokinetics was not affected by pregnancy trimester within the study population and a study with a non-pregnant control group is needed to evaluate the absolute effects of pregnancy. (5) Finally, a data-dependent power calculation methodology using the log likelihood ratio test was successfully used for sample size calculations of mixed pharmacokinetic study designs (i.e. sparsely and densely sampled patients). Such sample size calculations can contribute to a better design of future pharmacokinetic studies.

In conclusion, this thesis showed lower exposures for drugs used to treat uncomplicated *Plasmodium falciparum* malaria during the second and third trimester of pregnancy. More pharmacokinetic studies in pregnant women with a non-pregnant control group are urgently needed to confirm the current findings and to enable an evidence-based dose optimisation. The data-dependent power calculation methodology using the log likelihood ratio test can contribute to an effective design of these future pharmacokinetic studies.

Contents

List of abbreviations

ACT	Artemisinin combined therapy
AUC	Area under the curve
BIO	First-pass artesunate metabolism
CL	Elimination clearance
CL_H	Hepatic elimination clearance
CL_{int}	Intrinsic clearance
CL_R	Renal elimination clearance
C	Total drug concentration
C_{MAX}	Maximum plasma concentration
C_{MIN}	Minimum plasma concentration prior to a new dose administration
C_{SS}	Plasma concentration at steady state
Cu	Unbound drug concentration
D	Dose
DUR	Duration of infusion
E	Drug effect
E_0	Baseline effect
EC_{50}	Concentration realising 50% of the maximum effect
ED_{50}	Dose realising 50% of the maximum effect
E_H	Hepatic extraction ratio
E_{MAX}	Maximum effect
E_R	Renal extraction ratio
F	Bio-availability

fb	Fraction bound drug
fu	Fraction unbound drug
GFR	Glomerular filtration rate
h	Hazard rate
IIV	Inter-individual variability
IOV	Inter-occasion variability
I.V.	Intravenous administration
$\mathbf{k_a}$	Absorption rate constant
$\mathbf{k_e}$	Elimination rate constant
MTT	Mean Transit Time
OFV	Objective function value
P.O.	Per oral administration
Q	Inter-compartmental clearance
$\mathbf{Q_H}$	Hepatic blood flow
$\mathbf{Q_R}$	Renal blood flow
RSE	Relative standard error
S	Survival function
$\mathbf{t_{LAG}}$	Time to first observed plasma concentration after dosing
$\mathbf{t_{MAX}}$	Time to reach the maximum plasma concentration
$\mathbf{t_{1/2}}$	Elimination half-life
$\mathbf{V_{TOT}}$	Apparent volume of distribution
$\mathbf{V_C}$	Central apparent volume of distribution
$\mathbf{V_P}$	Peripheral apparent volume of distribution

$\mathbf{V_S}$	Apparent volume of distribution in the sampling matrix
$\mathbf{V_{SS}}$	Apparent volume of distribution at steady state
$\mathbf{V_T}$	Apparent volume of distribution in the tissue
$\mathbf{V_Z}$	Apparent volume of distribution in the elimination phase

List of tables

List of figures

List of equations

EQ 2.1	$F = \frac{AUC_{oral} * DOSE_{intravenous}}{AUC_{intravenous} * DOSE_{oral}}$	Bioavailability
EQ 2.2	$CL = CL_H + CL_R + CL_{OTHERS}$	Elimination clearance
EQ 2.3	$CL_H = Q_H * E_H = Q_H * \left[\frac{fu * CL_{int}}{Q_H + fu * CL_{int}}\right]$	Hepatic clearance
EQ 2.4	$CL_R = Q_R * E_R = (1 - F_R) * [CL_f + CL_S]$	Renal clearance
EQ 2.5	$C_t = C_0 * e^{-k_e * t}$	Drug concentration
EQ 2.6	$t_{1/2} = \frac{\ln(2)}{k_e} = \frac{\ln(2) * V}{CL}$	Elimination half-life
EQ 2.7	$V = V_S + V_T * \frac{fu}{fu_T}$	Apparent distribution volume
EQ.2.8	$E = slope * C$	Linear dose-effect relation
EQ 2.9	$E = E_0 - \frac{C * E_{MAX}}{EC_{50} + C}$	E_{MAX} dose-effect relation
EQ 2.10	$E = E_0 - \frac{C^{\gamma} * E_{MAX}}{EC_{50}^{\gamma} + C^{\gamma}}$	Sigmoidal E_{MAX} dose-effect relation
EQ 2.11	$S(t) = P(time_{event} \geq time) = e^{-\int h(t)}$	Survival function

EQ 2.12	$P(event) = 1 - e^{-(\int h(t)_{event} - \int h(t)_{startinterval})}$	Probability of event during interval
EQ 2.13	$h(t) = \lambda$	Constant hazard model
EQ 2.14	$h(t) = \lambda * e^{-time*\frac{ln(2)}{t_{1/2}}}$	Gompertz hazard model
EQ. 2.15	$h(t) = \alpha^2 * \lambda * time^{\alpha-1}$	Weibull hazard model
EQ 2.16	$k_e = \frac{ln(2)}{t_{1/2}}$	Elimination rate-constant
EQ 2.17	$AUC_{0-\infty} = \sum AUC_{T1} + AUC_{T2} + ... + \frac{C_{LAST}}{\lambda}$	Area Under the Curve
EQ 2.18	$\frac{V_Z}{F} = \frac{DOSE}{k_e * AUC}$	Apparent volume of distribution
EQ 2.19	$\frac{CL}{F} = \frac{DOSE}{AUC}$	Elimination clearance
EQ 2.20	$P_i = \theta_{TV} * e^{\eta_i}$	Parameter log-normal distribution
EQ 2.21	$\eta_i = \eta_{IIV,i} + \eta_{IOV,i}$	Sum of IIV and IOV variability

EQ 2.22 $$\eta_{i\_box-cox} = \frac{e^{\eta_i^{\theta_i}} - 1}{\theta_i}$$ Box-cox transformed variability

EQ 2.23 $$\eta_{i\_heavy-tailed} = \eta_i * |\eta_i|^{\theta_i}$$ Heavy-tailed transformed variability

EQ 2.24 $$\eta_{i\_logit} = \left(\frac{e^{\ln\left(\frac{\theta_1}{(1-\theta_1)}\right)+\eta_i}}{1+e^{\ln\left(\frac{\theta_1}{(1-\theta_1)}\right)+\eta_i}} - \theta_1 \right) * \theta_2$$ Logit-transformed variability

EQ 2.25 $$\text{Observation}_{ij} = \text{individual prediction}_{ij} + \varepsilon_{ij}$$ Additive residual error model

EQ 2.26 $$\text{Observation}_{ij} = \text{individual prediction}_{ij} * (1 + \varepsilon_{ij})$$ Proportional residual error model

EQ 2.27 $$\text{Observation}_{ij} = \text{individual prediction}_{ij} * (1 + \varepsilon_{\text{proportional},ij}) + \varepsilon_{\text{additive},ij}$$ Combined error model

EQ 2.28 $$h(t) = \lambda * \left(E_0 - \frac{C^{\gamma} * E_{MAX}}{EC_{50}^{\gamma} + C^{\gamma}} \right)$$ Constant hazard model with sigmoidal E_{MAX} drug effect

EQ 2.29 $$P_i = \theta_{TV} * (1 + \theta * \text{covariate}) * e^{\eta_i}$$ Categorical covariate

EQ 2.30 $P_i = \theta_{TV} * (1 + \theta * covariate) * e^{\eta_i}$ Linear covariate

EQ 2.31 $P_i = \theta_{TV} * e^{\theta * covariate} * e^{\eta_i}$ Exponential covariate

EQ 2.32 $P_i = \theta_{TV} * covariate^{\theta} * e^{\eta_i}$ Power covariate

EQ 2.33 $sh_{\eta} = 1 - \frac{standard\ deviation(\eta_{EBE})}{\omega}$ Eta shrinkage

EQ 2.34 $sh_{\varepsilon} = 1 - standard\ deviation(IWRES)$ Epsilon shrinkage

EQ 2.35 $RSE = 100 * \frac{standard\ deviation}{mean}$ Relative standard error

EQ 8.1 $\Delta OFV = \sum_{i=1}^{n} iOFV_{covariate} - \sum_{i=1}^{n} iOFV_{base}$ Delta Objective Function

Value

EQ 8.2 $RSE(\%) = 100 * \frac{standard\ error}{mean\ parameter\ estimate}$ Relative Standard Error

EQ 8.3 $Budget = cost(hospitalisation) * days(n) + cost(assay) * samples(n)$

Study cost

Author’s contribution

The original research performed for this thesis comprises non-compartmental pharmacokinetic analyses, population pharmacokinetic analyses, population pharmacokinetic-pharmacodynamic analyses and statistical analyses. The clinical studies were finished already by the time the analyses were started and Frank L. Kloprogge was not involved in the design and execution of the clinical studies as well as quantification of drug plasma concentration levels.

1.0 Introduction

1.1 Aim

The primary objective was to study the pharmacokinetics and pharmacodynamics of the most commonly used drugs for the treatment of uncomplicated *Plasmodium falciparum* malaria during the second and third trimester of pregnancy using a pharmacometric approach. The specific objectives were to study:

- Population pharmacokinetics of oral quinine in pregnant women with uncomplicated *Plasmodium falciparum* malaria in Uganda (chapter 3)
- Population pharmacokinetics of oral and intravenous artesunate and dihydroartemisinin for the treatment of uncomplicated *Plasmodium falciparum* malaria in pregnant and 3 months post-partum women in Thailand (chapter 4)
- Population pharmacokinetics of oral artemether and dihydroartemisinin in pregnant women with uncomplicated *Plasmodium falciparum* malaria in Uganda (chapter 5)
- Population pharmacokinetics of lumefantrine in pregnant and non-pregnant women with uncomplicated *Plasmodium falciparum* malaria in Uganda (chapter 6)
- Population pharmacokinetics and pharmacodynamics of lumefantrine and desbutyl-lumefantrine in pregnant women with uncomplicated *Plasmodium falciparum* malaria in Thailand (chapter 7)
- Power calculations for mixed pharmacokinetic study designs using the population approach (chapter 8)

1.2 Background of malaria

Malaria is the most important parasitic disease in man and it is a major problem in many tropical countries. During 2010 approximately 3.3 billion people were at risk worldwide and an estimated (range) 219 (154-289) million people became infected. The majority of these infections occurred in Africa (79%) followed by South East Asia (15%) and the Eastern Mediterranean region (5%) (Figure 1.1). The rest of the infections occurred in the Western Pacific region (0.78%), the Americas (0.50%) and Europe (0.000091%) [1].

There are five different parasite species (*Plasmodium falciparum*, *Plasmodium vivax*, *Plasmodium ovale*, *Plasmodium malariae* and *Plasmodium knowlesi*) which can cause malaria in human beings. *Plasmodium falciparum* is the most common species and accounts worldwide, in Africa, the Easter Mediterranean region, Western pacific region, South-East Asia and the Americas for 90%, 98%, 83%, 79%, 53% and 35% of the infections, respectively [1]. *Plasmodium vivax* is widespread across the world while *Plasmodium ovale*, *Plasmodium malariae* and *Plasmodium knowlesi* are relatively rare [2].

Malaria can be deadly and approximately (range) 660,000 (490,000-836,000) patients died from malaria in 2010. The vast majority of the lethal cases occurred in Africa (90%), South-East Asia (6.5%) and the Eastern Mediterranean region (2.3%). The remainder of the cases occurred in the Western Pacific region (0.61%) and the Americas (0.17%) [1].

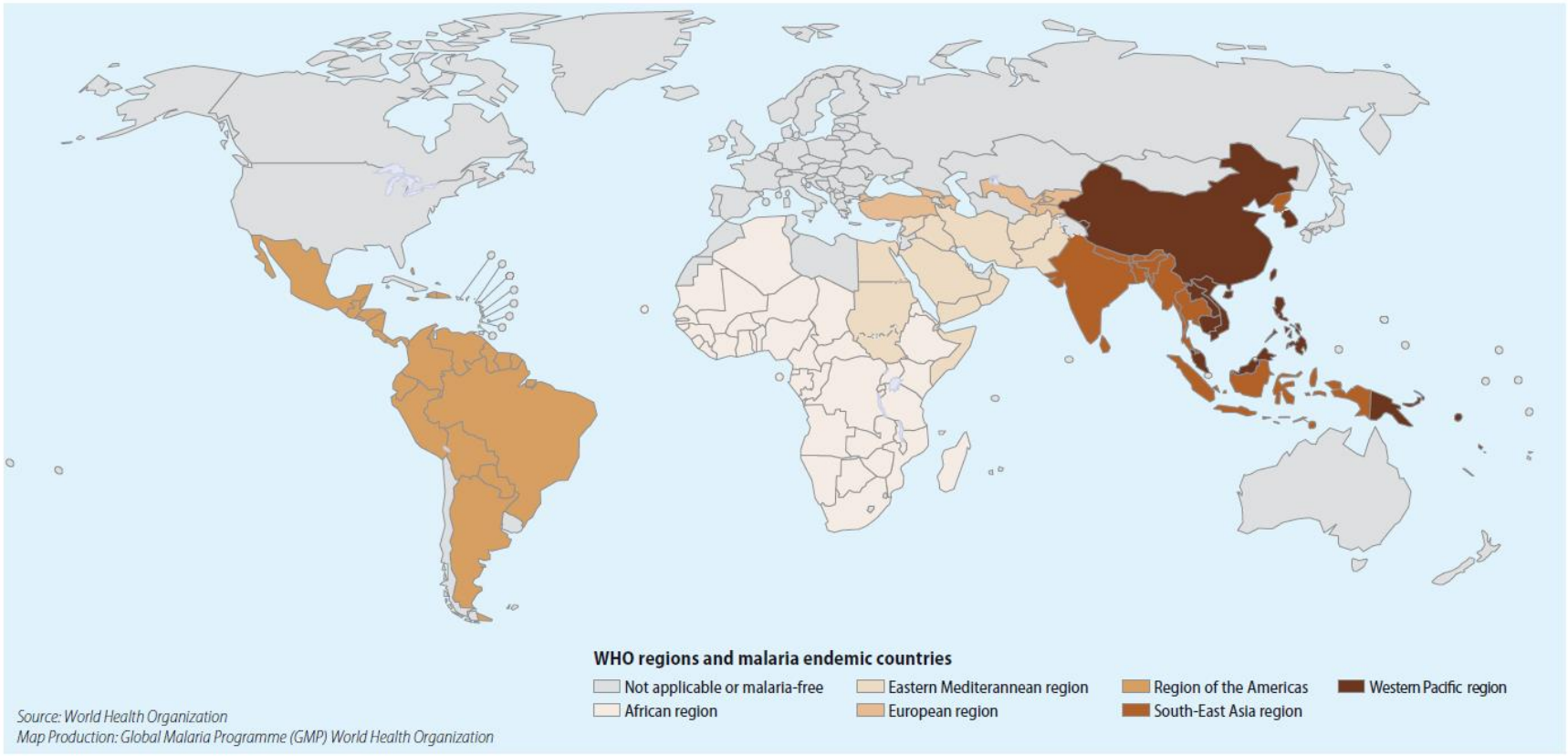

Figure 1.1 A visual representation of the different geographical regions. © World Malaria report 2012, World Health Organisation, ISBN/WHO Reference Number: 978 92 4 156453 3, “WHO regions and malaria endemic countries (page 64) [1].

Young children are especially vulnerable to malaria due to a less well developed immune system and children below 5 years of age accounted during 2010 for 86% of the deaths [1]. Also pregnant women are vulnerable to malaria due to a modulated activity of the immune system and malaria during pregnancy can cause lowered birth weight, stillbirth and it increases the mortality rate in the mother [1, 3, 4]. The total number of pregnancies in malaria transmission areas emphasise the risk for pregnant women as approximately 125 million pregnancies occurred in areas with *Plasmodium falciparum* and/or *Plasmodium vivax* transmission during 2007 (85.3 million pregnancies occurred in areas with *Plasmodium falciparum* and 92.9 million pregnancies occurred in areas with *Plasmodium vivax* transmission) [5].

1.3 Pathophysiology of malaria

1.3.1 The malaria life-cycle

Female anopheles mosquitoes can transmit *Plasmodium* parasites and the anopheles mosquito family consists of approximately 400 species. However, only 50 of them are clinically important as a vector [6]. The malaria life cycle in the mosquito starts with transmission of gametocytes during a blood meal. The gametocytes form eggs in vesicles in the mosquito mid-gut and when they are fertilized they form zygotes (Figure 1.2 #1). The fertilised zygotes become oocytes (Figure 1.2 #2) and consequently sporozoites will be formed and released from the salivary glands (Figure 1.2 #4). The released sporozoites enable a new human infection during a future blood meal. The life cycle from

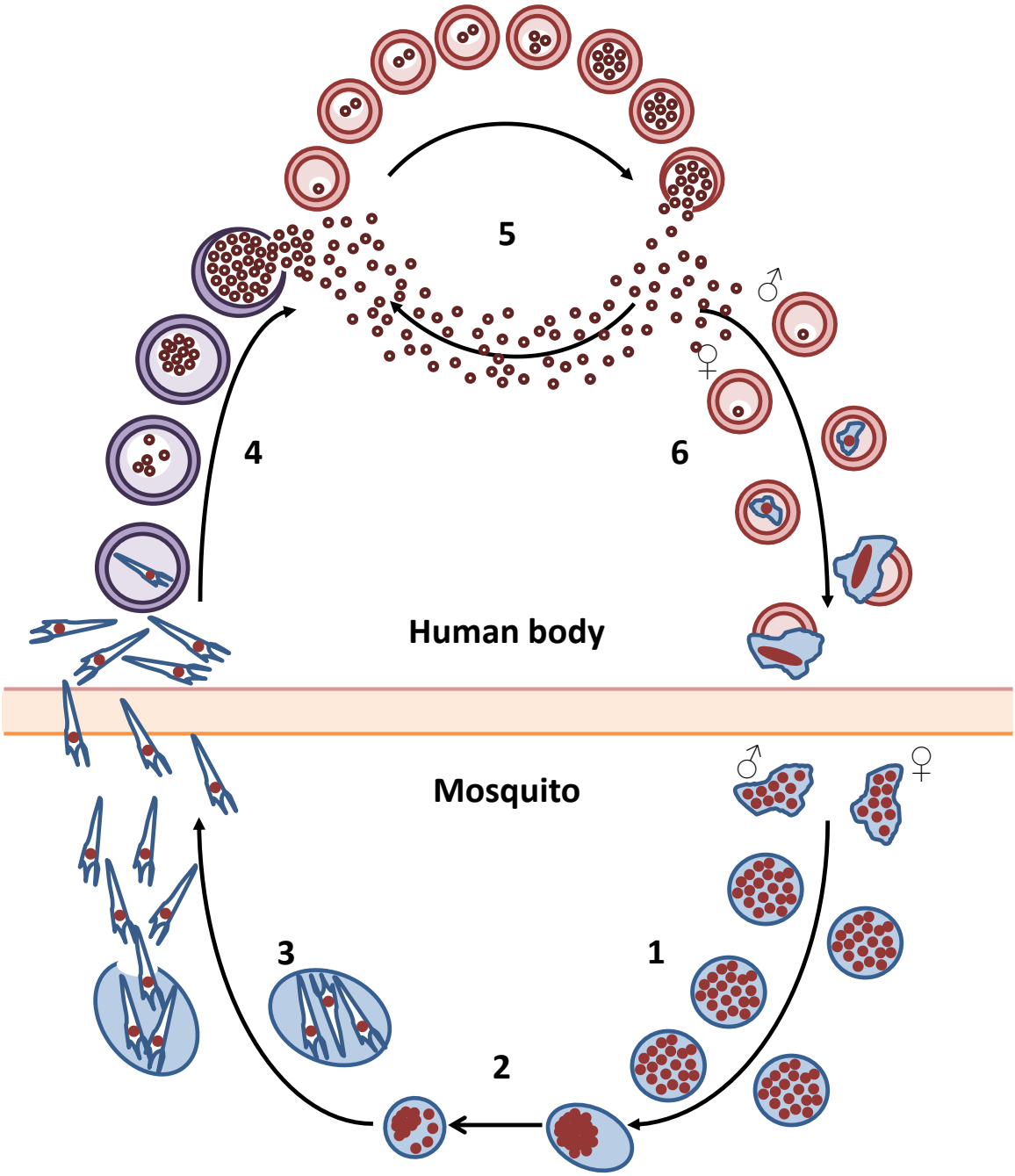

Figure 1.2 A visual representation of the malaria life cycle. 1-2: fertilisation in the mosquito gut to produce zygotes and oocytes 3: sporozoites production, 4: the liver stage, 5: the blood stage, 6: the sexual stage.

gametocyte to sporozoite release in the mosquito takes approximately 6 to 12 days.

The malaria life cycle in human starts with the transmission of *Plasmodium* parasites by an infected female mosquito from the anopheles mosquito family [3]. An estimated 5 to 100 sporozoites are injected into the bloodstream during a blood meal [7, 8]. Sporozoites migrate to the liver to form schizonts and stay there between 5 (*Plasmodium falciparum*) and 15 (*Plasmodium malariae*) days (Figure 1.2 #4) [3].

However, *Plasmodium vivax* and *Plasmodium ovale* sporozoites can enter the dormant stage in the liver (i.e. hypnozoites) and consequent malaria relapses can occur due to the reactivation of the hypnozoites in the liver [2]. Merozoites are released into the systemic circulation due to the rupture of schizonts and red blood cells are consequently entered for the asexual replication (Figure 1.2 #5). First immature throphozoites (ring stage) mature to throphozoites and consequently schizonts are formed. Parasites consume haemoglobin available in the erythrocyte in order to replicate and the toxic haeme released during digestion is detoxified by the formation of an insoluble crystalline form (haemozoin) [9]. The asexual blood cycle takes approximately 3 days for *Plasmodium malariae*, 1 day for *Plasmodium knowlesi* and 2 days for *Plasmodium falciparum*, *Plasmodium vivax* and *Plasmodium ovale* [3]. Released merozoites can then enter either the asexual stage again (Figure 1.2 #5) or the sexual blood stage (Figure 1.2 #6). Gametocytes are formed (male and female)

during the sexual stage and mosquitos can ingest them during a blood meal (Figure 1.2 #6).

1.3.2 The different malaria stages

The detection limit for malaria using microscopy is a parasite biomass of 10^8 and this is reached 6 days after the liver rupture what corresponds to 2-3 asexual blood cycles. A parasite biomass of 10^8 is also the threshold for symptomatic malaria and necrosis of the parasitised red blood cells results in acidosis, anaemia and fever. *Plasmodium ovale* and *Plasmodium vivax* parasites continue growing until a parasite biomass of 10^{12} has been reached although *Plasmodium falciparum* parasite loads can continue growing beyond this level. At the critical biomass of 10^{12} approximately 2% of the red blood cells are infected with parasites [3, 10].

Typical for red blood cells infected with *Plasmodium falciparum* is the formation of certain proteins on the surface of the erythrocytes [3]. The presence of these proteins on the outer wall of red blood cells acts as glue and enables the *Plasmodium falciparum* infected red blood cells to stick both to each other (rosetting) and to capillary blood vessels (sequestration). Sequestration in capillary blood vessels can cause ischemia which can have critical consequences if it happens in the brain or placenta. The pathophysiology of *Plasmodium falciparum* malaria and the fact that *Plasmodium falciparum* malaria can continue growing beyond the critical parasite biomass of 10^{12} explains the fact that the majority of the mortality in malaria disease is on account of *Plasmodium falciparum* malaria [11].

Malaria infected erythrocytes do not cross the placenta and thereby the foetus does not get infected. However, during pregnancy, *Plasmodium falciparum* infected erythrocytes can also sequester in the placenta [12-15] and this can cause intra-uterine growth retardation resulting in a lower birth weight, preterm delivery and an increased infant and maternal mortality [3, 4]. Cytoadherence in *Plasmodium vivax* malaria is less clear and contra-intuitive due to the absence of certain proteins on the surface of the infected erythrocytes. Nevertheless, sequestration of *Plasmodium vivax* in the placenta has been described although at a multiple fold lower level compared to *Plasmodium falciparum* malaria [14, 16].

1.4 Malaria drugs: mechanism of action

Different theories regarding the mechanism of action have been suggested for the artemisinin drugs, but it is believed that the antimalarial activity in general is based on a reduction of the peroxide bridge and the production of free radicals or other reactive intermediates [17-23]. The artemisinin drugs are effective during the asexual blood stage from the ring stage to schizonts [24-26]. By killing parasites already during their ring stage, artemisinin drugs can prevent young parasites from maturing. The artemisinin derivatives also inhibit the development of *Plasmodium falciparum* gametocytes and thereby reduce its transmission potential [27-29].

The quinolones (4-aminoquinolines, 8-aminoquinolines and amino alcohols) and related compounds (chloroquine, quinine, lumefantrine, mefloquine, piperaquine,

primaquine and amodiaquine) act during the asexual blood stage. This drug class inhibits the formation of haeme crystals by stopping the detoxification of haeme and therefore this class of drugs only acts during the later asexual blood stages [30, 31]. Primaquine has the additional capability to kill hypnozoites (dormant parasites in the liver) and is therefore the only radical cure for *Plasmodium vivax* [32]. Primaquine also kills mature gametocytes and thereby reduces the transmission of malaria [28, 29].

Anti-folate drugs (e.g. Proguanil [cycloguanil] and pyrimethamine) interfere with the folate pathway in the parasite and thereby inhibit the production of folate which is involved in the methylation of DNA [3]. The anti-folate drugs have been playing a central role as prophylactic drugs for travellers [24].

1.5 Treatment of malaria

Depending on the disease status (i.e. severe or uncomplicated), different treatment regimens and administration routes are being used.

1.5.1 Severe malaria

For the treatment of severe malaria parenteral artesunate is now recommended as first line treatment by the WHO but parenteral quinine is still used in areas where parenteral artesunate is not available [10]. Parenteral artesunate reduced the mortality in adults and children with severe *Plasmodium falciparum* malaria by 34.7% and 22.5%, respectively, compared to parenteral quinine in large trials conducted in South-East Asia (n=1461) and Africa (n=5425) [33, 34]. Parenteral artesunate is given for the first 24 hours after admission or until the patient is

able to reliably swallow tablets if this is later than 24 hours after the start of the treatment. At this stage patients are consequently treated with drugs used for the uncomplicated malaria stage. Parenteral quinine dihydrocloride treatment starts with a loading dose at admission followed by maintenance doses until the patient is able to reliably swallow tablets if this is later than 24 hours after the start of the treatment.

1.5.2 Uncomplicated *Plasmodium falciparum* malaria

The first line treatment for uncomplicated *Plasmodium falciparum* malaria is an artemisinin combined therapy (ACT). However, quinine is still widely used in areas where resistance is not reported [10]. An ACT consists of one artemisinin derivative (i.e. artemisinin, artemether, artesunate, artemotil [i.e. arteether] or dihydroartemisinin) combined with a more slowly eliminated partner drug (e.g. lumefantrine, mefloquine, pyronaridine, amodiaquine, sulfadoxine-pyrimethamine or piperaquine). The artemisinin derivatives are potent but rapidly eliminated and therefore have a short acting antimalarial effect which quickly reduces the malaria parasite biomass. Once the treatment has stopped residual parasites can start multiplying and therefore all artemisinin short course monotherapies are associated with high recrudescence rates. The slowly eliminated partner drug in an ACT prevents recrudescent malaria infections due to elimination of the residual parasites. The combination of antimalarials with different modes of action decreases the probability of selecting drug-resistant parasites [35, 36].

1.5.2.1 Artemisinin

Artemisinin (molecular weight (MW): 282.33 g/mol), is a sesquiterpene lactone drug extracted from *Artemisia annua* leaves [20]. Artemisinin mono-therapy (for six days in Tanzanian patients with *Plasmodium falciparum* malaria) was associated with a 41% recrudescence/reinfection rate after four weeks of follow-up [37]. However, when artemisinin was administered with mefloquine, piperaquine or piperaquine/primaquine as partner drugs, cure rates of >98% were reported [37-40].

1.5.2.2 Dihydroartemisinin

Dihydroartemisinin (MW: 284.34 g/mol) is relatively insoluble in water [41]. It is the main active metabolite of several artemisinin drugs (i.e. artemether, artesunate and arteether) but can also be administered as oral treatment in combination with piperaquine [41]. This drug combination is a promising new ACT and overall high cure-rates (>95%) at days 28, 42, 56 and 64 have been reported although children below 5 years of age were at higher risk for treatment failure [42-50]. A recent report suggested that lower piperaquine exposure in small children compared to adults after a standard weight-based dose regimen might explain the lower cure-rates [51].

1.5.2.3 Artesunate

Artesunate (MW: 384.42 g/mol) is a water soluble sodium salt of the hemisuccinate ester of dihydroartemisinin [41]. Artesunate in combination with mefloquine has shown high cure rates (>95%) in Thailand but the combination of artesunate and amodiaquine has shown more variable cure rates [39, 52-54].

This was initially attributed to amodiaquine resistance, although recent analyses show significantly higher cure rates with the fixed dose combination compared to loose tablets which points to underdosing as a significant contributor to lower cure rates.

1.5.2.4 Artemether

Artemether/lumefantrine is the most widely used ACT and accounted for 77% of the delivered ACT's during 2011 [1]. Artemether (MW: 298.37 g/mol) is a methyl ether of dihydroartemisinin and a relatively lipophilic compound compared to artemisinin or artesunate [41]. The fixed combination treatment shows good cure rates in adult and children (>95% at day 28) [55, 56].

1.5.2.5 Lumefantrine

Lumefantrine (MW: 528.9 g/mol) is a racemic fluorine derivative and the long acting partner drug in the artemether/lumefantrine drug combination. Lumefantrine belongs to the aryl aminoalcohol group of antimalarials [41].

1.5.2.6 Quinine

Quinine (MW: 324.4 g/mol) belongs to the alkaloids [41] and has shown variable cure rates and resistance patterns, however there is no clear picture of the quinine efficacy worldwide [57]. Quinine has been administered in different formulations for the treatment of uncomplicated malaria. A 7 day quinine combination therapy with tetracycline or clindamycin resulted in day 28 cure rates of 92- 98%, and 100%, respectively [58-60]. However, generally lower cure rates

have been obtained using quinine monotherapy with reported day 28 cure rates of 38% and 87% for 3 and 7 day treatments, respectively [58, 61].

Also 3 day quinine combination treatments were generally less effective with day 28 cure rates of 76%, 92% and 91% for tetracycline, clindamycin and doxycycline concomitant therapy, respectively [60, 61]. But a 3 day quinine treatment concomitantly administered with sulphadoxin-pyrimethamine on the other hand resulted in a day 42 cure rate of 98% [62].

1.6 Malaria treatment during pregnancy

During the first trimester of pregnancy quinine is the treatment of choice [10]. A recent study with artesunate mono-therapy during the first trimester of pregnancy did not indicate additional toxic effects [63]. This may result in a changed treatment guideline for pregnant women in their first trimester in the future. The first line treatment for uncomplicated *Plasmodium falciparum* malaria in women during the second and third trimester of pregnancy is an ACT [41]. However, quinine is often used in areas without resistance [41].

1.6.1 Artemether/lumefantrine during pregnancy

Artemether/lumefantrine has shown high cure rates (>95%) in non-pregnant adult populations [55, 56, 64, 65] although contradictory results have been published in pregnant women [64, 66, 67]. For example, low cure rates have been reported after a standard 3 day artemether-lumefantrine treatment (82.0% [74.8%-89.3%] at delivery or day 42 if later) in pregnant women with uncomplicated *Plasmodium falciparum* malaria on the Thai-Myanmar border [66]. However, pregnant women

with uncomplicated *Plasmodium falciparum* malaria from Uganda showed a cure rate of 98.2% (93.5%-99.7%) at delivery or day 42 if later [64].

1.6.2 Artesunate during pregnancy

Artesunate has shown good cure rates (cure rate >95% at day 28 or 63) for the treatment of uncomplicated malaria in adults [39, 52-54]. However, decreased cure rates in pregnant women at the Thai-Myanmar border were reported between 2004 and 2006 (89.2% [82.3%-96.1%] at delivery or day 42 if later) compared to between 1997 and 2000 (>95% at day 42) after an artesunate mono-therapy [66, 68]. This tendency may indicate a loss of efficacy although one should interpret this trend with caution since no long acting partner drug was co-administered in these studies and this has a major impact on recrudescent rates [66]. For example, artesunate-amodiaquine and artesunate-mefloquine has been reported to be effective (>95% at day 28 and day 63) during pregnancy in Tanzania and on the same Thailand-Myanmar border [69, 70].

1.6.3 Quinine during pregnancy

Contradictory quinine efficacy results have been reported in pregnant women. Low day 63 cure rates (<70%) have been reported in Thailand after a 7 day quinine mono-therapy [70, 71] although high day 42 cure rates (>95%) have been reported in Uganda and Thailand with 7 day quinine [64] and quinine-clindamycin [68] treatments, respectively.

1.6.4 Intermittent preventive treatment

Intermittent preventive treatment programs have been started during pregnancy in Africa [1, 72]. The World Health Organisation recommends sulfadoxine-pyrimethamine for intermittent preventive treatment during pregnancy [1, 10]. Contradictory results of lower [73, 74], similar [74] and higher [75] exposures have been reported for sulfadoxine and pyrimethamine in pregnant women and also resistance against sulfadoxine and pyrimethamine have been reported. Dose optimisation studies or alternative drugs may therefore have to be considered [73, 75].

1.7 The immune system during pregnancy

Malaria incidence rates and disease severity are increased during pregnancy [76]. Cell-mediated immunity is thought to be suppressed during pregnancy to avoid a rejection of the foetus. Immunological changes on account of pregnancy may consequently increase the susceptibility to certain viruses, bacteria and pathogens although a general hormonal immunosuppression does not seem to occur [77]. This indicates that the immune system is rather modulated instead of generally suppressed [78]. The increased susceptibility to malaria during pregnancy is thought to be caused by depletion of selected components in the immune system, increased production of a variety of hormones and proteins [79]. Altered patterns in the immune system activity may consequently lead to an increased workload for the drugs to clear the residual parasites and in particular for the long acting partner drug in an ACT.

In areas with low transmission rates (i,e. pregnant women have little acquired immunity before the pregnancy) both the mother and the foetus are susceptible to the most severe forms of malaria irrespective of the parity. Whereas in areas with high transmission rates (i.e. pregnant women have acquired a significant immunity before the pregnancy) both the mother and foetus have less severe effects and primigravidae are most affected. This can be partly explained by placental malaria as the placenta has not acquired immunity as it is a new organ. Primigravidae women in high transmission areas therefore have a higher risk of severe symptoms compared to pregnant women at multiple parities. In low transmission areas women show similar symptoms in all parities as only little immunity to malaria has been acquired before the pregnancy.

1.8 Antimalarial drug exposure during pregnancy

As well as the changed activity patterns of the immune system the altered antimalarial drug exposure also plays a role in lowered cure rates during pregnancy. Lower exposures result in insufficient cure-rates and sub-therapeutic drug exposure might lead to the development of drug resistance. Lowered drug exposures have been reported for artemether/dihydroartemisinin [80], artesunate/dihydroartemisinin [81], dihydroartemisinin [82], lumefantrine [83], atovaquone [84] and proguanil [84] in pregnant women. However, some antimalarials show similar (e.g. piperaquine [82, 85-87], amodiaquine and desethylamodiaquine [88, 89]) drug exposure in pregnant women compared to the non-pregnant adult patient population. Contradictory results of lower [73, 74],

similar [74] and higher [75] exposures have been reported for sulfadoxine and pyrimethamine in pregnant women.

The changes in antimalarial drug exposure may have been caused by several physiological changes that occur during pregnancy. For example, increased renal blood flow, glomerular filtration and cardiac output, decreased plasma protein binding and altered cytochrome P450 (CYP) enzyme and UDP glucuronosyltransferases (UGT) activities may affect the elimination clearance [90-92]. For example CYP isoenzymes 3A4, 2D6, 2C9 and UGT isoenzymes 1A4 and 2B6 are increased during pregnancy but CYP isoenzymes 1A2 and 2C19 are decreased during pregnancy [91, 92]. A decreased gut motility may affect the absorption of the drug and an increased plasma volume, water content and fat content may affect the distribution of the drug [90].

1.8.1 Pharmacometric models

Pharmacometrics is a general term for the quantitative analysis of drugs using mathematical/statistical models based on pharmacology, physiology and diseases. Pharmacometric models can be effectively used to study the impact of physiological changes during pregnancy on antimalarial drug exposure. The models consist of a pharmacokinetic component, pharmacodynamic component or a combination of both components. The pharmacokinetic component describes what the body does to the drug by an empirical or mechanistic representation of the absorption, distribution and elimination of the drug. The pharmacodynamic component on the other hand, describes what the drug does to the body by an empirical or mechanistic representation of the

pharmacodynamic endpoints. A population pharmacokinetic-pharmacodynamic model can combine the two facets and explain the underlying processes leading to the drug effect.

The objective of this thesis was to study the pharmacokinetics and pharmacodynamics of the most commonly used drugs for the treatment of uncomplicated *Plasmodium falciparum* malaria during the second and third trimester of pregnancy using a pharmacometric approach.

2.0 Methods

2.1 Pharmacokinetic parameters

Pharmacokinetic parameters are used to describe what the body does to the drug. Certain pharmacokinetic parameters can be directly retrieved from the data. For example the time to the first observed plasma concentration after dosing (t_{LAG}), maximum plasma concentration (C_{MAX}), time to reach the maximum plasma concentration (t_{MAX}), plasma concentration at steady state (C_{SS}) and minimum plasma concentration before the next dose is administered (C_{MIN}) [93]. However, other pharmacokinetic parameters cannot directly be retrieved from the data.

The Area Under the concentration Curve (AUC) (i.e. integral of the concentration-time profile) needs to be calculated (e.g. using the trapezoidal rule) and reflects the drug exposure. The oral bioavailability (F) represents the fraction of unchanged drug that reaches the systemic exposure after extravascular administration. F can be calculated by the following equation [93]:

EQ 2.1

$$F = \frac{AUC_{oral} * DOSE_{intravenous}}{AUC_{intravenous} * DOSE_{oral}}$$

Elimination clearance (CL) reflects the volume of sampling matrix cleared per time unit and is the sum of hepatic clearance (CL_H), renal clearance (CL_R) and other sources of clearance (CL_{OTHERS}) as for example esterases in the blood (EQ 2.1).

EQ 2.2

$$CL = CL_H + CL_R + CL_{OTHERS}$$

Usually blood clearance is assumed to be equal to plasma clearance under the condition that the blood to plasma ratio is 1. Hepatic elimination clearance (CL_H) can be described by the well-stirred model which assumes the rate of elimination to be a function of unbound drug, the liver to be a homogenous compartment and an instantaneous and complete mixing in the liver, portal and venous blood [93]:

EQ 2.3 $$CL_H = Q_H * E_H = Q_H * \left[\frac{fu * CL_{int}}{Q_H + fu * CL_{int}} \right]$$

where Q_H represents the hepatic blood flow and E_H represents the hepatic extraction ratio. E_H can be described more detailed using intrinsic clearance (CL_{int}) and the ratio of unbound drug to total drug in the matrix (fu).

Renal elimination clearance (CL_R) can be described as follow [93]:

EQ 2.4 $$CL_R = Q_R * E_R = (1 - F_R) * [CL_f + CL_S]$$

where Q_R is the renal blood flow and E_R is the renal extraction ratio. For a more detailed description the fraction reabsorbed (F_R), the clearance by filtration (CL_f) and the clearance by secretion (CL_S) have to be defined.

The elimination rate constant (k_e) represents the rate at which the drug is removed from the body. After intravenous administration, following one compartment distribution disposition, this is a first order process and the following equation describes the concentration at time t (C_t) [93]:

EQ 2.5 $$C_t = C_0 * e^{-k_e * t}$$

where t is time and C_0 is the concentration at time 0. The elimination half-life ($t_{1/2}$) is the time required to decrease the concentration or amount of drug in the body by 50% and this can be calculated by the two following equations [93]:

EQ 2.6
$$t_{1/2} = \frac{\ln(2)}{k_e} = \frac{\ln(2) * V}{CL}$$

The apparent volume of distribution (V) reflects a hypothetical volume in which the drug is distributed. For a compound with a high value for apparent volume of distribution a relatively big proportion of the drug is accommodated by the tissue compared to the sampling matrix. While for a compound with a low value for apparent volume of distribution a relatively big proportion of the drug is accommodated by the sampling matrix compared to the tissue. Apparent volume of distribution (V_{TOT}) can be described as follow [93]:

EQ 2.7
$$V_{TOT} = V_S + V_T * \frac{fu}{fu_T}$$

where V_S is the apparent distribution volume in the sampling matrix, V_T is the apparent distribution volume in tissue, fu is the fraction unbound drug in the sampling matrix and fu_T is the fraction unbound drug in the tissue.

All pharmacokinetic parameters describe different phases in the absorption, distribution, metabolism and excretion of the drug. C_{MAX}, t_{MAX} and F describe the absorption phase, V describes the distribution phase and CL, k_e and $t_{1/2}$ describe the elimination phase. C_{MAX}, also represents the distribution and elimination phase since the parameter is also dependent on CL and V. Parameters used to

describe the overall exposure of the drug are AUC, C_{MAX}, C_{SS} and C_{MIN}. The different pharmacokinetic parameters can be evaluated for correlation with treatment outcome or pharmacodynamic endpoints to enable a better pharmacological understanding of the drug.

2.2 Pharmacodynamic parameters

The pharmacodynamic parameters describe what the drug does to the body. Concentration-response relationships are often used to describe the pharmacodynamics with different models. A linear model between drug concentration (C) or dose (D: if no drug concentrations are available) and drug effect (E) is the most basic response model and can be defined by the following equation:

EQ.2.8 $$E = slope * C$$

An E_{MAX} model can also be used as response model using the following equation [93]:

EQ 2.9 $$E = E_0 - \frac{C * E_{MAX}}{EC_{50} + C}$$

The EC_{50} (or ED_{50} C is replaced with D) represents the plasma concentration which realises 50% of the maximum effect, the E_0 represents the baseline and the E_{MAX} represents the maximum effect. A more flexible version of the E_{MAX} model is the sigmoidal E_{MAX} model due to the implementation of the Hill-factor (γ). The sigmoidal E_{MAX} can be parameterised using the following equations [93]:

EQ 2.10 $$E = E_0 - \frac{C^{\gamma} * E_{MAX}}{EC_{50}^{\gamma} + C^{\gamma}}$$

A Kaplan-Meier analysis has often been used to describe the efficacy of the treatment. This type of analysis assesses the fraction of successful treatment outcomes until a certain time-point. The survival function (S[t]) is defined using the following equation [94]:

EQ 2.11 $$S(t) = P(time_{event} \geq time) = e^{-\int h(t)}$$

The hazard-rate (h[t]) is defined as rate constant representing the chance of having an event. However, in certain cases the time of the event is not known. If a weekly screening is available one can on the other hand be sure that an event should have occurred somewhere between the visit of detecting the event and last visit. In these cases interval censoring can be implemented in the Kaplan-Meier analysis and the probability that the event occurred during the interval can be defined using the following equation:

EQ 2.12 $$P(event) = 1 - e^{-(\int h(t)_{event} - \int h(t)_{startinterval})}$$

Different hazard distributions have been described in literature and the constant hazard model is most basic and describes a constant hazard rate over time using the following equation [94]:

EQ 2.13 $$h(t) = \lambda$$

The Gompertz distribution on the other hand enables the hazard rate to change exponentially over time (described by a hazard half-life [$t_{1/2}$]) using the following equation [94]:

EQ 2.14 $$h(t) = \lambda * e^{-time*\frac{\ln(2)}{t_{1/2}}}$$

The Weibull distribution also enables the hazard rate to change over time with an additional shape parameter (α) using the following equation:

EQ. 2.15 $$h(t) = \alpha^2 * \lambda * time^{\alpha-1}$$

Dose-response relationships implemented in the survival analysis (e.g. applied on the hazard parameters) enable a better understand of the correlation between drug exposure and treatment outcome.

2.3 Analyses methodologies

Pharmacokinetic and pharmacodynamic data can be investigated using different types of analysis. The conventional methodology of studying pharmacokinetic and pharmacodynamic data uses non-compartmental analysis. The population approach can also be used for the analysis of pharmacokinetic and pharmacodynamic data. Depending of the aim of the analyses one of the two different methods can be applied.

2.3.1 Non-compartmental analysis

Dense sampled individual plasma concentration-time data from relatively few patients (chapter 5) was evaluated by non-compartmental analysis using

WinNonlin version 5.3 (Pharsight Corporation, California, USA). Complete *in-vivo* conversion of a drug into the metabolite was assumed for the analysis of drug-metabolite data and the administered dose of the metabolite was calculated using the relative difference in molecular weights.

Observed pharmacokinetic parameters for non-compartmental analysis (t_{LAG}, C_{MAX} and t_{MAX},) were directly retrieved from the data. Patients who did not provide a sufficient number of samples for a full pharmacokinetic evaluation were excluded from the analysis but were included in the summary statistics for C_{MAX}, T_{MAX} and T_{LAG} if the data allowed.

The $t_{1/2}$ was estimated by best-fit log-linear regression of the observed concentrations in the terminal elimination phase and k_e was calculated using the following equation [93]:

EQ 2.16
$$k_e = \frac{\ln(2)}{t_{1/2}}$$

$AUC_{0-\infty}$ was calculated using the linear trapezoidal method for ascending concentrations and the logarithmic trapezoidal method for declining concentrations to avoid over-estimation of the AUC using the following equation [93]:

EQ 2.17
$$AUC_{0-\infty} = \sum AUC_{T1} + AUC_{T2} + ... + \frac{C_{LAST}}{\lambda}$$

Lambda (λ) was obtained using log linear regression. The last observed concentration (C_{LAST}) and λ were subsequently used to obtain the drug exposure during the elimination phase.

Apparent volume of distribution during the elimination phase (V_z/F) and oral clearance (CL/F) were computed individually using equation 2.18 and 2.19, respectively [93]:

EQ 2.18
$$\frac{V_Z}{F} = \frac{DOSE}{k_e * AUC}$$

EQ 2.19
$$\frac{CL}{F} = \frac{DOSE}{AUC}$$

Individual pharmacokinetic parameter estimates and exposures (i.e. AUC, C_{MAX}) did not follow a normal distribution and were therefore compared between groups (e.g. second versus third trimester) using the Mann-Whitney test in STATA v.11. A regression analyses between exposure and continuous variables (e.g. estimated gestational age) were performed using GraphPad Prism 6.0.

2.3.2 Population approach

Non-linear mixed effect modelling was used for the population approach in chapter 3, 4, 5, 6, 7 and 8. This methodology estimates the fixed effects (population mean parameters and covariates) and random effects (between subject variability, between occasion variability and residual variability) simultaneously. Therefore both relatively small and large study populations consisting of densely, sparsely or mixed densely and sparsely sampled patients

are suitable for this type of analysis. Population pharmacokinetic and pharmacodynamic analyses in this thesis were performed using NONMEM 7.1 (chapter 5 and 6) and NONMEM 7.2 (chapter 3, 4, 7 and 8).

NONMEM is the most frequently used software package for population pharmacokinetic and pharmacodynamic analyses. It is available since the 1970's and is constantly being updated and further developed ever since. Furthermore, it has a large user community sharing knowledge about bugs and ways to implement specific problems which is the main reason why NONMEM was selected for the analyses in this thesis. However, there are concerns about the robustness of the estimation methods available in NONMEM and alternative software packages claim to have more precise and accurate estimation methods. These alternative software packages on the other hand also have limitation and often have substantially smaller user groups which make bug solving and help with implementation of problems more complicated.

2.3.2.1 Pharmacokinetic model

All pharmacokinetic data was transformed into their natural logarithm and drug-metabolite data (chapter 4, 5 and 7) was transformed into molar units. It was assumed that physiological parameters cannot be smaller than 0 due to the physiological boundaries. Therefore, all pharmacokinetic parameters were coded following a log-normal distribution:

EQ 2.20 $$P_i = \theta_{TV} * e^{\eta_i}$$

where P_i represents the individual parameter estimate for the i^{th} individual, θ represents the typical parameter estimate in the population (with a lower boundary of 0) and η_i represents the random difference between θ and P_i. Variability could be classified as inter individual variability (IIV) and/or inter (dose) occasion variability (IOV). The different variability components were consequently added up as per below:

EQ 2.21 $$\eta_i = \eta_{IIV,i} + \eta_{IOV,i}$$

The variability components in equation 2.20 and 2.21 (normal distribution with a mean of 0) enable the parameter to follow a log-normal distribution, but there are circumstances where that the log-normal distribution needs to be modified. For example, apparent volume of distribution might be skewed because the lowest value is not 0 but the volume of the sampling matrix, elimination clearance might be skewed due to an upper limit of liver blood flow and bio-availability might be skewed due to the range between 0 and 1. Therefore, also box-cox (EQ 2.22), heavy tailed (EQ 2.23) and logit (EQ 2.24) transformations were tested [95].

The box-cox transformation of the variability was parameterised as follow:

EQ 2.22 $$\eta_{i\_box-cox} = \frac{e^{\eta_i^{\theta_i}} - 1}{\theta_i}$$

The normally distributed variance (η_i) in the box-cox transformation is modified by the shape parameter (θ_i) that enables more flexibility in describing the variability.

Heavy-tailed transformation of the variability was parameterised as follow:

EQ 2.23

$$\eta_{i\_heavy-tailed} = \eta_i * |\eta_i|^{\theta_i}$$

A negative, zero and positive value for the shape parameter (θ_i) in the heavy-tailed transformation result in a bimodal, normal and heavy-tailed distribution of the parameter, respectively.

The logit transformation of the variability was described as follow:

EQ 2.24

$$\eta_{i\_logit} = \left(\frac{e^{\ln\left(\frac{\theta_1}{(1-\theta_1)}\right)+\eta_i}}{1+e^{\ln\left(\frac{\theta_1}{(1-\theta_1)}\right)+\eta_i}} - \theta_1 \right) * \theta_2$$

The skewness parameter varies between 0 and 1 and is represented by θ_1. The distribution width must be a positive number and is represented by θ_2.

Different residual variability models on the pharmacokinetic data were assessed (additive [EQ 2.25], proportional [EQ 2.26] and combined additive and proportional error [EQ 2.27] model structures).

EQ 2.25

$$\text{Observation}_{ij} = \text{individual prediction}_{ij} + \varepsilon_{ij}$$

EQ 2.26

$$\text{Observation}_{ij} = \text{individual prediction}_{ij} * (1+\varepsilon_{ij})$$

EQ 2.27

$$\text{Observation}_{ij} = \text{individual prediction}_{ij} * (1+\varepsilon_{\text{proportional,ij}}) + \varepsilon_{\text{additive ij}}$$

In all residual error models, the j^{th} observation in the i^{th} individual can be approximated by the individual prediction plus an unexplained variability component (e.g. EQ 2.25, EQ 2.26 and EQ 2.27).

Pharmacokinetic models were executed using the first-order conditional estimation method with interaction. The objective function value (OFV) computed as minus twice the log likelihood of the data, physiological plausibility and goodness-of-fit diagnostics were used to evaluate competing hierarchical models during the model building process. Goodness-of-fit diagnostics were four different graphs representing the observed versus population predictions, observed versus individual predictions, conditional weighted residuals versus population predictions and conditional weighted residuals versus time.

Different disposition models were fitted to the data in order to best describe the distribution of a drug through the body (Figure 2.1#A). An ascending number of distribution compartments was assessed and a reduction in OFV of 3.84 or more was considered a significant (*p=0.05*) improvement of the model fit after the introduction of one new parameter (one degree of freedom).

Model misspecification may occur due to large fractions of censored data, which may be especially pronounced in the elimination phase of rapidly eliminated drugs (Figure 2.1#B). As a consequence, a two compartment distribution may fit the data better even though the true disposition of the drug follows a one-compartment distribution [82]. This may result in over estimation of the exposure and elimination half-life. Different methodologies to avoid bias in parameter estimates caused by multiple samples being below the limit of quantification (BLOQ) were evaluated while modelling artemether, artesunate and dihydroartemisinin. The first method is omitting the BLOQ data. Using the second method, BLOQ data were imputed by a fixed concentration at half the lower limit

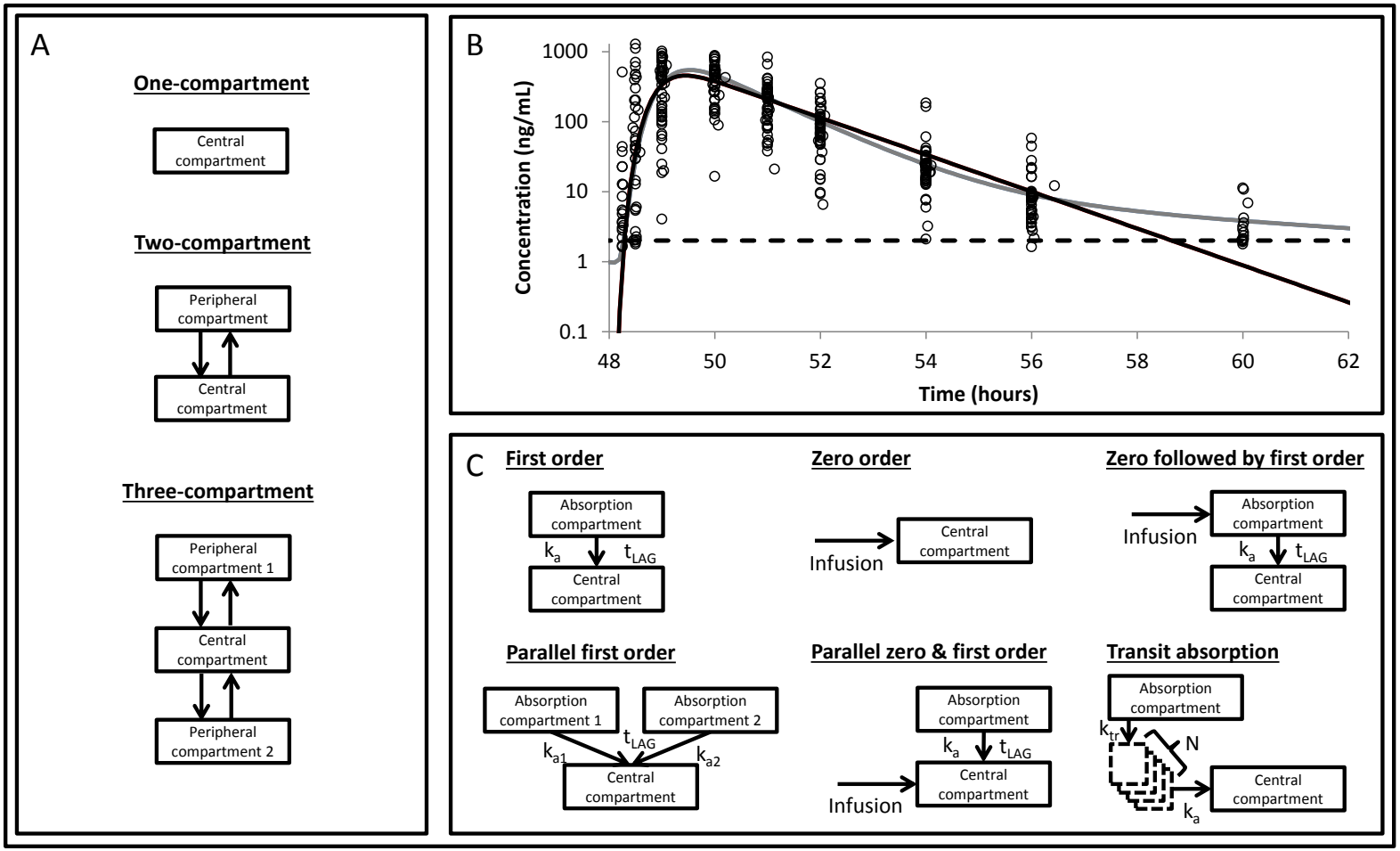

Figure 2.1 A schematic representation of the different tested disposition models (A), absorption models (C) and potential model misspecification on account of large fraction data below the limit of quantification (B; personal communication with Joel Tarning [82]). k_a: absorption rate constant, k_{tr}: transit rate constant, t_{LAG}: absorption lag-time and N: number of transit compartments.

of quantification (LLOQ/2) and modelled simultaneously with the data above the limit of quantification [96, 97]. Another methodology was to model the BLOQ data as censored data simultaneously with the data above the limit of quantification using the M3 method. The M3 method maximises the probability that BLOQ data will be predicted below the limit of quantification simultaneously with the conventional estimation of observed data above the limit of quantification [96, 97]. The Laplacian estimation method with interaction was used for the M3 method [96, 97].

A variety of absorption models was tested depending on the density of the data during the absorption phase. Hence, complex absorption model structures need dense data during the absorption phase. A first-order, parallel first-order, zero-order, parallel first- and zero-order and zero order absorption followed by first-order absorption with and without lag-time were tested. Furthermore, transit compartment absorption models with an individually estimated number of transit compartments [98] were tried and compared to a less flexible transit-compartment absorption model where the number of transit compartments (1-10) was evaluated and fixed for the population (Figure 2.1#C).

2.3.2.2 Pharmacodynamic model

The pharmacodynamic data (no recurrent malaria, recrudescent malaria or novel infection) was modelled simultaneously with pharmacokinetic data using a survival analysis (chapter 7). Pharmacokinetic parameters were fixed in the simultaneous pharmacokinetic-pharmacodynamic model and models were executed using the Laplacian estimation method with interaction. Three different

hazard distributions for having a recrudescent malaria infection (i.e. constant hazard [EQ 2.13], Gompertz hazard [EQ 2.14] and Weibull hazard [EQ 2.15]) have been evaluated. For a novel infection only the constant hazard model was assessed. Both the effect of plasma concentration and accumulated AUC was subsequently assessed on the best performing hazard function using an E_{MAX} model (EQ 2.9) and a sigmoidal E_{MAX} model (EQ 2.10) as described per below:

EQ 2.28

$$h(t) = \lambda * \left(E_0 - \frac{C^{\gamma} * E_{MAX}}{EC_{50}^{\gamma} + C^{\gamma}} \right)$$

The hazard rate (h[t]) defined in equation 2.28 represents a constant hazard model multiplied by the drug effect using a sigmoidal E_{MAX} model. The drug and metabolite effect could also be evaluated simultaneously by multiplying the drug effect using an E_{MAX} model and the metabolite effect using an E_{MAX} model with the hazard rate.

2.3.2.3 Covariate model

Random variability components in pharmacokinetic and pharmacodynamic base models were preferably explained by physiological plausible covariates. Covariate modelling was therefore done using the best performing structural model. Body weight was evaluated as an allometric function on all clearance (using a fixed power of 2/3 or 3/4) and volume parameters (using a fixed power of 1) [99]. Furthermore, all parameter-covariate relationships were screened for a significant correlation (*$p<0.05$* in Pearson, Spearman and/or Kendall test). Parameter-covariate relationships which were considered physiologically

plausible and/or significant parameter-covariate relationships from the screening were evaluated using forward addition and backward elimination covariate selection [100, 101]. In the forward step a p-value of 0.05 was considered significant for retaining the covariate in the model and a p-value of 0.01 or 0.001 (ΔOFV>6.63 or ΔOFV>10.83) was considered as significant in the backward elimination. A p-value of 0.001 was used for studies with relative sparse sampled data or relatively small number of enrolled patients (chapter 3, 4, 5 and 7) and a p-value of 0.01 was used for more densely sampled studies and/or studies with relatively large numbers of included patients (chapter 6).

Categorical covariates were implemented as proportional effect and described as per below:

EQ 2.29 $$P_i = \theta_{TV} * (1 + \theta * \text{covariate}) * e^{\eta_i}$$

The covariate was multiplied with the population parameter of interest and the coefficient (θ) was estimated in the case that the covariate was 1.

Two different types of continuous covariates were available; baseline covariates and time varying covariates. The implementation of time varying covariates was assessed via three different methods (i.e. last observed covariate value carried forward, linear interpolation of observed covariate values and a disease model explaining the covariate). All continuous covariates (i.e. baseline covariates and time varying covariates) were assessed using three different types of parameterisation. Linear covariate-parameter relationships were assessed first. Subsequently exponential and thereafter power relationships were assessed if a

significant improvement for a linear and exponential continuous covariate-parameter relationship was realised. A linear (EQ 2.30), exponential (EQ 2.31) and power (EQ 2.32) covariate-parameter relationship were coded as follow:

EQ 2.30 $$P_i = \theta_{TV} * (1 + \theta * \text{covariate}) * e^{\eta_i}$$

EQ 2.31 $$P_i = \theta_{TV} * e^{\theta * \text{covariate}} * e^{\eta_i}$$

EQ 2.32 $$P_i = \theta_{TV} * \text{covariate}^{\theta} * e^{\eta_i}$$

All continuous covariate relationships were multiplied with a population-parameter of interest and the coefficient (θ) was estimated. Continuous covariates may be centralised around the median of the population. The population mean estimate represents then an individual with the median value for the covariate within the study population rather than an individual with value 0 for the covariate. The absorption and disposition models were reconsidered using the final covariate model.

The full covariate approach enabled visualisation of (potential/non-significant) pregnancy related covariate effects on all clearance, volume and absorption parameters [102]. The covariate of interest was applied on all parameters but not at the same time on bio-availability to avoid identifiability problems. Bio-availability is correlated with clearance and volume parameters what would result in many different values with the same fit. Results from 200 non-parametric bootstrap runs were visualised using a box-plot and covariate effects were

considered potentially significant in the full covariate model if the 95% confidence interval did not include zero effect.

2.3.2.4 Model validation

All models were validated by assessing the goodness-of-fit diagnostics. Eta (EQ 2.33) and epsilon (EQ 2.34) shrinkage calculations obtained by NONMEM were evaluated in order to assess the reliability of the individual parameter estimates and the goodness-of-fit diagnostics [103]. Eta and epsilon shrinkage was calculated using the following equations:

EQ 2.33
$$sh_{\eta} = 1 - \frac{\text{standard deviation}(\eta_{EBE})}{\omega}$$

EQ 2.34
$$sh_{\varepsilon} = 1 - \text{standard deviation}(IWRES)$$

EBE and IWRES in equation 2.33 and 2.34 stand for empirical bayes estimates and individual weighted residuals, respectively. Parameter estimates with shrinkage values higher than 20%-30% should be interpreted with caution [103].

A bootstrap was performed by the execution of the model using 1,000 resampled datasets. The resampling of the dataset should be stratified to retain a similar covariate distribution across all resampled datasets. The relative standard error (RSE) and the non-parametric 95% confidence intervals (calculated as 2.5% and 97.5% percentiles) of parameter estimates were consequently retrieved from the 1,000 bootstrap runs. The relative standard error was calculated as:

EQ 2.35

$$RSE = 100 * \frac{\text{standard deviation}}{\text{mean parameter estimate}}$$

The predictive power of the model to accurately and precisely describe the data was assessed by numerical predictive checks and visual predictive checks. The numerical predictive check verified the percentage of observed data outside the simulated 90% confidence interval from the model (chapter 3 and 6). The visual predictive check for pharmacokinetic data was visualised by overlaying the 95% confidence intervals of the simulated (n=2,000) 5^{th}, 50^{th} and 95^{th} percentiles with the 5^{th}, 50^{th} and 95^{th} percentiles of the observed data. The visual predictive check may also be weighted with the population prediction in order to correct for different dosages, biological matrices or time varying covariates [104]. The visual predictive check for the Kaplan-Meier analysis (chapter 8) was visualised by overlaying the 95% confidence interval from the simulated (n=2,000) Kaplan-Meier analyses with the observed Kaplan-Meier analysis. The relative hazard versus plasma concentrations visual predictive check (chapter 8) was visualised by plotting the 90% confidence interval from the simulated relative hazard (compared to the baseline hazard) and the individual predicted plasma concentrations.

Post-hoc parameter estimates as for example AUC, C_{MAX}, t_{MAX} and $t_{1/2}$ were produced using the final model to enable comparison to literature findings which have been mainly analysed using non-compartmental analysis. AUC was calculated by taking the integral of the sampling compartment in the pharmacokinetic model (appendix A). C_{MAX} and t_{MAX} were calculated in the

sampling compartment of the pharmacokinetic model (appendix A) and $t_{1/2}$ was calculated using the code in appendix B. Post-hoc estimates and literature values were reported as median (range) unless mentioned otherwise.

Parameter estimates from a drug metabolite data analysis obtained with non-compartmental analysis, sequential drug-metabolite modelling using the population approach and simultaneous drug-metabolite modelling using the population approach were transformed into their natural logarithms (chapter 5). A student t-test was used to compare parameter estimates between two methodologies and ANOVA with regression analysis was performed to compare parameter estimates between more than two methodologies.

2.4 Advantages of the population approach

The population pharmacokinetic approach is, other than the traditional non-compartment analyses approach, not restricted to analyse solely traditional dense sampled concentration-time data from a relatively few patients. The population pharmacokinetic approach also enables the analysis of sparse sampled concentration-time data from relatively large patient groups or a combination of both sparsely and densely sampled data.

The models developed using the population approach also enable a mechanistic understanding of the disposition pharmacokinetics by complex distribution models. A model independent non-compartmental analysis on the other hand is not able to do this. For example a non-compartmental analysis is therefore not

able to mechanistically explain the phenomenon of a significantly different $t_{1/2}$ but not substantially different exposure.

Furthermore, the population approach enables a careful analysis of drug-metabolite data using a simultaneous pharmacokinetic drug-metabolite model. These models produce physiologically plausible parameter estimates for both the drug and the metabolite. A model independent non-compartmental analysis or a separate drug and metabolite model using the population approach on the other hand might produce non-physiological parameter estimates for both the drug and metabolite. The standard procedure of analysing a metabolite using non-compartmental analysis is to adjust the input dose for the metabolite by the relative difference in molecular weight between the parent drug and the metabolite. The metabolite is then assumed to be absorbed from the gut into the systemic circulation. This is inaccurate since the drug in most cases is absorbed as parent drug and then converted to metabolite *in-vivo*. The same mistake can also be made while using the wrong models for the population approach, for example if the drug and metabolite pharmacokinetic data is modelled separately.

Moreover, random variability can be estimated by the population approach although it is preferably described with physiologically explainable covariates (i,e, body weight, age, estimated gestational age etc.). Both the size and shape of the parameter-covariate relationship can be determined with high statistical power and covariate models thereby enable a physiological interpretation of the drug and disease and even physiological based models can be developed. This is

impossible using a non-compartmental analysis, which only allows a correlation analysis between covariates and parameters.

2.4.1 Simulations using a population approach model

Pharmacokinetic and/or pharmacodynamic models can be used for Monte-Carlo simulations. Final estimates of the fixed and random effects from a developed model can be used to perform studies *in-silico*. This can be useful to evaluate the effects of detected covariates on pharmacokinetic and/or pharmacodynamic endpoints. Also dose optimisations can be performed by the interpolation of the data using *in-silico* studies which can reliably guide follow op studies and adaptive study designs [83, 105].

2.4.2 Study design using a population approach model

The pharmacokinetic and pharmacodynamic models can also be used for power calculations with the Monte Carlo mapped power or stochastic simulation estimation method [106]. Sample size calculations can calculate the minimum required number of patients to detect a covariate-parameter relationship with a predefined chance (e.g. 80% power at a 5% significance level). It was shown that sample size calculations performed with Monte Carlo mapped power or stochastic simulation estimation method were statistically more powerful compared to traditional t-tests and analyses of variance [106, 107]. Furthermore, pharmacokinetic and pharmacodynamic models can also be used to optimise sampling schedules. The optimisation criterion is a minimum residual standard error on the model parameters [108]. The appropriate use of power calculations

and optimal design methods for the design of pharmacokinetic and/or pharmacodynamic studies can improve the efficiency in clinical research.

3.0 Quinine

3.1 Background

Oral quinine is still frequently used for the treatment of uncomplicated malaria in areas with low resistance patterns or in areas where ACT's are not available [41]. A 7 day mono therapy or combination treatment of quinine with tetracycline, doxycycline or clindamycin, dosed 3 times daily at 10 mg quinine sulphate per kg bodyweight is commonly used [41, 59, 60]. Quinine in combination with clindamycin is even recommended during all pregnancy trimesters [41].

There is only limited pharmacokinetic quinine data during pregnancy available, even though quinine is still widely used. A non-compartmental analysis of quinine in pregnant (n=8) and non-pregnant (n=8) women with uncomplicated *Plasmodium falciparum* malaria in Sudan did not show a significantly different exposure or elimination half-life after intravenous administration [109]. However, a study in pregnant women with *Plasmodium falciparum* malaria (n=10) [110] reported a shorter elimination half-life (11.3 vs 16.0 and 18.2 hr) and a smaller apparent volume of distribution (0.96 vs 1.67 and 1.18 L/kg) compared to a literature reference population (i.e. patients with uncomplicated *Plasmodium falciparum* malaria and cerebral malaria) after intravenous administration [111]. This suggests that pregnancy might affect the distribution of intravenous quinine and therefore the terminal elimination half-life but not the elimination clearance and therefore not the exposure of the drug.

3.1.1 Study aim

The objective of this study was to evaluate the population pharmacokinetics of orally administered quinine in pregnant women in the second and third trimester with uncomplicated *Plasmodium falciparum* malaria in Uganda.

3.1.2 Absorption

The absolute bioavailability of oral quinine tablets is approximately 75% [112, 113] and the maximum quinine plasma concentration of 0.552 (0.189-0.938) mg/l/ per mg/kg dose is reached 2.4 (1.4-5.9) hours after oral administration [114-124].

3.1.3 Distribution

To date no population pharmacokinetic analyses have been performed for oral quinine. However, population pharmacokinetic analyses were performed for intramuscular quinine and both one- and two-compartment disposition models have been used to describe the data [125, 126]. The different disposition models can be explained by the difference in dosing and sampling schedule.

3.1.4 Metabolism and elimination

Quinine is mainly metabolised via CYP3A4 in the liver and 3-hydroxyquinine is the metabolite with the most antimalarial activity equalling 10% of quinine antimalarial activity [127, 128]. Quinine elimination half-life is 11.9 (7.50-20.0) hours after oral administration [114-120, 122, 123]. Quinine elimination clearance is substantially lower during the acute phase of the disease as a result of

increased alpha-1-acid glycoprotein concentrations and thus increased plasma protein binding of quinine [124, 129-131].

3.2 Study design

This pharmacokinetic study was conducted in the Mbarara National Referral Hospital (MNRH) ante-natal clinic (ANC) in Uganda as a part of a larger efficacy study published elsewhere [64]. The trial was registered at ClinicalTrials.gov (NCT00495508) and patients were recruited from February to July 2008. Ethical approval was obtained from the Mbarara University Faculty of Medicine Research and Ethics Committee, the Mbarara University Institutional Ethics Committee, the Uganda National Council for Science and Technology (ethics committee) and the Comite d'Ethique de St. Germain en Laye (CCPPRN).

Inclusion criteria were an estimated gestation age (EGA) of at least 13 weeks, residence in the Mbarara Municipality (radius 15 km from MNRH), and *Plasmodium falciparum* mixed- or mono-infection (detected by microscopy). Exclusion criteria were known allergy to artemisinin derivatives, lumefantrine or quinine, inability to comply with the specified follow-up schedule, severe anaemia (Hb <7g/dL), signs or symptoms of severe malaria requiring parenteral treatment, or *Plasmodium falciparum* parasitaemia above 250,000 parasitised red cells/µL. Patients were enrolled if written informed consent was obtained and if they fulfilled all inclusion criteria and none of the exclusion criteria.

3.2.1 Dosing regimen and blood sampling

Oral quinine sulphate (Remedica, Limassol, Cyprus, 300 mg salt per tablet; 10 mg salt/kg/dose) was administered under supervision three times daily (0, 8 and 16 hours) for 7 days. A full or a half replacement dose was given if the dose was vomited within 30 minutes or between 30 to 60 minutes, respectively. When the dose was vomited again within 30 minutes, the patient was withdrawn from the study and treated with rescue treatment (artemether –lumefantrine [Coartem®], 4 tablets twice daily for 3 days). Venous blood samples (2 mL) were collected in heparinised tubes at 0, 1, 2, 3, 4, 8, 16, 24, 48, 72, 96, 120, 144, 160, 161, 162, 163, 164, 168, 170, 172, 176, and 184 hour after the first dose. Blood samples were centrifuged for 5 minutes at 1400 g and plasma was stored at -70°C or in liquid nitrogen until analysis.

3.2.2 Drug analysis

Quinine drug analysis was performed using LC with fluorimetric detection. Fifty µL of NaOH 0.1 M and 50 µL of the internal standard (hydroquinidine 7.5 µg/L) were added to 50 µL of plasma. Liquid/liquid extraction was performed with 4 mL of dichloromethane:isopropylic alcohol (80:20). After 10 minutes of mixing, the samples were centrifuged and the supernatant was separated and evaporated under a stream of nitrogen. The dry residue was reconstituted with 100 µL of the mobile phase and 30 µL were injected in the chromatographic system. Chromatographic separation was performed on a Cluzeau C8+ satisfaction column (250x3 mm; 3 µm; Sainte Foy la Grande, France) with a mobile phase consisting of dihydrogen potassium phosphate 0.1 M:acetonitrile:acetic acid

(695:300:5). The retention times of quinine and the internal standard were 4.9 minutes and 6.1 minutes, respectively. Excitation and emission wavelengths were 350 and 440 nm, respectively. The recovery was between 76% and 80% within the calibration range of 1-10 µg/mL. Duplicates of quality control samples were analysed at three concentrations at 2 µg/mL, 6 µg/mL and 8 µg/mL. Overall accuracy (bias) and precision (RSD) was less than 5.0% and 9.9%, respectively, and the LLOQ was set to 1 µg/mL.

3.3 Results

Twenty three women in the second and third trimesters of pregnancy were enrolled in this pharmacokinetic study, but one patient was excluded from data analysis because of an unreliable dosing history (Table 3.1). The treatment was well tolerated and efficacious with no cases of vomiting or reappearance of malaria during the follow-up until delivery or day 42 if later.

3.3.1 Population pharmacokinetic quinine model

A first-order absorption model followed by a two-compartment disposition model with an additive residual error model described the quinine data accurately. Simpler structural models resulted in model miss-specification and more complex models did not result in significant improvement ($p>0.05$). Adding inter-individual variability ($\Delta OFV=-34.7$) and inter-occasion variability between doses ($\Delta OFV=-60.4$) on a fixed (100%) relative bioavailability parameter improved the model fit significantly.

Table 3.1. Admission demographics of patients included in the pharmacokinetic study.

	Pregnant women (n=22)
Age (years)	21.0 (18.0-37.0)
Body weight (kg)	56.5 (44.0-71.0)
Gestational age (weeks)	26.0 (13.0-37.0)
2nd trimester (%)	54.5
3rd trimester (%)	45.5
Body temperature (°C)	37.2 (36.0-38.9)
Plasmodium falciparum parasitaemia (parasites/μL)	2,240 (39.0-44,500)
Platelets (10^9/uL)	131 (15.0-313)
Bilirubin (mg/dL)	1.31 (0.310-3.36)
Haematocrit (%)	31.3 (22.1-39.8)
Diastolic blood pressure (mmHg)	63.0 (45.0-80.0)
Haemoglobin (g/dL)	10.4 (7.40-12.7)
Red blood cell (10^{12}/L)	3.43 (2.37-4.50)
Neutrophils (10^9/L)	2.56 (0.550-6.53) [a]
Eosinophils (10^9/L)	80.0 (10.0-300) [a]
Basophils (10^9/L)	30.0 (10.0-80.0)
Lymphocytes (10^9/L)	2.22 (0.690-3.61)
Monocytes (10^9/L)	0.645 (0.170-1.34)
ALAT results (IU/L)	16.5 (8.00-26.0)
Creatinine results (mg/dL)	0.510 (0.380-1.29)

Values are reported as median (range).

[a] Based on 21 patients

Parasitaemia, implemented linearly (EQ 2.30) as a time-varying covariate (last observation carried forward) had a significant effect on relative bioavailability (ΔOFV=-88.6) resulting in a 38.9% increase in relative bioavailability per log10 parasitaemia. Body weight, allometrically scaled on clearance (power exponent of 2/3) and volume (power exponent of 1) parameters, realised an improvement (ΔOFV= -4.01) of the model.

The following covariate-parameter relationships were identified (physiological plausibility and/or graphical screening) and tried formally in a stepwise covariate approach using the base model with body weight implemented allometrically on all clearance and volume parameters and parasitaemia as time-varying covariate on relative bioavailability: body temperature, baseline parasitaemia, age, trimester and estimated gestational age on all parameters; alanine aminotransferase on elimination clearance and inter-compartmental clearance; systolic blood pressure on inter-compartmental clearance and body weight on absorption rate constant. Body temperature on elimination clearance (exponential relationship), estimated gestational age on bioavailability (linear relationship) and body weight on absorption rate constant (power relationship) were significant covariates in the forward addition. However, only body temperature on elimination clearance was retained in the model in the backward elimination (51.8% lower at 39 °C compared to 36 °C).

Goodness-of-fit plots from the final model did not show any model misspecification (Figure 3.1) and the visual predictive check demonstrated a reasonable predictive power of the model (Figure 3.2). The numerical predictive

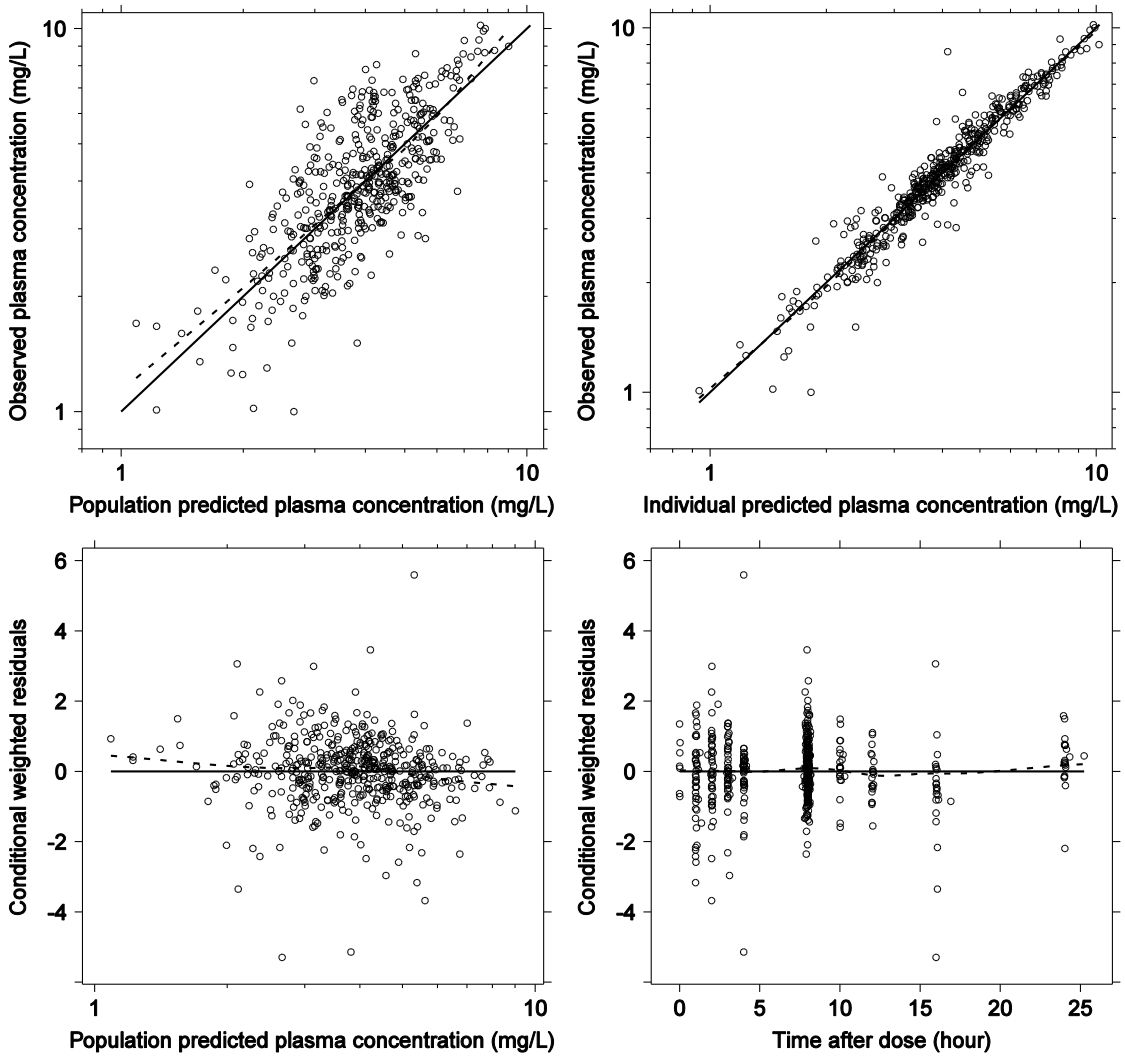

Figure 3.1 Quinine goodness-of-fit diagnostics. The solid black line represents the line of identity and a local polynomial regression is represented by the dashed black line. Observed data are represented by the black circles.

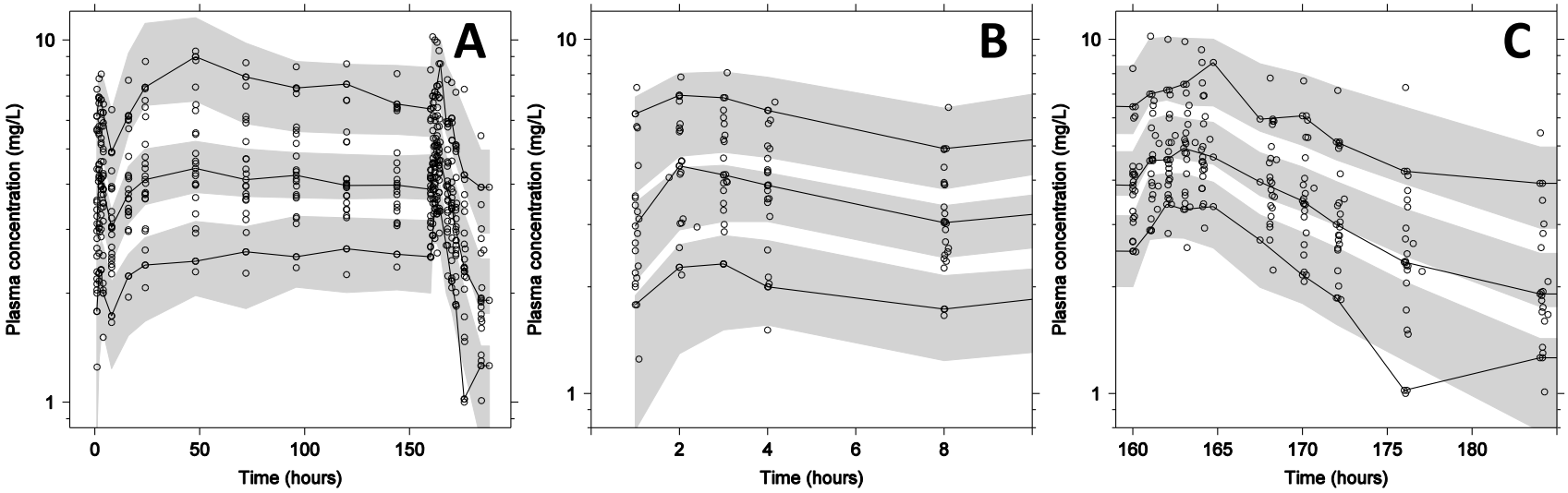

Figure 3.2 Visual Predictive Check of the final quinine model. Open circles represent the observed data, solid lines represent the 5th, 50th and 95th percentiles of the observed data and the shaded areas represent the 95% confidence interval of the simulated 5th, 50th and 95th percentiles. Panel A displays a visual predictive check of all data, Panel B display a visual predictive check of the first dose and Panel C display a visual predictive check of the last dose.

check computed 5.45% (95% CI 1.26% - 10.5%) and 3.56% (95% CI 1.26% - 10.5%) of the observed quinine concentration above and below the 90% prediction interval, respectively. Eta shrinkages for absorption rate constant, elimination clearance, central apparent distribution volume, peripheral apparent distribution volume, bioavailability (IIV) and bioavailability (IOV) were 14.0%, 27.1%, 39.4 %, 33.6%, 30.2% and 25.5%-84.5%, respectively. Epsilon shrinkage was 20.1%. High relative standard errors for parameter estimates of inter-compartmental clearance (44.6%) and apparent peripheral distribution volume (29.1%) were observed (Table 3.2).

The bootstrap diagnostics of the full covariate approach (Figure 3.3) showed a substantial effect of estimated gestational age on elimination clearance (1.73% median change per week age of gestation) but no significant effects on other parameters. This would result in 41.5% higher clearance for a patient in week 37 of pregnancy compared to a patient in week 13 of pregnancy. Similar trends were observed in the parameter distributions calculated for women in their second and third trimester (data not shown).

3.3.2 Simulations

Simulations showed substantially higher exposures during the acute phase of the disease in patients with a high admission body temperature and total parasite biomass load compared to patients with a lower admission body temperature and total parasite biomass (Figure 3.4 and 3.5). Simulated median quinine exposures during the first 8 hours of treatment were 29.2, 36.5, 43.7, 51.1 and 57.6 mg/L×hr for patients with a total parasite biomass of 10^7, 10^8, 10^9, 10^{10} and 10^{11},

Table 3.2. Population pharmacokinetic parameter estimates from the final quinine model.

Parameter	Population estimate [a] (% RSE) [b]	95% CI [b]	IIV/IOV [%CV] [a] (% RSE) [b]	95% CI [b]
k_a (1/hr)	0.817 (18.8)	0.479-1.03	58.7 (32.7)	40.5-107
CL/F (L/hr)	10.4 (4.36)	9.51-11.4	7.69 (65.4)	1.16-47.4
V_C/F (L)	174 (14.0)	112-195	-	-
F (%)	100 % (fixed)	-	12.3 (77.0)/21.4 (48.8)	0.170-48.8/19.3-93.3
Q/F (L/hr)	10.7 (44.6)	7.06-36.9	-	-
V_P/F (L)	54.3 (29.1)	33.6-112	70.8 (65.3)	8.00-128
Parasitaemia on F (%)	38.9 (9.33)	32.4-47.2	-	-
Temperature on CL/F (%)	-24.3 (21.1)	(-42.7)-(- 18.0)	-	-
Additive error	0.016 (41.6)	11.4-41.0	-	-
Post-hoc estimates [c]	all patients	second trimester	third trimester	
$AUC_{0\text{-}8\ hr.}$ (hr*mg/L)	26.6 (16.0-53.2)	26.2 (16.3-43.8)	27.7 (16.0-53.2)	
$AUC_{0\text{-}12\ hr.}$ (hr*mg/L)	36.9 (24.0-49.7)	36.7 (26.8-49.7)	36.9 (24.0-45.3)	
C_{MAX} (mg/L)	4.06 (2.40-7.92)	3.95 (2.54-6.62)	4.16 (2.40-7.92)	
T_{MAX} (hr)	3.01 (1.85-8.00)	3.01 (2.00-8.00)	2.75 (1.85-4.34)	
$T_{1/2}$ (hr)	15.3 (10.4-30.8)	14.6 (11.0-29. 3)	16.1 (10.4-30.8)	
CL/F (L/hr/kg)	0.188 (0.113-0.247)	0.196 (0.149-0.238)	0.181 (0.113-0.247)	
V_{SS}/F (L/kg)	4.05 (3.53-5.68)	4.07 (3.53-5.68)	4.02 (3.62-5.08)	

[a] Population mean and inter-individual variability (IIV; presented as 100* ((mean variance estimate)-1)1/2) estimates by NONMEM.
[b] The relative standard error (RSE) is calculated as 100*(standard deviation/mean value) from 1,000 runs of a non-parametric bootstrap. The 95% confidence interval (95% CI) is displayed as the 2.5 to 97.5 percentile of the bootstrap estimates
[c] Post-hoc estimates were calculated as the median and ranges of the empirical bayes estimates
k_a: absorption rate constant, *CL/F*: elimination clearance, V_C/F: central apparent volume of distribution, *Q/F*: inter compartmental clearance, V_P/F; peripheral apparent volume of distribution, F: relative bioavailability, *AUC*: area under the plasma concentration-time curve, C_{MAX}: maximum concentration after the last dose, T_{MAX}: Time to maximum concentration, $T_{1/2}$: elimination half-life and V_{SS}: sum of the posthoc apparent central and peripheral volume estimates. All clearance and volume parameters are centralised around median body weight of the study population using allometry.

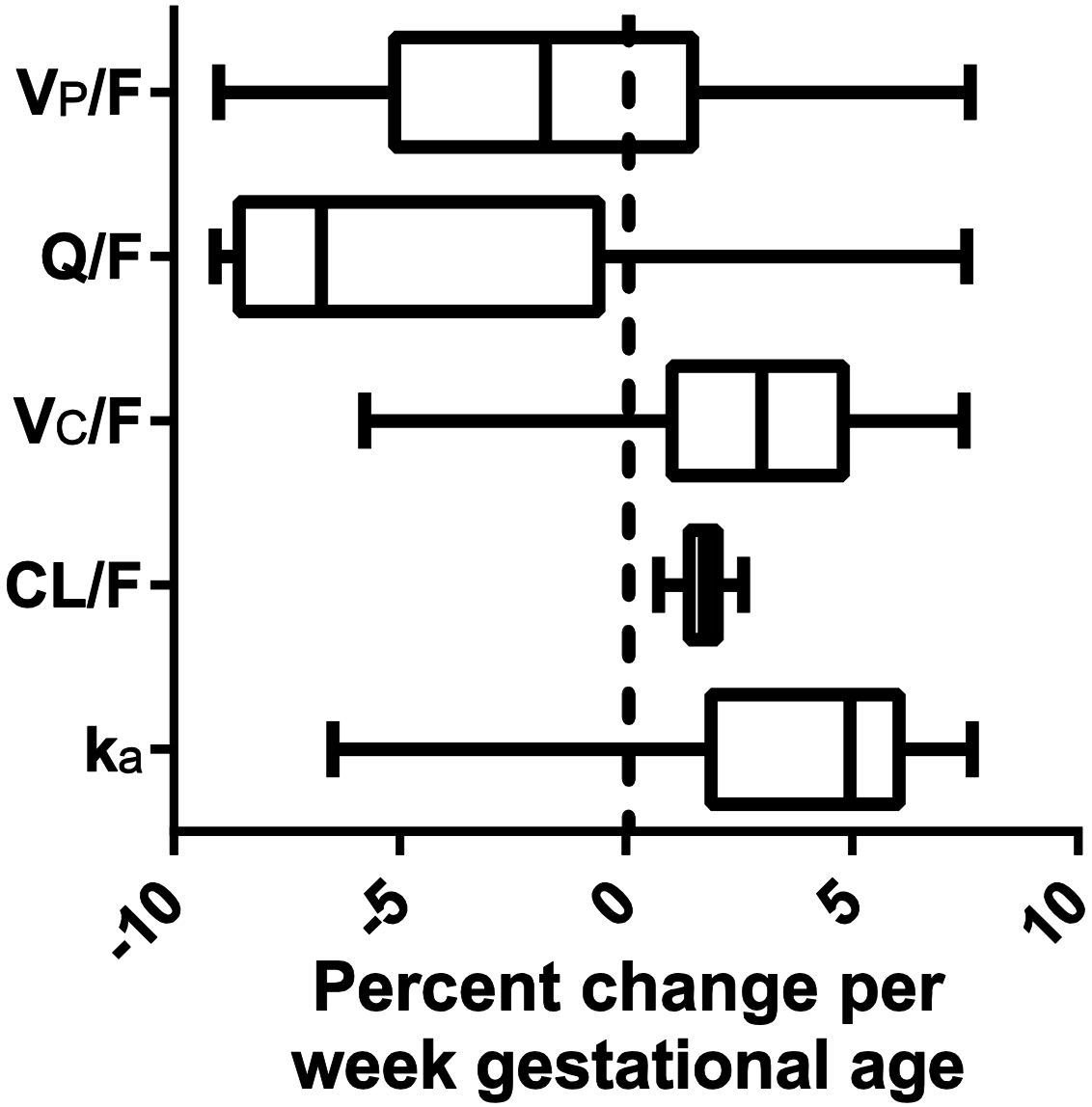

Figure 3.3 Box and whisker plot visualising the effect of estimated gestational age on pharmacokinetic parameters from 200 bootstraps of the full covariate approach (boxes represent 25%-75% and whiskers represent 2.5%-97.5%). Absorption rate constant (K_a) , elimination clearance (CL/F), apparent volume of distribution central compartment (V_2/F), inter-compartmental clearance (Q/F) and apparent volume of distribution peripheral compartment (V_3/F).

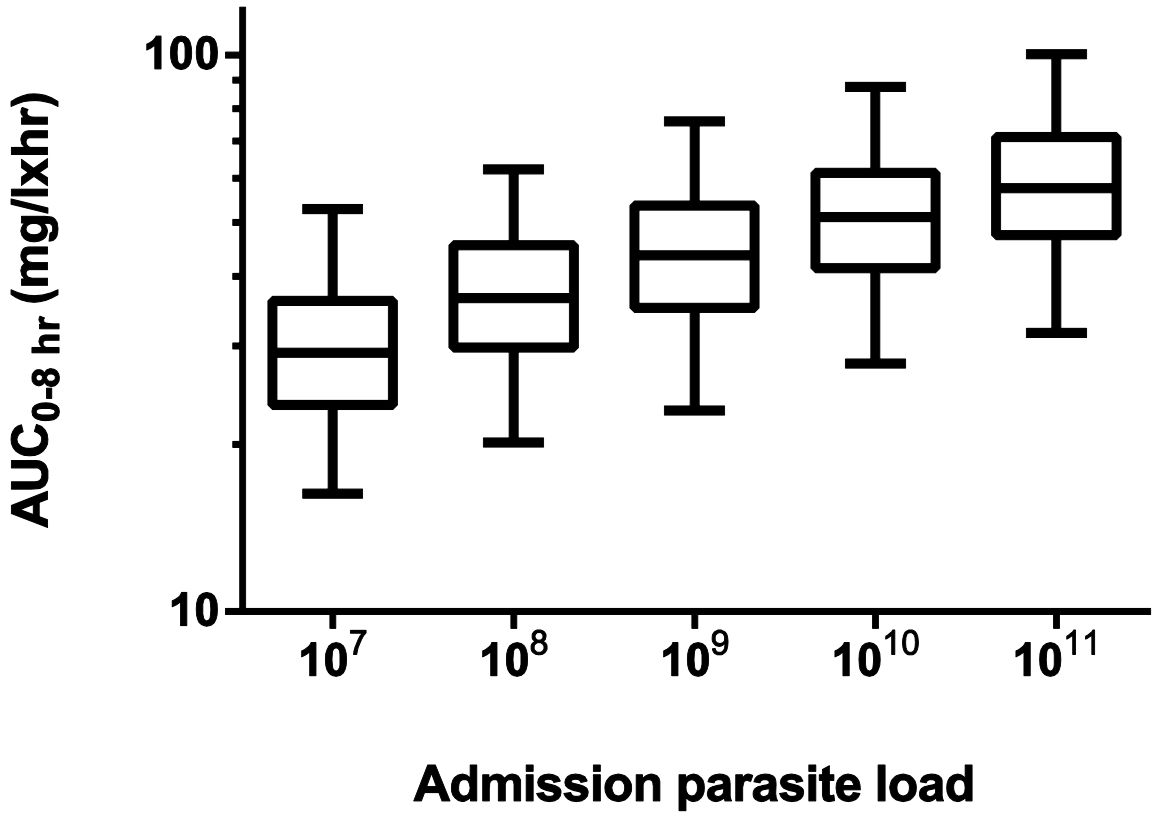

Figure 3.4 Simulated (n=1,000) first dose-exposure ($AUC_{0\text{-}8\ hr}$) after 560 mg quinine sulphate administered to a typical patient (weighting 56 kg with a body temperature of 37.1°C) at a total parasite load of 10^7, 10^8, 10^9, 10^{10} and 10^{11}. Data is represented by box and whiskers plots (boxes represent 25%-75% and whiskers represent 2.5%-97.5%).

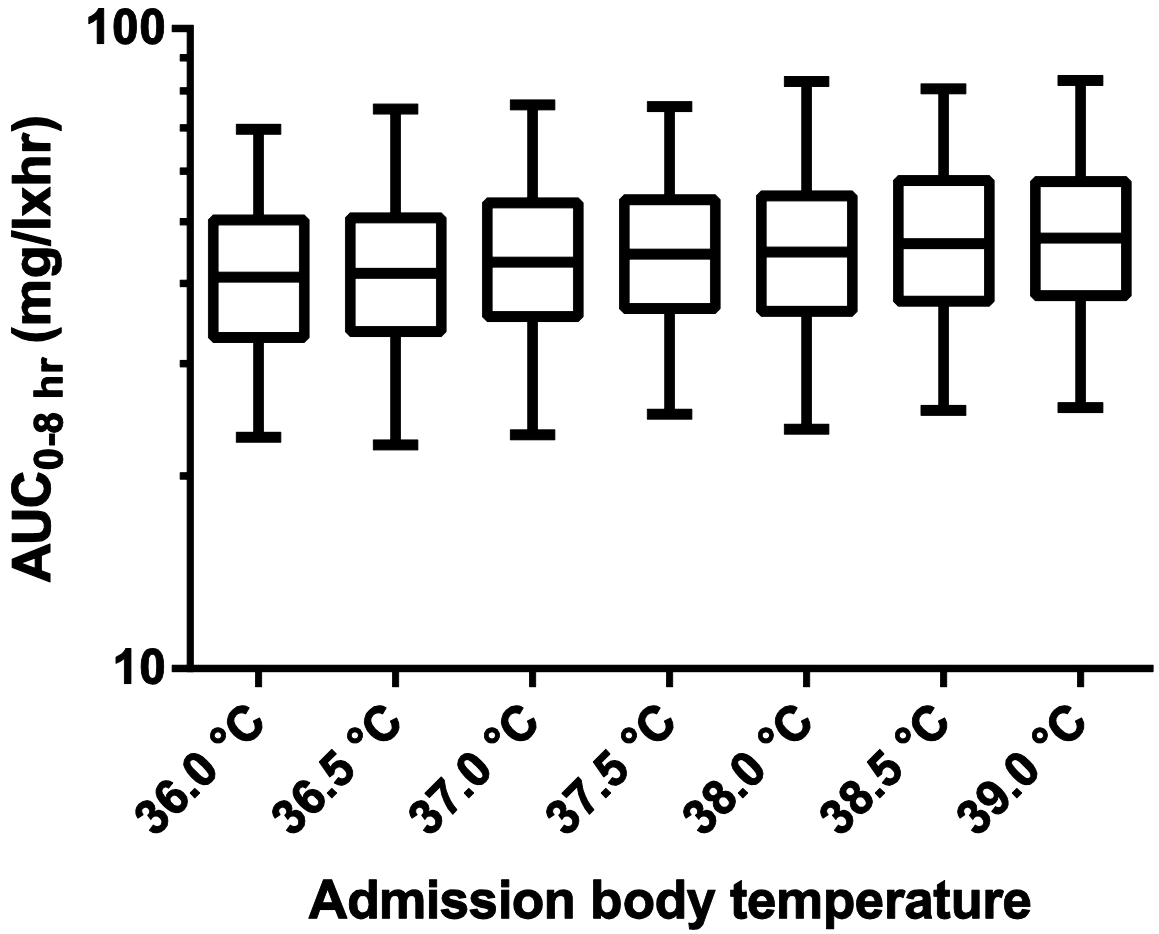

Figure 3.5 Simulated (n=1,000) first dose-exposure ($AUC_{0\text{-}8\ hr}$) after 560 mg quinine sulphate administered to a typical patients (weighting 56 kg and with a 12.1^9 total parasite biomass) with admission body temperatures ranging between 36 °C and 39 °C. Data is represented by box and whiskers plots (boxes represent 25%-75% and whiskers represent 2.5%-97.5%).

respectively. Quinine exposures during the first 8 hours of treatment increased with admission body temperature (Figure 3.5) at an average of 2.05 mg/L×hr per degree Celsius increase between 36°C and 39.0°C.

3.4 Discussion

Quinine is still an important antimalarial drug but the therapeutic window for the unbound drug is relatively narrow. Minor adverse effects such as tinnitus, dysphoria, and nausea (cinchonism) are common and hypoglycaemia is a particular problem in later pregnancy [132-134]. Despite intensive use, only limited information on quinine pharmacokinetics in pregnant women is available [109, 110]. In this study conducted in pregnant Ugandan women, oral quinine data were analysed using a population pharmacokinetic approach.

The best performing disposition model consisted of two distribution compartments. Both one [125, 135] and two [126] disposition models have been used previously to describe oral and intramuscular quinine pharmacokinetics. Differences between published disposition models might be caused by different sampling schedules. A first-order absorption model best described quinine absorption and more complex absorption models (i.e. first-order with lag-time and transit absorption) did not improve the model fit due to a lack of data in the absorption phase.

Body weight was implemented on clearance and apparent volume parameters using allometry, which has been shown in previous studies modelling antimalarial drugs [82, 89, 125]. A power coefficient of 2/3 on clearance parameters realised

a bigger drop in objective function compared to 3/4, which is in good agreement with observed physiology since clearance does not normally scale linearly with body weight [99].

Malaria affects the pharmacokinetic properties of quinine resulting in higher exposures during the acute phase of the disease in proportion to disease severity, but this has not been implemented previously with a modelling approach for quinine [124, 130, 131, 136]. The increase in quinine exposure with increasing disease severity is likely to be caused by increased alpha-1-acid-glycoprotein concentrations [129]. A time-varying covariate relation between parasitaemia and bioavailability was used to describe part of the disease effect in the current study. Parasitaemia was a significant covariate on bioavailability and resulted in a 50.7% higher exposure in a typical patient with a total parasite biomass of 10^{11} compared to 10^{7} parasites. As a consequence of the time varying aspect, exposure was only affected during the acute phase when parasitaemia was above the limit of detection. Parasite slides were taken only once daily but the exact time was not reported. The last observed parasite count was therefore carried forward and implemented as having a direct effect on quinine bioavailability. More complex models (i.e. interpolation of the parasite counts or a parasite disease model) were evaluated during the model building process but did not contribute to an improvement of the predictive power of the model based on the current data. It is possible that more frequent parasite counts and more accurate sampling times could have enabled a more mechanistic disease model.

A static covariate relation between admission body temperature and elimination clearance described the other part of the disease effect in the current study. Admission body-temperature was a significant covariate on elimination clearance and resulted in an approximately 15% higher quinine exposure across during the first 8 hours of treatment in patients with an admission body temperature of 39°C compared to 36°C. A time restriction to the first 24 or 48 hours for the covariate-parameter relationship admission body temperature-elimination clearance resulted in a significantly worse model (ΔOFV=16.1 and ΔOFV=18.7, respectively). This indicates that disease severity reflected by admission body temperature during the acute phase still influence quinine pharmacokinetics during the entire 7 day treatment. Elevated acute phase protein levels of alpha-1-acid-glycoprotein can last for up to three weeks after complete resolution of malaria infection [129] and it is possible that both admission body-temperature and parasitaemia serve as descriptors for alpha-1-acid-glycoprotein in this analysis.

Estimated gestational age was a significant covariate on the bioavailability of quinine in the forward addition of covariates ($p<0.05$) but this covariate could not be retained in the backward step ($p<0.001$). However, estimated gestational age resulted in a substantial increase in elimination clearance in the full covariate approach (Figure 3.4). This would result in decreased quinine exposures with increased estimated gestational age. Quinine is extensively metabolised by CYP3A4 enzymes [137, 138] and both hepatic and intestinal CYP3A4 activities have been reported to be induced during pregnancy compared with post-partum

women [139, 140]. However, no difference in CYP3A4 activity has been reported between the second and third trimesters of pregnancy which would explain the lack of a covariate effect in this study [139]. A comparison of pharmacokinetic parameters between the current study and previous studies was not possible due to the different analysis techniques (non-linear mixed effect modelling vs non-compartmental analysis) and routes of administration (oral vs intravenous). A study on the pregnancy effect during the first, second and third trimester using a non-pregnant control group with a sufficient sample size is therefore needed to enable an assessment of the impact of pregnancy as a categorical covariate.

The final model was validated using a variety of diagnostic tools (goodness-of-fit plots, visual predictive checks, numerical predictive checks, bootstrap statistics and shrinkage calculations). Simulation-based predictive checks of the final model resulted in a high predictive power with numerical values close to the theoretical values (i.e. 10% of observations outside the 90% prediction interval). Confidence intervals of simulated 5^{th}, 50^{th} and 95^{th} percentiles were large in the visual predictive check (Figure 3.2). However, this is not an uncommon phenomenon in studies with relative small sample sizes [141]. High relative standard errors on certain structural parameters and relatively high shrinkage values might also have been on account of a relatively small sample size and the sampling design. Caution is therefore warranted if the presented final model should be used for dose optimisation. Secondary parameter estimates (Table 3.2) and the performed simulations (Figures 3.4 and 3.5) should also be interpreted with caution since a relatively high shrinkage might under-estimate

the variability of these parameters. However, the median values are not likely to be affected by shrinkage and show accurately the important differences during the recovery from the disease in pregnant women.

3.5 Conclusion

The population pharmacokinetic properties of quinine in this study were described best by a first-order absorption with two distribution compartments. Pregnancy related covariates such as estimated gestational age or trimester did not affect the pharmacokinetics of quinine significantly. However, a non-significant trend of increased elimination clearance with trimester was observed. Quinine exposure was proportional to parasite density and increased by 50.7% in a typical patient with a total parasite biomass of 10^{11} compared to 10^{7} and the quinine exposure during the first 8 hours of treatment was 15% higher in patients with admission body temperature of 39°C compared to 36°C. A larger study with a non-pregnant control group is needed to quantify the effects of pregnancy on quinine pharmacokinetics and to assess the clinical implications of such alterations.

4.0 Artesunate-dihydroartemisinin

4.1 Background

Oral artesunate co-administered with amodiaquine, mefloquine, piperaquine or sulfadoxine-pyrimethamine is recommended by the WHO as first line treatment for uncomplicated *Plasmodium falciparum* malaria and it is even used for treatment during the second and third trimester of pregnancy [41]. The recommended artesunate dose for oral artesunate combinations is 4 mg/kg/day for three days.

Malaria alters the pharmacokinetic properties of dihydroartemisinin after oral artesunate administration because the illness reduces first-pass metabolism resulting in increased systemic exposures during the acute phase of malaria compared to convalescence (>5 days after treatment initiation) and healthy volunteers [142-145].Pregnant women [66] are especially vulnerable to malaria infections due to a modulated immune system. Furthermore, several physiological changes occur during pregnancy, potentially resulting in altered pharmacokinetics of administered drugs. For example, changed CYP450 enzyme and UGT activities may affect elimination clearance. Decreased gut motility may affect the drug absorption and increased plasma volume, water content and fat content may affect the distribution of the drug [90-92]. Altered pharmacokinetics might result in lower drug exposures with potentially lowered treatment efficacy and an increased risk of the development of drug resistance. For example, pregnant patients from Congo had increased dihydroartemisinin elimination clearance (1.39 L/kg/h) compared to post-partum healthy volunteers (1.26 L/kg/h) and non-pregnant patients (1.07 L/kg/h) after a single oral artesunate dose [146].

A population pharmacokinetic model on the same data showed a 42% increased dihydroartemisinin elimination clearance during pregnancy and suggests the exposure to be substantially decreased in pregnant women compared to non-pregnant patients [147].

4.1.1 Study aim

The aim of this study was to re-evaluate the pharmacokinetic properties of artesunate and dihydroartemisinin in pregnant patients with uncomplicated *Plasmodium falciparum* malaria on the Thailand-Myanmar border and compare these again post-partum [145] using a simultaneous population pharmacokinetic drug-metabolite modelling approach. Non-compartmental analysis has been published previously [145] and showed significant differences between pregnant malaria patients and post-partum healthy volunteers. However, a model-independent analysis could not dissect and quantify the individual contributions of disease and pregnancy to the altered pharmacokinetics.

4.1.2 Absorption

The absolute oral bioavailability of artesunate and dihydroartemisinin in uncomplicated malaria patients is 9.9-22% and 73-82%, respectively [145, 148]. Artesunate C_{MAX} after oral administration is not substantially different in uncomplicated malaria patients (54.6 [12.8-113] ng/mL/mg/kg) compared to healthy volunteers (42.7 [16.5-120] ng/mL/mg/kg) [81, 142-146, 148-166]. Similarly, dihydroartemisinin C_{MAX} values after oral artesunate administration are not substantially different between uncomplicated malaria patients (362 [84.8-

690] ng/mL/mg/kg) and healthy volunteers (286 [51.4-575] ng/mL/mg/kg) [81, 142-146, 148-166].

Artesunate absorption can be affected by several factors. Concomitant intake with a high fat/calorie meal results in a reduced absorption rate what may delay the onset of the antimalarial effect [167]. Different generic oral formulations have shown some variability in absorption profiles, most likely on account of differences in preparation [153]. A fixed dose formulation of artesunate-mefloquine and a loose oral formulation gave similar pharmacokinetic profiles of dihydroartemisinin [159].

4.1.3 Distribution

Both, artesunate and dihydroartemisinin distribution pharmacokinetics have been described by two-compartment disposition models after intravenous administration [168, 169]. The brief distribution phase is masked by the absorption phase after extravascular administration. Thus, the disposition pharmacokinetics of artesunate and dihydroartemisinin after oral artesunate has been described adequately by a one-compartment disposition model [147, 167].

4.1.4 Metabolism and elimination

Oral artesunate is completely metabolised into dihydroartemisinin by rapid and extensive hydrolysis of artesunate at gastric pH [170], CYP2A6 [171] and esterases in the blood [170]. The apparent elimination half-life of artesunate varies depending on route of administration. After intravenous administration, the elimination half-life of artesunate is fastest at 0.19 (0.043-0.24) and 0.063 (0.037-

0.22) hour in healthy volunteers and uncomplicated malaria patients, respectively [81, 142-146, 148-166]. The elimination half-life of artesunate is longer after oral (volunteers: 0.49 [0.24-1.1] hour uncomplicated malaria patients: 0.499 [0.35-1.2] hour), administration reflecting absorption limited “flip-flop” pharmacokinetics (Table 1 & 2). Dihydroartemisinin elimination half-life estimates after different administration routes are less affected, and is similar in all patient groups (intravenous volunteers: 1.34 [0.783-2.37] hour intravenous uncomplicated: 0.720 [0.300-1.07] hour oral volunteers: 1.14 [0.550-3.20] hour oral uncomplicated: 0.882 [0.640-1.41] hour) [81, 142-146, 148-166].

4.2 Study design

This study was conducted on the North Western border of Thailand in the clinics of the Shoklo Malaria Research Unit from April 2008 until March 2009. The pregnant patients were screened for malaria (via an antenatal clinic programme) using blood smears on a weekly basis. Pregnant women in the second and third trimester with acute uncomplicated *falciparum* malaria and haematocrit values not lower than 25% were enrolled in the study if written informed consent was given. Post-partum women were followed monthly and the 3 months post-partum visit was postponed in case of malaria detection or any other illness.

Patients were allocated as moderately unwell if plasma creatinine, blood urea nitrogen or liver function tests, including bilirubin (total or direct), aspartate aminotransferase or alanine aminotransferase were raised (25th percentile) or if patients had fever (>37.5°C) and tachycardia (>100 beats min-1). The patients

were classified as mildly unwell if none of the above conditions were met. The disease count status was calculated as the sum of the criteria used for mildly/moderately unwell allocation

Ethical approval for the pharmacokinetic study was obtained from the Faculty of Tropical Medicine, Mahidol University Ethics Committee (TM-IR 029/2005) and Oxford Tropical Research ethics Committee (OXTREC 007-05).

4.2.1 Dosing regimen and blood sampling

Patients were assigned to either group 1 or 2 and all drug intakes were done under supervision. Group 1 received 4 mg/kg intravenous artesunate on admission followed by 4 mg/kg oral artesunate for the consecutive 6 days. Group 2 received 4 mg/kg oral artesunate on admission, 4 mg/kg intravenous artesunate on day 2 followed by 4 mg/kg oral artesunate for the consecutive 5 days. The same women were followed-up monthly for 3 months during the post-partum period before receiving the exact same dose regimen and sample schedule as during the pregnant period. Intravenous and oral artesunate was manufactured by the Guilin Pharmaceutical Factory, Guangxi in China and repackaged in Thailand by Atlantic Pharmaceuticals.

Venous blood samples (2 mL) were drawn on day 1 and on day 2 at 0, 5, 15, 30, 60, 120, 180, 240 and 360 minutes or 0, 15, 30, 60, 90, 120, 180, 280 and 360 minutes after intravenous or oral administration, respectively. Additional venous blood samples were also drawn on day 7 at 0, 60, 120 and 240 minutes after dose in all patients.

4.2.2 Drug analysis

Samples were collected in pre-chilled tubes containing sodium fluoride/potassium oxalate as anticoagulant. Samples were inverted 5 to 6 times and stored on wet ice until centrifugation at 2,000 g for 7 min at 4 °C. Plasma samples were stored in liquid nitrogen until transfer to -80 °C for storage. After completion of the study, all samples were transferred on dry ice to the Department of Clinical Pharmacology, Bangkok, Thailand.

Artesunate and dihydroartemisinin was quantified using liquid chromatography-tandem mass-spectroscopy. The coefficient of variation of the assay was less than 8% at each level of quality control samples and the limit of quantification was set to 1.2 ng/mL and 2 ng/mL for artesunate and dihydroartemisinin, respectively [172].

4.3 Results

Twenty pregnant women with uncomplicated falciparum were enrolled in the study and 15 women returned 3 months later as post-partum healthy volunteers (Table 4.1). Full non-compartmental analysis results are presented in full elsewhere [145].

A nonlinear mixed-effects model consisting of a flexible transit absorption model (6 transit compartments; ΔOFV=-82.7) with first-pass metabolism of artesunate into dihydroartemisinin (ΔOFV=-41.5) described the absorption phase well. A structural two-compartment disposition model for both artesunate and

Table 4.1: Demographic summary of the study population		
	Pregnant	Post-partum
Number of patients	20	15
Total artesunate dose (mg/kg)	27.9 (26.8-28.6)	27.4 (4.08-29.0)
Total number of samples	920	651
Sample size (samples/patient)	46 (46-46)	45 (17-47)
Admission covariates		
Bodyweight (kg)	48.0 (40.0-64.0)	46.0 (37.0-52.0)
Height (cm)	154 (143-161)	153 (148-161)
Age (years)	27 (17-40)	27 (17-40)
Parasitaemia (parasites/μL)	4,390 (109-63,600)	-
Body temperature (°C)	37.6 (36.0-40.0)	37.0 (36.2-37.5)
Number of fever days	2 (0-7)	-
Pulse (beats/minute)	94 (75-113)	80 (64-96)
Systolic blood pressure (mmHg)	100 (90-120)	110 (90-160)
Diastolic blood pressure (mmHg)	60 (50-70)	70 (60-100)
Mildy/moderately unwell (n)	7/13	-
Smoker/non-smoker (n)	4/16	4/11
Second/third trimester (n)	10/10	-
Estimated gestational age (weeks)	25.7 (14.0-38.0)	-
Number of pregnancies	3 (1-8)	-
Number of deliveries	1 (0-6)	-
Days after delivery	-	100 (84-264)

Values are presented as median (range)

dihydroartemisinin (ΔOFV=-590) provided a satisfactory fit to the data (Figure 4.1). Inter-individual variability could not be estimated for first-pass metabolism of artesunate, artesunate elimination clearance, central distribution volume of artesunate and peripheral distribution volume of dihydroartemisinin (Table 4.2). Inter-occasion variability could only be estimated for the first- pass metabolism of artesunate and residual variability was best described using an additive error model on the log-transformed data (Table 4.2).

Bodyweight was implemented using allometry on all clearance (power fixed to 3/4) and volume parameters (power fixed to 1) (ΔOFV=-1.49). Disease effect as a categorical covariate on bioavailability during day 1 and 2 of the study (ΔOFV=-66.4) was superior over all other combinations of categorical disease effect, disease status effect or disease count effect on bioavailability, first-pass artesunate metabolism, artesunate or dihydroartemisinin elimination clearance. Pregnancy as a categorical covariate on dihydroartemisinin elimination clearance (ΔOFV=-45.1) was superior over all other combinations of pregnancy as categorical covariate, trimester or estimated gestational age on bioavailability, first-pass artesunate metabolism, artesunate or dihydroartemisinin elimination clearance. Pregnancy as an additional categorical covariate on absolute oral bioavailability had a significant effect (ΔOFV=-6.06) in the forward step during covariate model building but could not be retained during the backward step ($p \leq 0.01$).

Basic goodness of fit plots did not indicate model misspecification (Figure 4.2) and the visual predictive check (Figure 4.3) indicate an adequate predictive

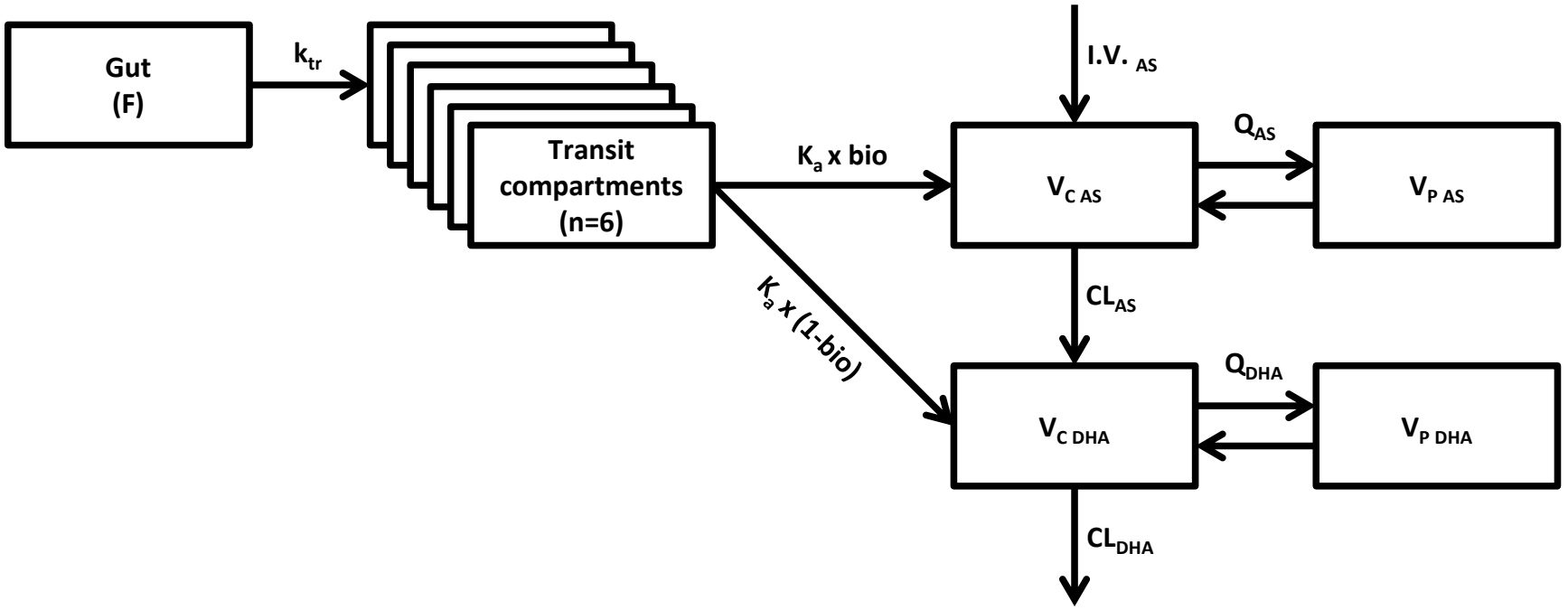

Figure 4.1 Visual representation of the simultaneous population pharmacokinetic artesunate-dihydroartemisinin model. AS: artesunate, DHA: dihydroartemisinin, F: Bio-availability, k_{tr}: transit rate constant, k_a: absorption rate constant, bio: fraction absorbed as AS, I.V.: Intra-Venous administration, V_C: apparent volume of distribution central compartment, V_P: apparent volume of distribution peripheral compartment, Q: inter-compartmental clearance, and CL: elimination clearance.

Table 4.2: Population pharmacokinetic parameter estimates from the final simultaneous artesunate-dihydroartemisinin model

Parameters	Population estimates [a] (%RSE) [b]	IIV/IOV * [%CV] [a] (%RSE) [b]
F (%)	40.6 (5.36)	28.2 (23.0)
BIO (%)	25.0 (19.3)	69.1 (47.8)/34.7 (41.3)
MTT (hour)	0.34 (10.0)	34.4 (16.5)
Transit compartments (n)	6 (fixed)	-
DUR (hour)	0.0167 (fixed)	-
$k_{a\ ART}$ (hr^{-1})	1.59 (9.39)	10.8 (62.3)
$V_{C\ ART}$ (L)	9.64 (11.1)	-
$Q_{\ ART}$ (L/hr)	6.69 (15.6)	8.8 (28.7)
$V_{P\ ART}$ (L)	2.23 (18.3)	64.3 (12.0)
$CL_{\ ART}$ (L/hr)	188 (9.83)	-
$V_{C\ DHA}$ (L)	57.9 (6.39)	6.35 (20.8)
$Q_{\ DHA}$ (L/hr)	5.14 (30.3)	7.91 (51.0)
$V_{P\ DHA}$ (L)	18.5 (53.1)	-
$CL_{\ DHA}$ (L/hr)	49.8 (5.43)	8.18 (19.4)
Disease effect on F	90.3 (20.3)	-
Pregnancy effect on $CL_{\ DHA}$	27.2 (27.5)	-
$\sigma_{\ ARS}$	1.26 (7.06)	-
$\sigma_{\ DHA}$	0.44 (7.49)	-

[a] Population mean values, Inter-Occasion Variability (IOV) and Inter-Individual variability (IIV) estimated by NONMEM. IIV is presented as coefficient of variation (%CV) and calculated as $100 \text{ x } \sqrt{e^{\text{estimate}} - 1}$.

[b] The Relative Standard Error (RSE) is calculated as $100 \text{ x } \frac{\text{standard deviation}}{\text{mean parameter estimate}}$ from 99 (out of a total of 100) iterations of a non-parametric bootstrap.

[*] Inter Occasion Variability

F: absolute oral bio-availability of artesunate, BIO: first-pass artesunate metabolism, MTT: mean transit time, DUR: infusion duration, k_a: absorption rate constant, V_C: apparent volume central compartment, Q: inter-compartmental clearance, V_P: apparent volume peripheral compartment and CL: elimination clearance. All parameters are centralised around the median bodyweight for pregnant and post-partum women from the study population.

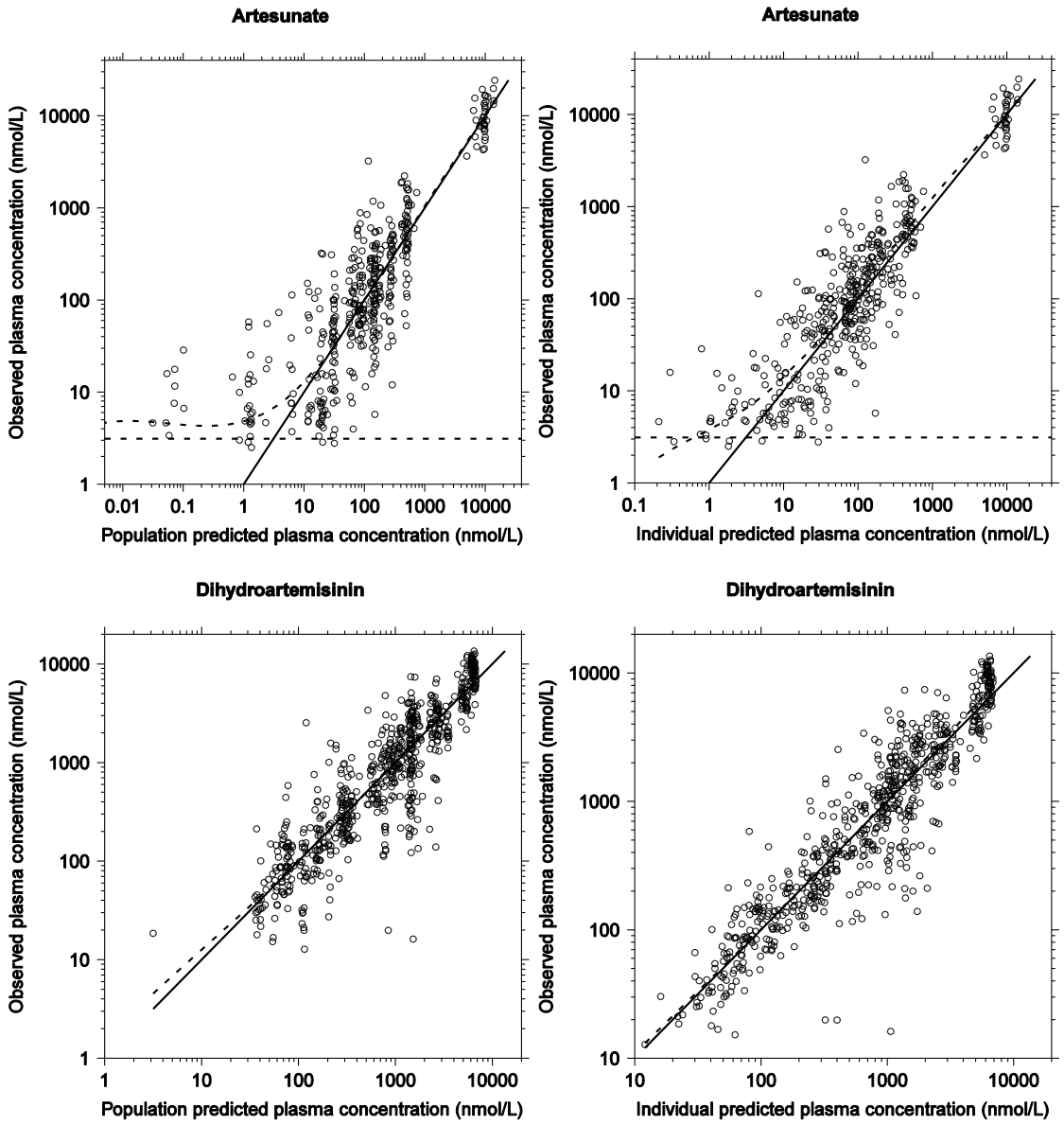

Figure 4.2 Basic goodness-of-fit plots from the final simultaneous artesunate-dihydroartemisinin model. The line of identity is represented by the black solid line and the trend line (Local Polynomial Regression Fitting using 50 evaluations) is represented by the black dashed line.

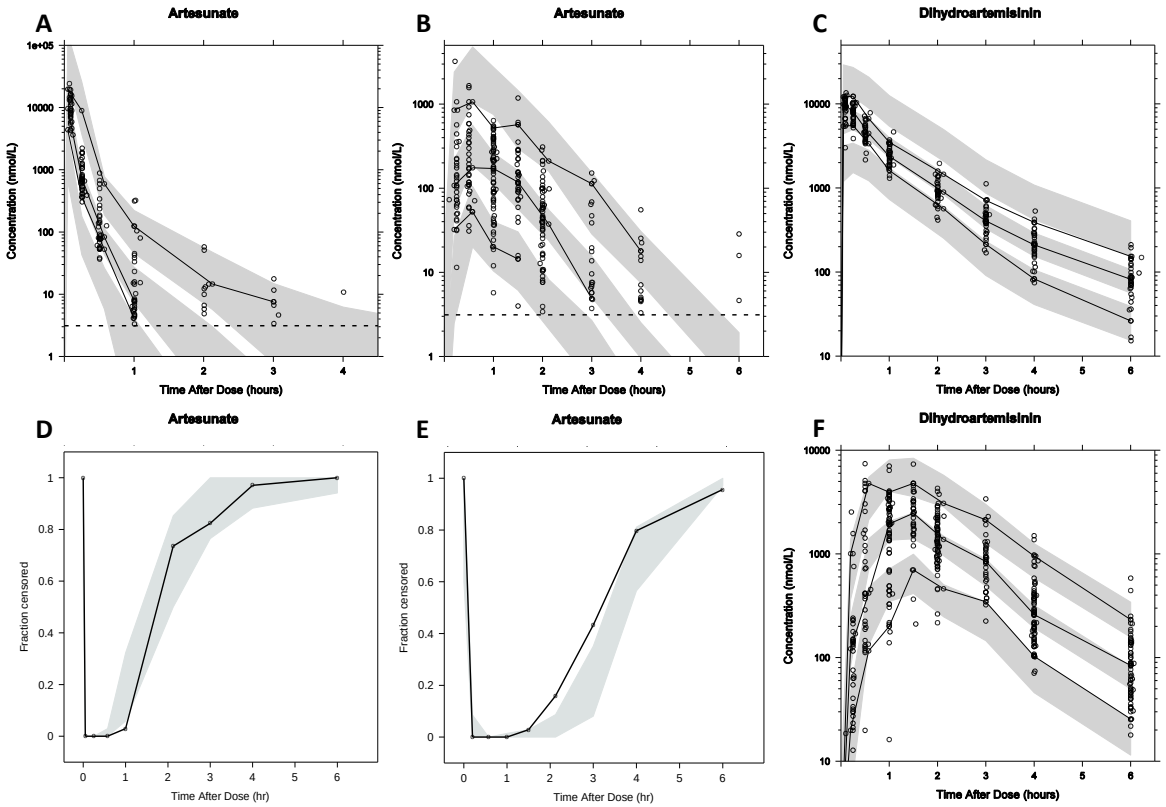

Figure 4.3 Visual predictive checks for intravenous and oral artesunate (A & B) and dihydroartemisinin (C & F) data. The dots represent the observed plasma concentration data, the black solid line represents the 5th, 50th and 95th percentile of the observed plasma concentration data and the grey shaded areas represent the confidence interval of the simulated (n=2,000) 5th, 50th and 95th percentiles. Panel D and E represent the visual predictive check for censored artesunate data. The black solid line represents the observed fraction of plasma samples below quantification limit and the grey shaded area represents the confidence interval of the simulated (n=2,000) fraction plasma samples below quantification limit.

power of the final model of oral data. The visual predictive check for intravenous artesunate displays an acceptable predictive power (Figure 4.3A) but the variability on intravenous dihydroartemisinin was overestimated (Figure 4.3C). The M3-method was used to avoid bias in parameter estimates on account of a high percentage of artesunate data below the limit of quantification (>45%) [97]. Figure 4.3 shows satisfactory model predictions of the fraction of censored data.

Eta- and epsilon-shrinkages were calculated to determine the reliability of the individual parameter estimates and diagnostic plots. Epsilon-shrinkage was 8.56% for artesunate and 5.42% for dihydroartemisinin. Eta shrinkages were 37.4%, 12.9%, 64.4%, 87.6%, 2.97%, 11.0%, 69.0%, 85.5%, 23.0%, and 22.8-52.1% for F, MTT, $k_{a\ ART}$, Q_{ART}, $V_{P\ ART}$, $k_{a\ DHA}$, $V_{C\ DHA}$, Q_{DHA}, $V_{P\ DHA}$, CL_{DHA} and BIO (inter-occasion variability), respectively.

Simulations and post-hoc estimates, using the final model, displayed altered artesunate and dihydroartemisinin exposures on account of both disease and pregnancy (Figure 4.4 and Table 4.3). Higher median artesunate and dihydroartemisinin exposures were observed during the acute malaria phase (F_{ART}: 21.6% and F_{DHA}: 79.9%) compared to both the convalescence phase (F_{ART}: 10.9% and F_{DHA}: 41.0%) and healthy status (F_{ART}: 12.5% and F_{DHA}: 40.9%) (Table 4.3). A lower dihydroartemisinin exposure was observed during pregnancy compared to the post-partum period (Figure 4.4B), and the decreased dihydroartemisinin exposure during pregnancy could be compensated by a 25% dose increase. This resulted in equal dihydroartemisinin exposures during

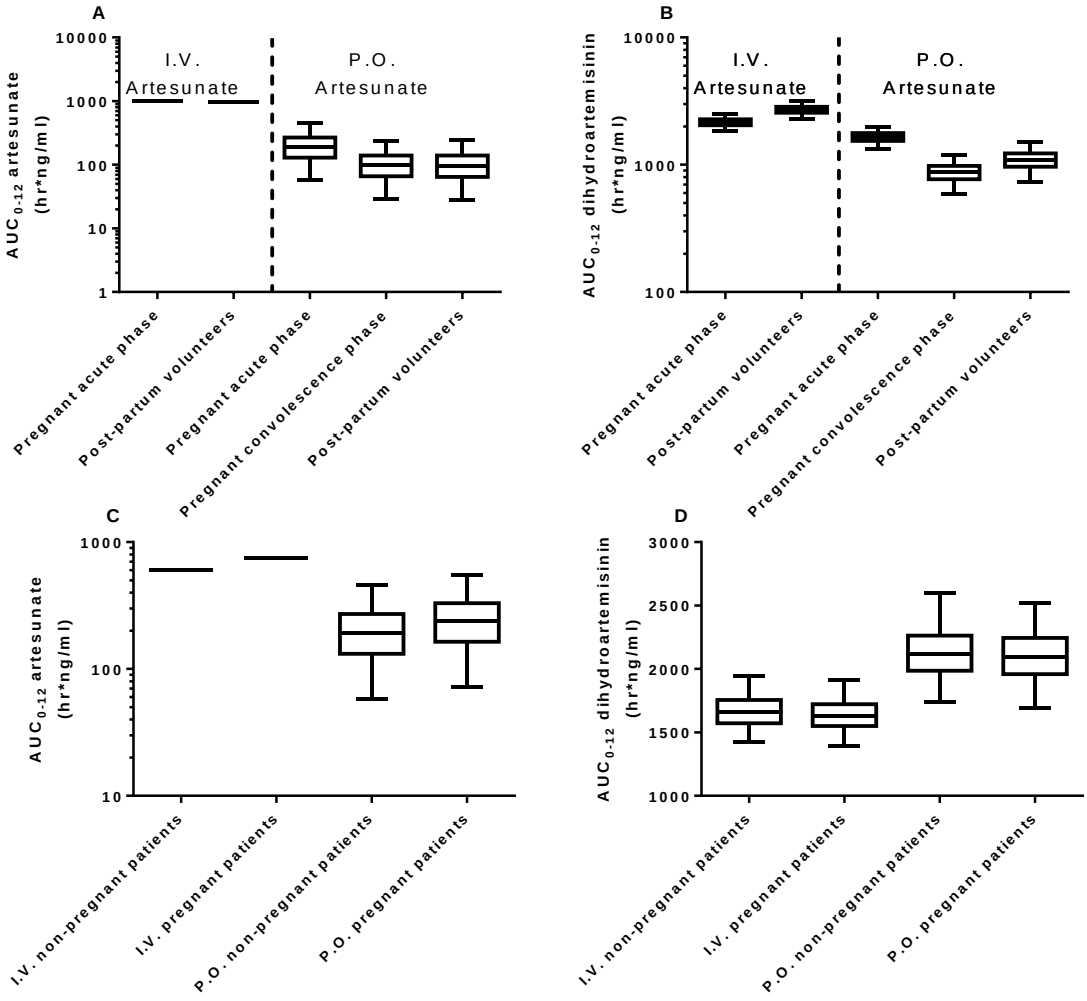

Figure 4.4 Artesunate and dihydroartemisinin simulated (2,000 simulations) $AUC_{0\text{-}6hr}$ using the simultaneous population pharmacokinetic artesunate-dihydroartemisinin model. Panel A & B represent the AUC characteristics after intravenous (4 mg/kg) and oral (4 mg/kg) dosing during the acute and convalescence malaria phase in pregnant patients (48 kg) and during the post-partum visit as healthy volunteers (46 kg). Panel C & D represent the artesunate and dihydroartemisinin AUC after intravenous (2.4 mg/kg) and oral (4 mg/kg) dosing in post-partum women (50 kg) and in pregnant women (50 kg) receiving a 25% increased dose. Results are presented using box and whiskers plots (boxes represent 25%-75% and whiskers represent 2.5%-97.5%).

Table 4.3: Summary of artesunate post-hoc parameter estimates from the simultaneous population pharmacokinetic artesunate-dihydroartemisinin model.

	Pregnant patients			Post-partum volunteers		
	Acute malaria (day 1 & 2)		Convalescent malaria (day 7)	Day 1 & 2		Day 7
	I.V.	P.O.	P.O.	I.V.	P.O.	P.O.
AUC_{0-12} (hrxng/mL)	989 (824-1070)	166 (74.5-242)	76.4 (34.3-129)	981 (939-1020)	79.1 (47.2-145)	83.7 (33.6-128)
C_{MAX} (ng/mL)	16200 (13500-16500)	160 (75.2-235)	78.9 (34.1-135)	16200 (16100-16400)	72.6 (46.9-153)	77.9 (33.4-133)
T_{MAX} (h)	-	0.594 (0.363-0.807)	0.595 (0.360-0.800)	-	0.600 (0.300-0.800)	0.600 (0.300-0.800)
$T_{1/2}$ (h)	0.199 (0.138-0.770)	0.199 (0.138-0.772)	0.199 (0.138-0.772)	0.253 (0.136-0.741)	0.235 (0.136-0.741)	0.253 (0.136-0.741)
CL (L/hr/kg)	4.04 (3.76-4.23)	23.8 (16.1-53.7)	51.6 (30.4-117)	4.08 (3.96-4.32)	50.1 (28.1-91.7)	46.6 (32.0-122)
V_{SS} (L/kg)	0.249 (0.237-0.361)	1.53 (1.03-4.55)	3.15 (1.91-7.66)	0.260 (0.237-0.360)	3.11 (1.69-6.08)	2.88 (1.88-8.06)
F (%)	-	17.1 (7.46-23.3)	7.91 (3.43-12.4)	-	8.29 (4.32-14.8)	8.91 (3.26-12.9)

Estimates were calculated as median values [range] from the empirical Bayes estimates. AUC_{0-12}: area under the plasma concentration curve from 0 to 12 hours after the dose, C_{MAX}: maximum plasma concentration, T_{MAX}: Time to reach maximum plasma concentration, $T_{1/2}$: elimination half-life, CL: elimination clearance after intravenous administration, V_{SS}: apparent volume of distribution at steady state after intravenous administration calculated as the sum of central and peripheral apparent volume of distribution and F: oral bioavailability. After oral administration elimination clearance and distribution volume at steady state are represented as CL/F and V_{SS}/F. P.O.: Per Oral and I.V.: Intravenous

pregnancy compared to post-partum volunteers but artesunate exposures were higher (Figure 4.4C & 4.4D). Furthermore, dihydroartemisinin exposure after intravenous dosing for severe malaria (2.4 mg/kg) was lower compared to that after standard oral dosing for uncomplicated malaria (4 mg/kg) although the opposite trend was observed for artesunate exposure (Figure 4.4C & 4.4D).

4.4 Discussion

Absolute oral bio-availability of artesunate and dihydroartemisinin, as well as disease and pregnancy effects have been evaluated previously, although in separate studies. Covariate effects in separate studies may be confounded on account of an overlap of disease and pregnancy status. A simultaneous analysis of the pregnancy and disease effect using a drug-metabolite model was therefore needed.

Disposition pharmacokinetics after intravenous administration were satisfactorily described using two distribution compartments. However, a one-compartment distribution model was adequate if only oral artesunate and dihydroartemisinin data were modelled. These findings were in agreement with previous studies [144, 147, 167, 169, 173, 174] and indicate that the distribution phase of artesunate and dihydroartemisinin is attenuated by the absorption phase after oral administration.

The first-pass conversion of artesunate into dihydroartemisinin was implemented in the model and improved the model fit significantly. The first-pass artesunate conversion can be physiologically explained by hepatic and intestinal CYP2A6

Table 4.4: Summary of dihydroartemisinin post-hoc parameter estimates from the simultaneous population pharmacokinetic artesunate-dihydroartemisinin model.

	Pregnant patients			Post-partum volunteers		
	Acute malaria (day 1 & 2)		Convalescent malaria (day 7)	Day 1 & 2	Day 7	Day 1 & 2
	I.V.	P.O.	P.O.	I.V.	P.O.	P.O.
AUC_{0-12} (hrxng/mL)	2180 (1810-2550)	1670 (1410-1950)	880 (669-11205)	2740 (2450-3060)	1110 (892-1440)	1080 (874-1440)
C_{MAX} (ng/mL)	1930 (1530-1960)	740 (592-848)	397 (283-482)	1970 (1860-2040)	416 (328-545)	409 (328-545)
T_{MAX} (h)	0.162 (0.154-0.179)	1.13 (0.940-1.44)	1.13 (0.940-1.43)	0.200 (0.0100-0.200)	1.20 (1.00-1.50)	1.25 (1.00-1.50)
$T_{1/2}$ (h)	2.77 (2.66-3.02)	2.77 (2.66-3.02)	2.77 (2.66-3.02)	2.86 (2.72-2.89)	2.86 (2.72-2.89)	2.86 (2.72-2.89)
CL (L/hr/kg)	1.35 (1.16-1.51)	1.77 (1.47-2.09)	3.33 (2.55-4.39)	1.07 (0.968-1.20)	2.61 (2.06-3.42)	2.66 (2.06-3.42)
V_{SS} (L/kg)	1.66 (1.61-1.72)	2.16 (1.99-2.38)	4.09 (3.51-5.05)	1.66 (1.61-1.72)	4.07 (3.51-5.05)	4.09 (3.51-5.05)
F (%)	-	77.3 (71.8-81.5)	40.7 (33.8-46.9)	-	40.8 (33.8-47.0)	40.5 (33.8-46.9)

Estimates were calculated as median values [range] from the empirical Bayes estimates. AUC_{0-12}: area under the plasma concentration curve from 0 to 12 hours after the dose, C_{MAX}: maximum plasma concentration, T_{MAX}: Time to reach maximum plasma concentration, $T_{1/2}$: elimination half-life, CL: elimination clearance after intravenous administration, V_{SS}: apparent volume of distribution at steady state after intravenous administration calculated as the sum of central and peripheral apparent volume of distribution and F: oral bioavailability. After oral administration elimination clearance and distribution volume at steady state are represented as CL/F and V_{SS}/F. P.O.: Per Oral and I.V.: Intravenous

activity. A liver compartment was also assessed in the model building process but did not converge. This was not unexpected due to the direct esterase activity in the blood, which cannot be captured adequately by the liver model.

Bodyweight was implemented on all clearance and volume parameters using allometry, to correct for the differences in bodyweight between the pregnant and post-partum group [82]. Subsequently, selected disease (categorical effect, mildly/moderately unwell or disease count status) and pregnancy (categorical effect, trimester as categorical effect or estimated gestational age) related covariates were tested on bio-availability, first-pass artesunate elimination, artesunate elimination clearance and dihydroartemisinin elimination clearance. A step-wise covariate model building procedure was not practically possible due to the complexity and consequently long run times of the model. Therefore, only physiologically plausible covariates were tested on parameters which could affect the systemic exposure of artesunate or dihydroartemisinin.

The increased exposure of artesunate and dihydroartemisinin during the acute malaria phase (90.3% increase in oral bioavailability) compared to the convalescence and post-partum volunteer phase might be on account of decreased esterase, CYP enzyme. A more speculative explanation may be decreased efflux transporter activity, as artesunate is a substrate for P-glycoprotein-mediated transport [175].

Dihydroartemisinin elimination clearance increased by 27.2% during pregnancy compared to the 3 month post-partum phase. An additional pregnancy effect on

absolute oral bioavailability (resulting in an approximately 20% lower artesunate exposure and 40% lower dihydroartemisinin exposure) was not statistically retained in the final model. This is likely to be a consequence of a relatively small sample size studied here. The results are in agreement with previous findings where dihydroartemisinin elimination clearance increased by 42.3% in pregnant women compared to a non-pregnant control group [147]. Similarly, the bio-availability decreased by 37.5% in pregnant women compared to a non-pregnant control group after oral dihydroartemisinin treatment [82]. The increased dihydroartemisinin elimination clearance is most likely a result of increased activity of UGT 1A4 and UGT 2B7 during pregnancy [91]. The increase in dihydroartemisinin elimination clearance in pregnant women resulted in a similar decrease in total drug exposure. This can subsequently result in an increased risk of treatment failure and it might accelerate the development of resistance.

Variability on the dihydroartemisinin data was over predicted. This was on account of the relatively large residual variability for dihydroartemisinin which was driven by the oral data. Separating the residual variability for oral and intravenous dihydroartemisinin data reduced the overprediction of intravenous dihydroartemisinin variability but caused model misspecification in the oral dihydroartemisinin and artesunate data. Considering the fact that *in-silico* dose optimisation are performed without residual variability, overprediction of intravenous dihydroartemisinin data was not considered to have clinical implications using this model as the general trend of the data was satisfactorily

predicted. Therefore, residual variability for intravenous and oral data was modelled simultaneously.

In-silico dose optimisation was performed, using the final model, to get an equal exposure of dihydroartemisinin during pregnancy compared to that in the post-partum control group. This might reduce treatment failures and decrease the risk of the development of resistance against artesunate-dihydroartemisinin. The simulation results indicate that a 25% increase in artesunate dose compensates for the 27.2% higher dihydroartemisinin elimination clearance during pregnancy. Artesunate pharmacokinetics was not affected by pregnancy, thus resulted in a 25% higher artesunate exposure during pregnancy compared to that in post-partum women when using the new dose regimen. The increase in artesunate exposure was not expected to cause toxic side effects for the mother as dosages of 6 mg/kg and 8 mg/kg have been proven to be save in non-pregnant patients [176]. However, no information regarding toxicity for the foetus at these dose levels are available. Furthermore, the control group in this study are post-partum women. Post-partum women have proven to display a higher dihydroartemisinin elimination clearance after oral artesunate compared to non-pregnant women (1.26 [0.63-2.32] vs 1.07 [0.53-1.89]) [146]. The simulated variability has to be interpreted with caution due to high eta-shrinkages although the general trend of decreased dihydroartemisinin exposure is reliable. A meta-analysis with pregnant women, post-partum women and non-pregnant women is therefore urgently needed to confirm the current findings and enable eventual further dose

optimisation. A subsequent clinical study is needed to assess the implications of increased dose regarding toxicity and efficacy.

Moreover, the dose optimisation results indicated a substantially lower dihydroartemisinin exposure using the standard intravenous treatment for severe malaria (2.4 mg/kg) compared to the standard oral treatment for uncomplicated malaria (4 mg/kg). Dihydroartemisinin has the biggest clinical impact on the clearance of the parasite in the artesunate treatment. Severe patients need at least an equal dihydroartemisinin exposure compared to that in uncomplicated patients, if we assume that the disease effect is similar for severe and uncomplicated malaria. This advocates for further research for optimal dosing of severe malaria.

4.5 Conclusion

In conclusion, oral and intravenous artesunate and dihydroartemisinin pharmacokinetics were satisfactorily described using a transit compartment (n=6) absorption, first-pass artesunate elimination and two-compartment disposition model for artesunate and dihydroartemisinin. Bio-availability was estimated to be 90.3% higher during the acute malaria phase as compared to the convalescence phase and dihydroartemisinin elimination clearance was 27.2% higher during pregnancy compared to non-pregnant women. To minimise the risk of treatment failures and the development of resistant parasites, intravenous and oral artesunate doses should be increased by 25% during pregnancy to realise a similar dihydroartemisinin exposure compared to that in post-partum women.

More modelling work and studies have to be performed to support the suggested dose optimisation in this vulnerable group.

5.0 Artemether-dihydroartemisinin

5.1 Background

Oral artemether has been intensively used for the treatment of uncomplicated malaria as a fixed combination with lumefantrine. It is even recommended as first line treatment during the second and third trimester of pregnancy. Four tablets (containing 20 mg artemether and 120 mg lumefantrine each) are recommended to be administered twice daily for three days [41]. For a person weighting approximately 50 kg this will result in a therapeutic dose of 3.4 mg/kg/day.

A non-compartmental analysis of 13 pregnant women (second and third trimester) on the Thai-Myanmar border indicated possible lower artemether and dihydroartemisinin exposures what might explain partly the lowered cure rates (82.0% [74.8-89.3]) in pregnant (second and third trimester) women on the same Thai-Myanmar border [66, 80]. A study in pregnant women (second and third trimester) in Uganda, receiving an identical treatment, on the other hand showed high cure rates (98.2% [93.5-99.7]) [64].

5.1.1 Study aim

The objective of this study was therefore to characterize the population pharmacokinetic properties of artemether and its metabolite dihydroartemisinin in pregnant women (second and third trimester) with uncomplicated P. falciparum malaria in Uganda.

5.1.2 Absorption

The absolute bioavailability of artemether and its metabolite dihydroartemisinin is not known but the mean bioavailability of artemether after oral administration has

been reported between 25% and 43% compared to intra muscular administration [177, 178] and 35% compared to intra rectal administration [178]. Dihydroartemisinin bioavailability after oral artemether administration compared to that after intra muscular administration was 89.6% [177]. Different oral formulations may affect the artemether and dihydroartemisinin exposures [179]. Dispersible and crushed tablets resulted in bioequivalent artemether and dihydroartemisinin exposure but these exposures were 20-35% lower compared to that after intact tablets [179].

Orally administrated artemether is used for treating uncomplicated malaria. Artemether and dihydroartemisinin C_{MAX} in healthy volunteers (artemether: 42.1 [3.80-221] ng/mL/mg/kg dihydroartemisinin: 68.0 [25.3-178] ng/mL/mg/kg) and uncomplicated malaria patients (artemether: 66.0 [15.0-116] ng/mL/mg/kg dihydroartemisinin: 76.0 [31.0-186] ng/mL/mg/kg) were similar [80, 141, 160, 177, 179-195]. Artemether and dihydroartemisinin T_{MAX} in healthy volunteers (artemether: 1.89 [0.5-3.6] hour dihydroartemisinin: 1.92 [0.800-6.00] hour) and uncomplicated malaria patients (artemether: 2.00 [1.00-3.00] hour dihydroartemisinin: 2.44 [1.00-7.4] hour) were also similar [80, 141, 160, 177, 179-195]. Oral administration of artemether results in erratic absorption profiles with multiple absorption peaks and this might be related to variable gastric emptying [141, 189]. However, variability in sample handling, sample preparation and quantification methodology might also have an influence on the variability in reported data.

5.1.3 Distribution

A one-compartment model has been used frequently to fit the artemether and dihydroartemisinin plasma concentration data after oral artemether administration [187-189, 191, 196]. However, two-compartment disposition models were reported to best fit the artemether plasma concentration data when using drug-metabolite models with a population pharmacokinetic approach [194, 197]. The two-compartment disposition model resulted in a 16 hour elimination half-life which is very long. Therefore, it is unlikely that oral artemether truly follows two-compartment disposition pharmacokinetics. A two-compartment structural model most likely suffers from model misspecification on account of large amount of data below the limit of quantification [82].

5.1.4 Metabolism and elimination

Artemether is thought to be predominantly converted into dihydroartemisinin by CYP3A4 in the liver [188]. The elimination half-life for artemether and dihydroartemisinin after oral administration in healthy volunteers (artemether: 2.00 [0.500-5.16] hour dihydroartemisinin: 1.65 [0.800-10.6] hour) and uncomplicated patients (artemether: 2.20 [0.860-16.4] hour dihydroartemisinin: 1.55 [0.950-12.5] hour) is similar [80, 141, 160, 177, 179-195]. Moreover time dependent pharmacokinetics have been reported and artemether elimination clearance increases with 57% and 67.8% after each consecutive dose in Tanzanian and Papua New Guinean children, respectively [194, 197]. However, the magnitude of auto-induction found in these models is only valid up to the sixth dose as the models were constructed on data from a standard dose.

5.2 Study design

This pharmacokinetic study was nested into a larger efficacy study conducted in the Mbarara National Referral Hospital (MNRH) ante-natal clinic (ANC) in Uganda [64]. Ethical approval was obtained from the Mbarara University Faculty of Medicine Research and Ethics Committee, the Mbarara University Institutional Ethics Committee, the Uganda National Council for Science and Technology (ethics committee) and the de Protection des Personnes de St. Germain in Laye, lle de France XI. The trial was registered at ClinicalTrials.gov (NCT00495508). The patients were recruited from March 2008 to September 2008. Inclusion criteria were *Plasmodium falciparum* mixed- or mono-infection (detected by microscopy), residence in the Mbarara municipality (radius 15 km from MNRH) and an estimated gestation age of at least 13 weeks. Exclusion criteria were *Plasmodium falciparum* parasitaemia above 250,000 parasite/uL, severe anaemia (Hb <7g/dL), signs or symptoms of severe malaria requiring parental treatment, known allergy to artemisinin derivates, lumefantrine or quinine, previous participation in the efficacy study or inability to comply with the specified follow-up schedule. Patients were enrolled if they fulfilled all of the inclusion criteria, none of the exclusion criteria, and if written informed consent was obtained.

5.2.1 Dosing regimen and blood sampling

Four tablets of the fixed oral combination of artemether and lumefantrine (Coartem® Novartis Pharma AG, Basel, Switzerland; each tablet contained 20 mg artemether and 120 mg lumefantrine) were administered twice daily for 3

days (0, 8, 24, 36, 48 and 60 hours) with 200 mL of milk tea at each dose to optimise the oral bioavailability of lumefantrine [198]. A full replacement dose was given if the dose was vomited within 30 minutes and a half replacement dose was given if the dose was vomited between 30 minutes and one hour. The patient was withdrawn from the study and treated with rescue treatment if the replacement dose was vomited again within 30 minutes. Venous blood samples (2 mL) were drawn from a cannula into heparinised tubes at 0, 0.25, 0.5, 0.75, 1, 1.25, 1.5, 1.75, 2, 2.5, 3, 4, 6, 8, and 10 hours after the last dose.

5.2.2 Drug analysis

Blood samples were centrifuged at 1,400g for 5 minutes and plasma was stored at -70°C until analysis. Plasma samples were shipped on dry ice to MORU Clinical Pharmacology Laboratory, Bangkok, Thailand for drug quantification. Quantification of artemether and dihydroartemisinin was performed by a previously published method [199]. Artemether and dihydroartemisinin and their stable isotope labelled internal standards were extracted from plasma using solid phase extraction (HLB u-elution SPE 96-well plate, Waters, USA) separated and quantified by liquid chromatography (Agilent 1200 system, Agilent technologies, USA) coupled to positive electrospray tandem mass spectroscopy (API 5000 triple quadrupole, Applied Biosystems/MDS SCIEX, USA). To ensure precision and accuracy during quantification, triplicates of quality control samples at three concentrations; 3.46 ng/mL, 36.0 ng/mL and 375 ng/mL for both artemether and dihydroartemisinin were analysed with every batch. The overall accuracy (i.e. relative standard deviation) was less than 5.4%. The limit of detection (LOD) was

set to 0.5 ng/mL and the lower limit of quantification (LLOQ) was set to 1.43 ng/mL for both compounds.

5.2.3 Comparison of analysis methodologies

The pharmacokinetic findings had to be compared to literature results due to the absence of a non-pregnant control group. The vast majority of the published studies on artemether-dihydroartemisinin pharmacokinetics were analysed using non-compartmental analysis [80, 81, 180] or using a separate drug and metabolite model using the population approach [160]. Since the current analysis was performed using a simultaneous drug-metabolite model, a comparison was performed to assess the potential discrepancies between the different analysis methodologies. Pharmacokinetic parameter estimates from the non-compartmental analysis and separate modelling were compared to that produced by a simultaneous modelling strategy.

5.3 Results

Twenty one (21) pregnant women in their second and third trimesters with uncomplicated *Plasmodium falciparum* malaria from Uganda were enrolled in the study (Table 5.1). The treatment was well tolerated and no cases of vomiting or recurrent malaria infections were recorded.

5.3.1 Comparison of analysis methodologies

All tested methodologies described the data reasonably well (Table 5.2). Significant differences in apparent volume of distribution and absorption rate constant (first order absorption) were evident when comparing non-

Table 5.1: Demographic information from the study population.

	Mean±S.D.	Median (range)
Number of patients	21	
Total artemether dose (mg/kg)	8.46±1.22	8.73 (5.46-9.80)
Total number of samples	316	
Sample size (samples/patient)	15.0±0.805	15 (12-16)
covariates		
Body weight (kg)	58.1±10.1	55 (49-88)
Age (years)	21.4±4.28	21 (16-35)
Gestational age (weeks)	25.8±7.77	27 (13-36)
Haemoglobin (g/dL)	11.1±1.72	11.3 (7.6-14.6)
Red blood cell (10^{12} /L)	3.74±0.629	3.71 (2.37-4.79)
Haematocrit (%)	33.7±5.14	34.0 (23.2-44.5)
Neutrophils (10^9/L) [a]	2.59±0.802	2.75 (1.14-4.13)
Eosinophils (10^9/L) [a]	83.7±148	70.0 (20.0-570)
Basophiles (10^9/L) [a]	24.9±14.0	20.0 (10.0-60.0)
Lymphocytes (10^9/L) [a]	1.98±0.667	1.98 (1.12-3.51)
Monocytes (10^9/L) [a]	0.552±0.214	0.550 (0.260-1.00)
Platelets (10^9/L) [a]	154±62.0	167 (64-285)
Alanine aminotransferase (IU/L)	16.1±6.77	14.0 (5.00-35.0)
Creatinine (mg/dL)	0.481±0.103	0.470 (0.330-0.660)
Bilirubin (mg/dL)	1.24±1.10	0.910 (0.560-5.53)
Systolic blood pressure (mmHg)	60.0±6.20	60.0 (46.0-75.0)
Temperature (°C)	36.8±0.747	36.7 (36.0-38.5)
Plasmodium falciparum parasitaemia (parasites/µL) [a]	1851±32,000	1570 (88.0-148,000)

Values are given as median (range).

[a] Reported as geomean ±S.D.

Table 5.2: Summary of parameter estimates for a comparative analysis of different methodologies.

Parameter	Approach 1 Non-compartmental analysis Median (range)	Approach 2 Sequential modelling Median (range)	Approach 3 Simultaneous modelling Median (range)	P-value (1 vs 2)	P-value (1 vs 3)	P-value (2 vs 3)
Artemether						
CL/F (L/hr)	753 (220-7,381)	904 (375-2,919)	858 (365-4,593)	0.975	0.899	0.972
V/F (L)	1,750 (547-11,045)	1,293 (1,279-1,301)	2,292 (951-4,967)	0.002	0.826	0.013
k_a (hr^{-1})	-	0.392 (0.137-2.25)	0.878 (0.381-2.17)	-	-	0.008
$AUC_{60h\text{-}LAST}$ (hr×ng/mL)	98.5 (7.24-355)	86.4 (26.5-207)	91.1 (17.4-215)	0.989	0.999	0.983
Dihydroartemisinin						
CL/F (L/hr)	381 (167-1,364)	534 (220-1,116)	496 (214-1,199)	0.311	0.459	0.910
V/F (L)	647 (374-4,154)	691 (325-1,699)	163 (97-200)	0.247	<0.001	<0.001
k_a (hr^{-1})	-	0.472 (0.472-0.472) [a]	-	-	-	-
$AUC_{60h\text{-}LAST}$ (hr×ng/mL)	196 (53.2-449)	140 (67.2-340)	150 (62.2-345)	0.304	0.502	0.930

CL/F: elimination clearance, V/F: apparent volume of distribution, k_a: absorption constant and $AUC_{60h\text{-}LAST}$: total area under the plasma concentration-time curve after the last dose to the last sample time. P- values were presented from an ANOVA test with regression analysis or a student t-test on log transformed parameter estimates. Non-compartmental analysis (Approach 1), sequential modelling (Approach 2) and simultaneous modelling (Approach 3) results.

[a] Small little variability was estimated.

compartmental analysis/ sequential modelling to simultaneous modelling (Table 5.2). The artemether absorption rate constant was approximately two times higher using simultaneous modelling compared to separate modelling. The artemether apparent volume of distribution obtained with separate modelling was approximately 25% and 50% lower compared to the estimates obtained with non-compartmental analysis and simultaneous modelling, respectively. The effect on the metabolite was even larger with an approximately four times lower estimated apparent volume of distribution for dihydroartemisinin using simultaneous modelling compared to the other two methodologies.

5.3.2 Simultaneous artemether-dihydroartemisinin model

A zero-order absorption followed by transit compartment absorption described the artemether and dihydroartemisinin absorption better (ΔOFV>-71) than all other tested absorption models (transit-compartment absorption model with an individually estimated number of transit compartments, a transit-compartment absorption model with a fixed number (1-10) of transit compartments, a zero order absorption followed by transit- absorption and first-order absorption, parallel first-order absorption, zero-order absorption, parallel first- and zero-order and zero order absorption followed by first order absorption with and without lag-time) and six transit compartments were sufficient to describe the data. A simultaneous one-compartment drug-metabolite model best described the disposition pharmacokinetics of artemether and dihydroartemisinin. Goodness-of-fit diagnostics of the final model showed an adequate description of observed data (Figure 5.1). The addition of a peripheral compartment for artemether

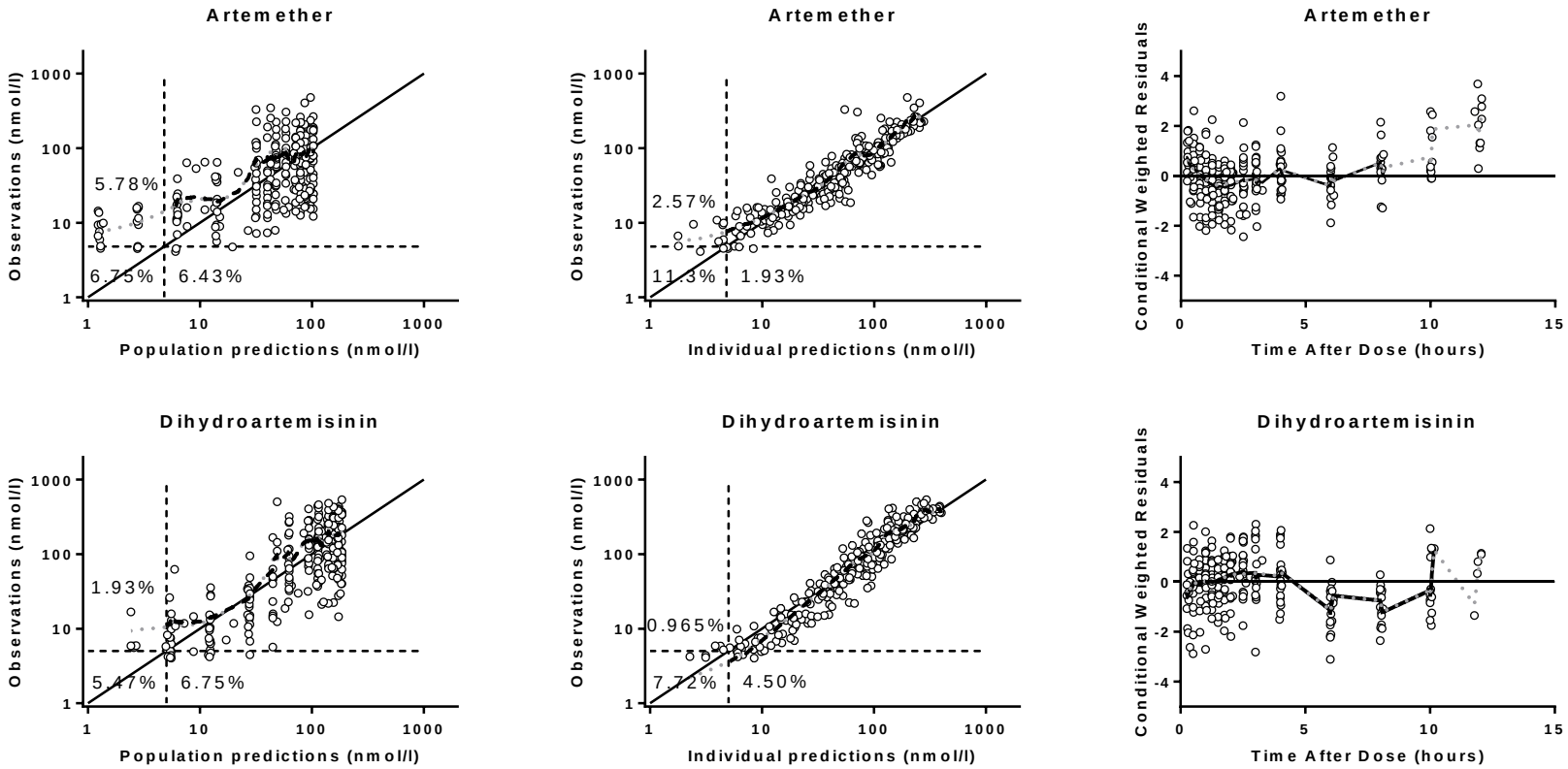

Figure 5.1 Artemether and dihydroartemisinin goodness-of-fit plots. The solid black line represents the line of identity, the local polynomial regression fitting for observations predicted above LLOQ is represented by the dashed black line and the local polynomial regression fitting for all observations is represented by the grey dashed line. The horizontal and vertical dashed black lines represent the lower limit of quantification (LLOQ). Clinical observations are represented by the black circles. Percentages mentioned in the diagnostic plots represent the percentages of the total amount of data in the particular subset.

improved the model fit (ΔOFV=-14.8) but could not be retained due to a combination of poor precision (RSE>30%) in additional parameters and misspecification of censored data. The implementation of a pre-systemic artemether elimination pathway in the model (ΔOFV=-12.5) was only possible in combination with a two-compartment disposition of artemether and the M3 method, but this resulted in an unrealistic artemether elimination half-life of 48.8 h (46.7-53.1) so this model structure was not considered as superior. Incorporation of inter-individual variability in the relative bioavailability significantly improved the model fit (ΔOFV=-133) due to variable absorption of artemether.

The residual error was sufficiently described by a combined additive error model for both the drug and the metabolite. The absorption rate constant in the final model was set to be identical to the rate constant between transit compartments because of the poor precision of the absorption rate constant (RSE>50%). Inter-individual variability for the distribution volume of artemether and dihydroartemisinin were fixed to zero because of poor precision (RSE>50%).

Clearance and volume parameters were not correlated (<50% correlation) in the final model. The relatively short half-life of artemether and dihydroartemisinin can cause a bias in parameter estimates because a large proportion of concentration measurements below the LLOQ at the later time-points (i.e. 47.6% of artemether and 33.3% of dihydroartemisinin samples were below the LLOQ at 10 hours after dose). Coding BLOQ data as missing data performed well with no trends of over- or under-predicting BLOQ data (Figure 5.2). Incorporation of the M3 method or

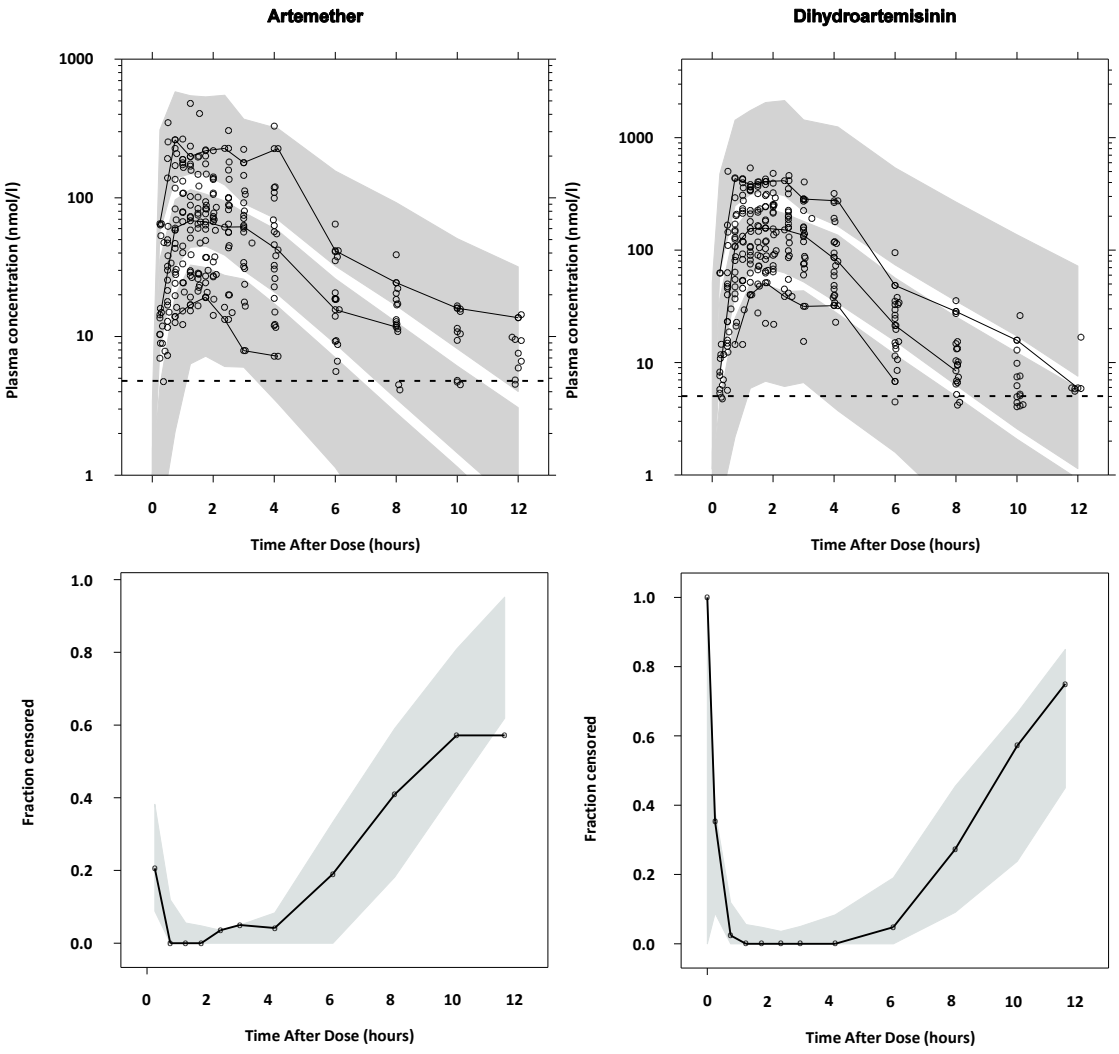

Figure 5.2 Visual Predictive Check of plasma artemether and dihydroartemisinin concentrations. Upper panel: open circles represent the observed data, the solid lines the 5th, 50th and 95th percentiles of the observed data and the shaded area the 95% confidence intervals of the 5th, 50th and 95th percentiles of the simulated plasma concentrations (nmol/L). The limit of quantification is represented by the black dashed line. Lower panel: the shaded area represents the simulated 95% confidence intervals for the fraction of BQL data. The black solid line represents the observed fraction of BQL data.

imputing BLOQ data with LLOQ/2 resulted only in minor improvements in the visual diagnostics. However, the M3 and LLOQ/2 approach resulted in much higher conditional numbers compared to the conventional method of coding BLOQ data as missing data. This implies that these models are less robust. BLOQ data were therefore coded as missing data in the final model.

No statistical significant covariates were found in this study using either stepwise covariate modelling or the full covariate approach. The full covariate approach indicated that the covariate effect was distributed with a certainty of 95% between -11% and 7% change in parameter estimate per estimated age of gestation in weeks and thereby confirming the absence of covariate effects from estimated age of gestation in the studied population (Figure 5.3).

The numerical predictive check of the final model computed 1.11% (95 % CI. 0.74 to 11.11%) and 2.96% (95% CI, 0.74-11.85%) of the observed artemether concentrations below and above the 90% prediction interval, respectively. For dihydroartemisinin 0% and 0.37% (95% CI. 0.37-12.45%) of observations were calculated below and above the 90% prediction interval, respectively. This indicated an over-prediction of the variability from both the drug and the metabolite. However, the central tendencies of the concentration-time profiles are adequately predicted and population parameter estimates were robust but showed large inter-individual variability as indicated by the predictive checks (Table 5.3 and Figure 5.2). All shrinkage estimates were below 20% indicating the reliability of the individual parameter estimates.

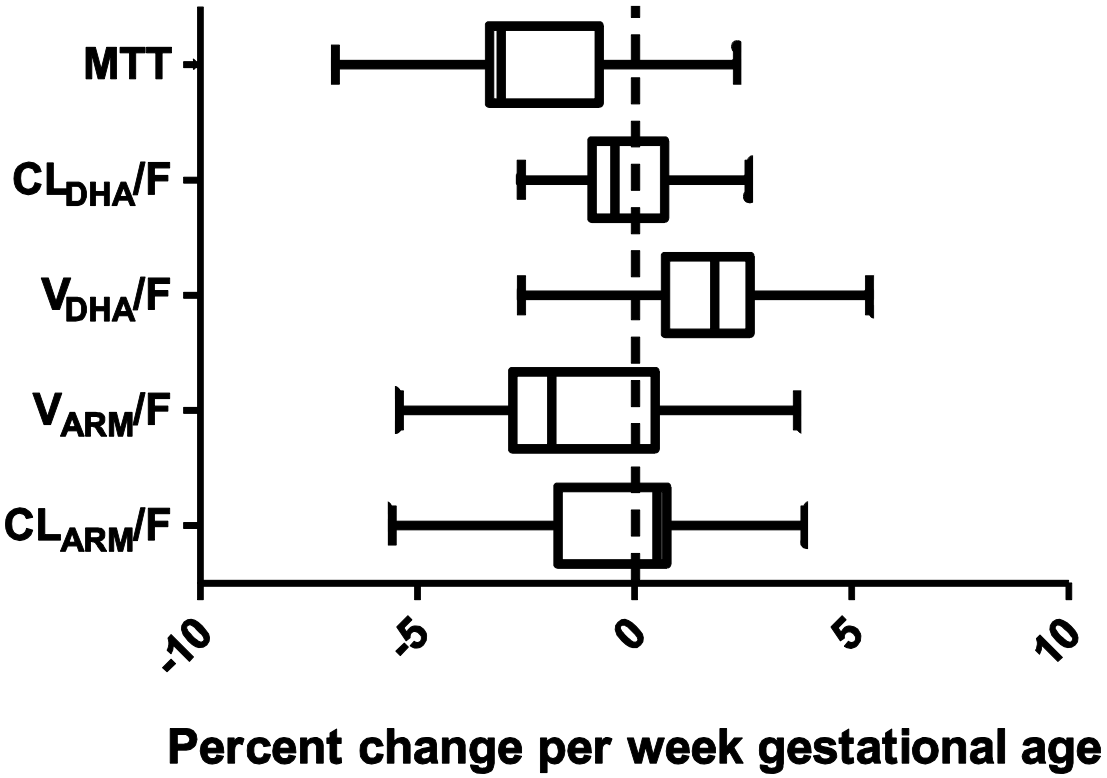

Figure 5.3 Box and whisker plot visualising the effect of estimated gestational age on pharmacokinetic parameters (boxes represent 25%-75% and whiskers represent 2.5%-97.5%). Mean transit time (MTT), apparent volume of distribution dihydroartemisinin (V_{DHA}/F), elimination clearance (CL_{DHA}/F), apparent volume of distribution artemether (V_{ARM}/F) and elimination clearance artemether (CL_{ARM}/F) from 250 bootstrap runs.

Table 5.3: Population pharmacokinetic parameter estimates from the simultaneous artemether-dihydroartemisinin model

Parameter	Population estimate [a] (% RSE) [b]	95% CI [b]	IIV[%CV] [a] (% RSE) [b]	95% CI [b]
CL_{ARM}/F (L/hr)	875 (18.7)	625-1,280	28.0 (47.6)	12.0-37.8
V_{ARM}/F (L)	2,160 (17.4)	1,620-3,110	-	-
CL_{DHA}/F (L/hr)	468 (10.2)	387-588	90.4 (39.0)	40.5-126
V_{DHA}/F (L)	57.1 (20.1)	41.7-88.8	-	-
MTT (hr)	0.274 (19.4)	0.170-0.380	75.2 (39.6)	41.4-121
D1 (hr)	0.687 (25.5)	0.400-1.19	151.2 (24.1)	90.6-209
F1	1 (fixed)	-	85.5 (24.8)	53.2-108
Transit compartments (N)	6 (fixed)	-	-	-
σ	0.166 (6.87)	0.130-0.221	23.1 (51.7)	8.35-35.2
Secondary parameters [c]	Artemether Median (range)	Dihydroartemisinin Median (range)		
AUC 60 - 72 (hr×ng/mL)	111 (16.2-317)	167 (55.3-437)		
$C_{MAX\ 60\ -\ 72}$ (ng/mL)	32.9 (7.5-82.8)	45.2 (14.1-114)		
$T_{MAX\ 60\ -\ 72}$ (hr)	1.16 (0.65-3.81)	1.37 (0.820-3.89)		

[a] Population mean values and inter-individual variability (IIV) estimated by NONMEM. IIV is presented as $100 \times \sqrt{e^{\text{mean variance estimate}} - 1}$.

[b] The relative standard error (RSE) is calculated as 100*(standard deviation/mean value) from 1,046 successful iterations of a non-parametric bootstrap. The 95%confidence interval (95% CI) is displayed as the 2.5 to 97.5 percentiles of the bootstrap estimates.

[c] Post-hoc estimates were calculated as the median and ranges of the empirical Bayes estimates.

CL_{ARM}/F: elimination clearance of artemether, V_{ARM}/F: apparent volume of distribution of artemether, CL_{DHA}/F: elimination clearance of dihydroartemisinin, V_{DHA}/F; apparent volume of distribution of dihydroartemisinin, MTT; mean transit time, DUR; duration of zero order-absorption and F; relative bioavailability. The additive error (σ) variance will essentially be exponential on arrhythmic scale data. AUC: total area under the plasma concentration-time curve after the last dose, C_{MAX}: maximum concentration after the last dose and T_{MAX}: Time to maximum concentration.

5.4 Discussion

Coartem® has been used with excellent cure rates in adults [55, 56, 65] but contradictory findings have been reported during the second and third trimester of pregnancy. Lowered cure rates have been reported on the Thai-Myanmar border (82.0% [74.8-89.3]) and contradictory findings were reported in Uganda (98.2% [93.5-99.7]) [64, 66]. A non-compartmental analysis indicated a tendency of lower artemether and dihydroartemisinin exposure on the Thai-Myanmar border what might contribute to the lowered cure rates [80]. An analysis to assess potential alterations of artemether-dihydroartemisinin pharmacokinetics on account of pregnancy in Uganda was therefore urgently needed.

5.4.1 Comparison of analysis methodologies

The comparative analysis between different analysis methodologies (non-compartmental analysis, separate modelling and simultaneous modelling) clearly shows that the volume of distribution estimate is affected by the actual absorption model for dihydroartemisinin. Therefore, different modelling approaches will lead to differences in the characterisation of both the absorption and the distribution phase for the drug and metabolite.

Although the approaches led to significant differences in pharmacokinetic parameter estimates, this may have little clinical relevance. Total exposure of both artemether and dihydroartemisinin were not significantly different for the different approaches. However, a trend of lower dihydroartemisinin exposure after sequential and simultaneous modelling compared to after NCA was

observed. This phenomenon resulted from difficulties with fitting the erratic absorption phase.

5.4.2 Simultaneous artemether-dihydroartemisinin model

Pharmacokinetic data from 21 pregnant women with *uncomplicated Plasmodium falciparum* malaria in Uganda was analysed using the population approach. A zero-order absorption followed by transit (n=6) compartment absorption best described the absorption of the drug combination artemether-dihydroartemisinin and could be physiologically explained by the disintegration of the administered drug in the gut, resulting in a continuous drug supply, described by a zero-order process followed by transit absorption of drug into the systemic circulation.

The goodness-of-fit diagnostics in the present study (Figure 5.1) suggested that a two-compartment disposition model for dihydroartemisinin might be a better description of the data and a study in children (1-10 years old) with uncomplicated *Plasmodium falciparum* malaria in Tanzania was best described by a simultaneous artemether-dihydroartemisinin model consisting of two- and one-disposition compartments for artemether and dihydroartemisinin, respectively [197]. However, the addition of a peripheral compartment for artemether in this study resulted in poor precision and model misspecification and the addition of a peripheral compartment for dihydroartemisinin did not improve the model fit (ΔOFV=0.003). The general under-prediction of low artemether and dihydroartemisinin concentrations is a direct consequence of a high proportion of data below the LLOQ.

The incorporation of relative bioavailability significantly improved the model fit and it should theoretically de-correlate pharmacokinetic parameters (i.e. clearance and volume parameters) within a patient. This also explains the absence of correlation between variability components on clearance and volume parameters.

The additive error model structure for both artemether and dihydroartemisinin on logarithmic data is not unexpected since artemether and dihydroartemisinin plasma samples were obtained from the same blood sample and concentrations were quantified using a simultaneous bio-analytical method.

The big confidence intervals around the 5^{th}, 50^{th} and 95^{th} percentiles in the visual predictive check (Figure 5.2) and the over estimation of variability as indicated by the numerical predictive check was a result of problems with fitting the erratic absorption phase (Figure 5.4) and a relatively small study population. No cases of vomiting were reported or other possible explanations such as concomitant therapy or food intake to the observed absorption characteristics. However, similar erratic absorption profiles have been reported previously in healthy volunteers [189] and similar over prediction was reported in children with uncomplicated malaria in Tanzania [197].

Artemether is predominantly metabolised by CYP3A4 [188] and estimated gestational age could not be found as a significant covariate on artemether elimination clearance in this study. This was in line with the absence of a difference in CYP3A4 activity between the second and third trimester of

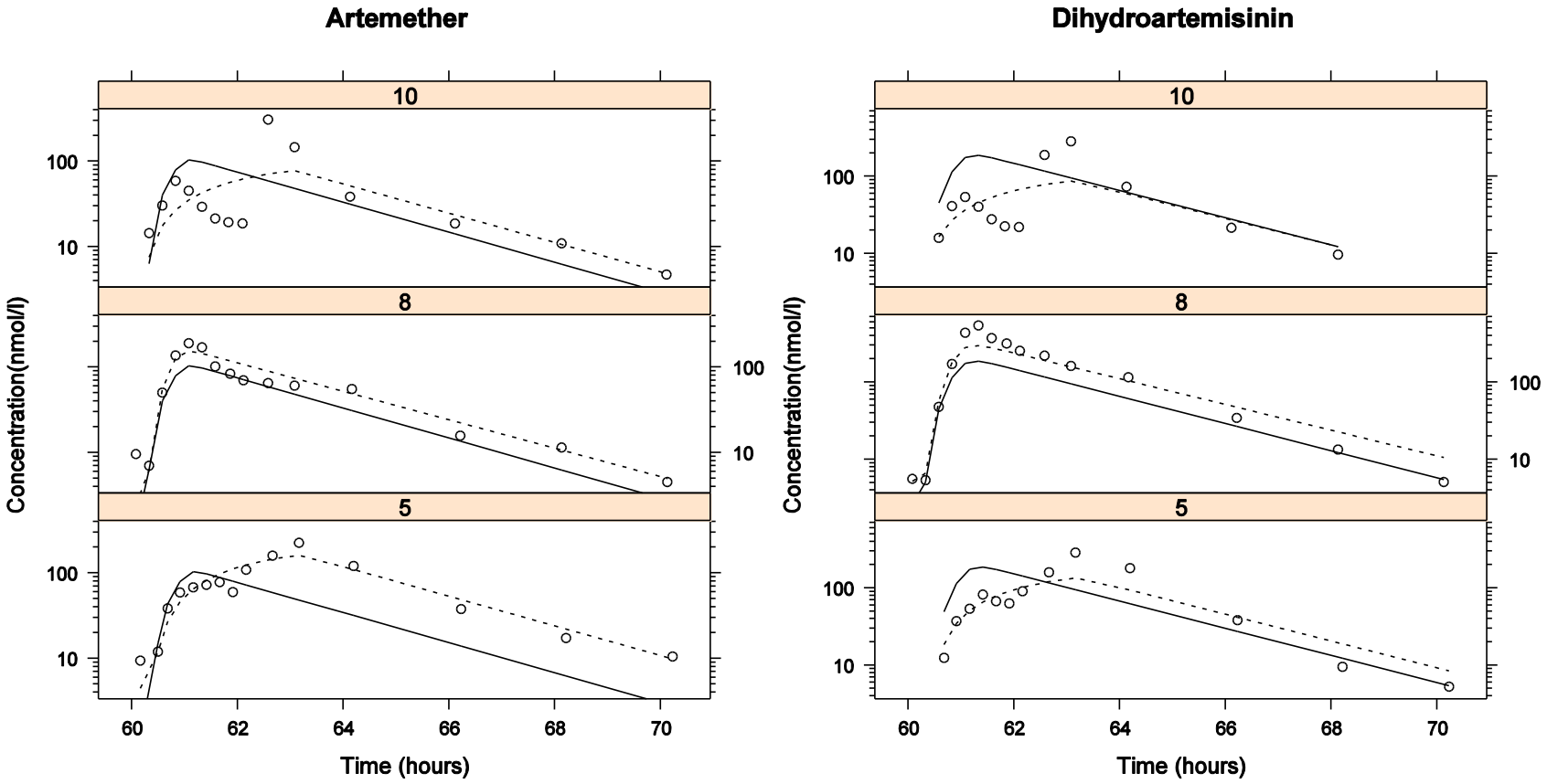

Figure 5.4 Observed (dots), population predicted (solid line) and individual predicted (dashed line) artemether and dihydroartemisinin plasma concentrations for selected patients with bi-phasic (ID 10), mono-phasic (ID 8) and plateau absorption (ID5).

pregnancy [139]. However, both hepatic and intestinal CYP3A4 activities have been reported to be induced during pregnancy compared with post- partum women but pregnancy could not be evaluated as a categorical covariate in this study due to the absence of a non-pregnant control group [139, 140]. Dihydroartemisinin is metabolised by UGT 1A9 and UGT 2B7 [200] and no significant covariate effect of estimated age of gestation was found on dihydroartemisinin elimination clearance. This might indicate that there is no difference in UGT 1A9 and UGT2B7 activity between the second and third trimester. The pregnant women in the current analysis were from Uganda, Africa and compared to literature values from non-pregnant patients from Thailand, South East Asia which may have resulted in genetic variation for the metabolising enzymes. However, this was not considered to have a major impact on the results since single nucleotide polymorphisms in a variety of CYP enzymes, including CYP3A4, had no substantial impact and did not significantly alter the pharmacokinetic properties of artemether [201].

Data collected in this study did not allow investigation of auto-induction since patients were sampled only after the last dose. However, a 57.0% and 67.8% increase in elimination clearance of artemether with each dose (auto-induction) has been suggested in a previous publication [194, 197] and lower artemether exposures were found after multiple dosing [187, 191, 192]. The elimination clearance in this study was 4.9-fold higher than that in healthy Pakistani volunteers when sampled after a single dose administration (15.1 L/hr/kg vs 3.11 L/h/kg). This could be a result of auto-induction. However, the effect of a

different sampling scheme, pregnancy, ethnic differences and/or disease should also be considered [180].

5.4.3 A comparison to literature

C_{MAX}, AUC, T_{MAX}, $T_{1/2}$ and CL results obtained by non-compartmental analysis and simultaneous population pharmacokinetic drug metabolite modelling were compared to literature non-compartmental analysis results from literature (Table 5.4 and Table 5.5). The elimination half-life of artemether (1.96 h) is longer compared to the elimination half-life of dihydroartemisinin (1.39 h), which suggests formation rate limited elimination of dihydroartemisinin. Therefore, the elimination half-life of dihydroartemisinin obtained with compartmental modelling did not reflect its physiological value as a result of flip-flop kinetics. Consequently, the non-compartmental analysis elimination half-life for dihydroartemisinin was considered as the true value.

Estimated artemether and dihydroartemisinin exposure in this African pregnant population was similar to that reported in pregnant Thai patients [80]. Both the present study and the previously published study in Thai pregnant women [80] showed artemether exposures in a similar range compared to a Thai adult non-pregnant patient population [192]. In contrast exposures were lower compared to another Thai adult non-pregnant patient population [193]. Dihydroartemisinin exposures in both African and Thai pregnant women were lower compared to the two Thai adult non-pregnant patient populations [192, 193]. This might suggest a

Table 5.4: A comparison of the artemether pharmacokinetic properties to literature values

	Parameter	AUC (hr×ng/mL/ mg dose)	C_{MAX} (ng/mL/ mg dose)	T_{MAX} (hr)	$T_{1/2}$ (hr)	CL (L/hr/kg)
Final model (N=21)	Median (range) [a]	1.34 (0.203-3.75)	0.411 (0.0930-1.04)	1.16 (0.653-3.81)	1.77 (0.773-2.49)	15.1 (18.6) [b]
NCA (N=21)	Median (range)	1.21 (0.0999-4.26)	0.443 (0.0710-1.79)	1.27 (0.500-4.00)	1.96 (0.590-4.01)	13.2 (3.21-130)
NCA in Thai pregnant patients (N=13) [80]	Median (90% ranges)	0.820 (0.131-3.50)	0.438 (0.175-1.30)	1.00 (0.500-2.00)	1.5 (1.20-7.20)	25.9 (6.0–162)
NCA in Thai patients (N=13) [c] [193]	Mean (range)	6.03 (3.21-10.2)	1.12 (0.730-1.50)	2.00 (2.00-2.00)	2.60 (1.80-4.70)	3.27
NCA in Thai patients (N=25) [192]	Mean ± S.D.	2.64 ± 1.36	0.828 ± 0.679	2.00 (1.00-8.00)	2.20±1.00	-
NCA in Pakistani subjects (N=12) [d][180]	Median (range)	4.53 (1.60-8.30)	2.16 (0.678-4.54)	1.50 (0.500-3.00)	1.88 (1.24-4.00)	3.11 (1.57-11.9)
NCA in Caucasian subjects (N=14) [185]	Mean ± S.D.	0.791 ± 0.906	0.343 ± 0.386	1.50 [1.00-4.00]	1.60	-
NCA in Caucasian subjects (N=8) [e][187]	Mean ± S.D.	0.350 ± 0.300	0.190 ± 0.130	1.60±0.800	0.500±0.100	-

[a] Median and ranges were derived from the empirical Bayes estimates.

[b] Population estimate (%RSE).

[c] After a single dose of 300 mg artemether and four consecutive 100 mg artemether doses daily.

[d] After a single dose of artemether-lumefantrine (Coartem).

[e] After five doses artemether mono-therapy.

AUC: area under the concentration-time curve, C_{MAX}: maximum concentration, T_{MAX}: time to maximum concentration and $T_{1/2}$: elimination half-life. AUC and C_{MAX} were normalized by artemether dose.

Table 5.5: A comparison of the dihydroartemisinin pharmacokinetic properties to literature values

	Parameter	AUC (hr×ng/mL/ mg dose)	C_{MAX} (ng/mL/ mg dose)	T_{MAX} (hr)	$T_{1/2}$ (hr)	CL (L/hr/kg)
Final model (N=21)	Median (range) [a]	2.11 (0.703-5.44)	0.593 (0.185-1.50)	1.37 (0.823-3.89)	0.0962 (0.0157-0.470)	8.06 (10.5) [b]
NCA (N=21)	Median (range)	2.571 (0.698-5.89)	1.09 (0.247-2.01)	1.83 (0.52-4.0)	1.39 (0.690-2.36)	6.91 (2.29-23.1)
NCA in Thai pregnant patients (N=13) [80]	Median (90% ranges)	4.68 (0.391-7.67)	2.16 (0.944-2.94)	1.0 (0.5-2.0)	1.3 (0.9-8.4)	4.5 (2.8–5.4)
NCA in Thai patients (N=13) [c] [193]	Mean (range)	11.1 (7.04-15.6)	1.41 (0.871-2.12)	4 (2-4)	3.6 (2.4-4.8)	-
NCA in Thai patients (N=25) [192]	Mean ± S.D.	7.92 ± 3.40	2.69 ± 1.34	2.0 (1.0-6.0)	1.6±0.4	-
NCA in Pakistani subjects (N=12) [d][180]	Median (range)	3.97 (2.57-4.74)	1.6 (0.704-2.56)	1.50 (0.750-3.00)	1.78 (1.34-2.20)	3.70 (3.05-5.27)
NCA in Caucasian subjects (N=14) [185]	Mean ± S.D.	2.51 ± 1.22	0.982 ± 0.547	1.5 [1-4]	1.5±0.6	-
NCA in Caucasian subjects (N=8) [e][187]	Mean ± S.D.	2.42 ± 0.682	0.818 ± 0.294	1.6±0.8	0.8±0.3	-

[a] Median and ranges were derived from the empirical Bayes estimates.
[b] Population estimate (%RSE).
[c] After a single dose of 300 mg artemether and four consecutive 100 mg artemether doses daily.
[d] After a single dose of artemether-lumefantrine (Coartem).
[e] After five doses artemether mono-therapy.
AUC: area under the concentration-time curve, C_{MAX}: maximum concentration, T_{MAX}: time to maximum concentration and $T_{1/2}$: elimination half-life. AUC and C_{MAX} were normalized by dihydroartemisinin dose.

lower artemether and dihydroartemisinin exposure in a pregnant population compared to a non-pregnant patient population. However, this comparison was based on only two available reference populations with different ethnicity [192, 193]. Therefore, studies in larger series with non-pregnant control groups are urgently needed to further assess the pharmacokinetics of artemether and dihydroartemisinin in pregnant women and guide dose optimisation.

5.5 Conclusion

In conclusion, the population pharmacokinetic properties of artemether and its metabolite dihydroartemisinin were well described by a simultaneous drug-metabolite model in 21 pregnant women with uncomplicated *Plasmodium falciparum* malaria in Uganda. Total exposure of artemether and dihydroartemisinin were somewhat lower in these pregnant women compared to adult patient populations from literature. However, these results should be interpreted with caution since ethnicity might have an impact on the pharmacokinetic properties of these drugs. Further studies in larger series with both pregnant and non-pregnant patients are urgently needed to study the pharmacokinetics in this vulnerable group.

6.0 Lumefantrine

6.1 Background

Oral lumefantrine has been intensively used together with artemether in a fixed combination for the treatment of uncomplicated malaria. The drug combination is even recommended as first line treatment during the second and third trimester of pregnancy. Four tablets (containing 20 mg artemether and 120 mg lumefantrine each) are recommended to be administered twice daily for three days [41]. For a person weighting approximately 50 kg this will result in a therapeutic dose of 9.6 mg/kg/day.

Lumefantrine (in the fixed combination artemether/lumefantrine) has shown to eliminate leftover parasites successfully in adults after artemether and dihydroartemisinin has been washed out from the body resulting in high cure rates [55, 56, 65]. However, a non-compartmental analysis of 13 pregnant women (second and third trimester) on the Thai-Myanmar border indicated possibly lower lumefantrine exposures what might explain the lowered cure rates (82.0% [74.8-89.3]) in pregnant (second and third trimester) women there [66, 80]. A study in pregnant women (second and third trimester) in Uganda, receiving the identical treatment, on the other hand showed high cure rates (98.2% [93.5-99.7]) [64].

6.1.1 Study aim

The objective of this study was therefore to characterise the population pharmacokinetic properties of lumefantrine in pregnant women (second and third trimester) and non-pregnant women with uncomplicated *Plasmodium falciparum* malaria in Uganda.

6.1.2 Absorption

The absolute oral bioavailability of lumefantrine in human beings is not known but a study in rat reports dose-dependent oral bioavailability of 11.6%, 4.80% and 5.24% after oral lumefantrine at 10 mg/kg, 20 mg/kg and 40 mg/kg, respectively [202]. It is recommended to administer artemether/lumefantrine with milk to optimise the low oral bioavailability and the time to reach the lumefantrine maximum plasma concentration is 4.0 [4.5-6.0] hour [80, 184-186].

6.1.3 Distribution

Lumefantrine is a lipophilic drug and follows multiphasic disposition pharmacokinetics. Two- and three-compartment distribution models have been reported in literature to best describe the lumefantrine plasma concentration-time data [83, 194, 197]. The additional peripheral compartment in Papua New Guinean children is a result of prolonged sampling schedule (28 days) compared to the studies reporting two-compartment disposition pharmacokinetics where patients were sampled for 3 and 14 days. Central volume of distribution has been previously reported to correlate with estimated gestational age within the second and third trimester of pregnancy [83].

6.1.4 Metabolism and elimination

Lumefantrine is thought to be metabolised by CYP3A4 enzymes into desbutyl-lumefantrine and the elimination half-life of oral lumefantrine is 3.80 (2.70-11.5) days [56, 80, 83, 181, 184-186, 203-206].

6.2 Study design

This nested pharmacokinetic study was conducted in the Mbarara National Referral Hospital (MNRH) ante-natal clinic (ANC) in Uganda and pregnant patients were recruited from October 2006 to December 2008 [64]. Inclusion criteria were pregnant women with *Plasmodium falciparum* mixed- or mono-infection (detected by microscopy), residence in the Mbarara municipality (radius 15 km from MNRH) and an estimated gestation age of at least 13 weeks. Exclusion criteria were *falciparum* parasitaemia above 250,000 parasites/uL, severe anaemia (Hb <7g/dL), signs or symptoms of severe malaria requiring parental treatment, known allergy to artemisinin derivates, lumefantrine or quinine, previous participation in the efficacy study or inability to comply with the specified follow-up schedule. Patients in the non-pregnant venous control group were recruited (from February to August 2009) as post-partum women (more than 8 weeks) if a match (with respect to history of fever, axillary temp >37.5, smoking and parasitaemia: <1,000, 1,001 – 25,000, 25,001-250,000/μL) could be found in the densely sampled venous lumefantrine pregnant arm. Written informed consent was obtained before inclusion.

Ethical approval was obtained from the Mbarara University Faculty of Medicine Research and Ethics Committee, the Mbarara University Institutional Ethics Committee, the Uganda National Council for Science and Technology (ethics committee) and the “Comité de Protection des Personnes” (Ile de France XI, France). The trial was registered at ClinicalTrials.gov (NCT00495508).

6.2.1 Dosing regimen and blood sampling

The combination of artemether and lumefantrine (Coartem® Novartis Pharma AG, Basel, Switzerland; each tablet contained 20 mg artemether and 120 mg lumefantrine) was administered with 200 mL of milk tea to optimize the oral bioavailability of lumefantrine [198]. Four tablets per dose were administered twice daily for 3 days (at 0, 8, 24, 36, 48 and 60 hours). If the dose was vomited within 30 minutes a full replacement dose was given. If the dose was vomited between 30 minutes and one hour a half replacement dose was given. If the replacement dose was vomited again within 30 minutes the patient was withdrawn from the study and treated with rescue treatment.

Two sample matrices were used for collecting pharmacokinetic samples. Venous blood samples (2 mL) in the venous sampling group were drawn from each patient from a cannula into heparinized tubes at 0, 4, 8, 12, 24, 28, 36, 40, 48, 52, 60, 60.5, 61, 62, 64, 66, 68, 72, 84, 108, 132, 156, 180, 204 and 228 hours after the first dose. Two capillary blood samples in the capillary sampling group were taken from each patient at 0 hours (pre-treatment) and at day 7 after treatment initiation. Additional capillary samples were taken from each patient in the capillary sampling group at random within the following time windows after the first dose 0-71, 72-95, 96-143 and 144-336 hours.

6.2.2 Drug analysis

Plasma was separated by centrifugation (1400 g for 5 minutes) and subsequently stored at -70°C or in liquid nitrogen until analysis. The plasma samples were transported on dry ice to the Mahidol-Oxford Tropical Medicine Research Unit,

Department of Clinical Pharmacology, Faculty of Tropical Medicine, Mahidol University, Bangkok, Thailand .

Lumefantrine was quantified by high performance liquid chromatography with UV-detection according to a validated and published method [207]. Triplicates of quality control samples at three concentrations were analysed within each batch to ensure precision and accuracy during quantification. The overall relative standard deviation was less than 10% and the lower limit of quantification was set to 26 ng/mL.

6.3 Results

This study was nested into a larger efficacy study and a total of 116 pregnant women in the second and third trimesters were enrolled into the pharmacokinetic cohort. In addition, 17 non-pregnant women with uncomplicated *falciparum* malaria in Uganda were enrolled in the pharmacokinetic cohort (Table 6.1). The standard oral fixed dose treatment of artemether and lumefantrine (twice daily for 3 days) was well tolerated and no cases of vomiting were reported. No patients presented with recurrent malaria infections during the follow-up (until delivery or day 42). Twenty six pregnant and 17 non-pregnant women contributed with densely sampled plasma, and 90 pregnant women contributed with sparsely sampled capillary plasma (Table 6.1). One individual in the capillary arm was omitted from the data analysis because of an unexplainable high baseline plasma lumefantrine concentration of 7,717 ng/mL. Demographic values were generally similar between pregnant and non-pregnant women except for a higher

Table 6.1: Demographic summary of the study population

	All	Venous non-pregnant	Venous pregnant	Capillary pregnant
Number of patients	132	17	26	89
Total lumefantrine dose (mg/kg)	51.4 (34.7-72.0)	58.8 (45.7-72.0)	51.4 (38.9-65.5)	50.5 (34.7-65.5)
Total number of samples	1580	440	620	517
Sample size (samples/patient)	6 (4-26)	26 (25-26)	25 (14-26)	6 (4-8)
A selection of covariates				
Body weight (kg)	56.0 (40.0-83.0)	49.0 (40.0-63.0)	56.0 (44.0-74.0)	57.0 (44.0-83.0)
Age (years)	21.0 (15.0-38.0)	21.0 918.0-29.0)	20.0 (18.0-38.0)	22.0 (15.0-38.0)
Parasitaemia (μL^{-1})	1,380 (24.0-194,000)	7,510 (48.0-152,000)	638 (32.0-11,800)	1,950 (24.0-194,000)
Gestational age (weeks)	21.0 (0-39.0)	0 (0-0)	22.5 (16.0-38)	22.0 (13.0-39.0)
Body temperature (°C)	36.9 (36.0-39.8)	36.7 (36.1-38.2)	36.7 (36.0-39.3)	37.0 (36.0-39.8)

Values are given as median (range).

body weight in pregnant women as compared to non-pregnant women (Table 6.1). Furthermore, pregnant women in the group with venous plasma sampling had lower admission parasitaemias as compared to both pregnant women with capillary sampling and non-pregnant women (Table 6.1).

6.3.1 Population pharmacokinetic lumefantrine model

The final nonlinear mixed-effects model consisted of a flexible transit absorption model (5 transit compartments) followed by a two-compartment disposition model and described the lumefantrine data well (Figure 6.1). Residual variability was best described using an additive error model on the log-transformed data. Implementation of between-patient variability, between-dose occasion variability, and a Box-Cox transformation of the relative bioavailability of lumefantrine resulted in a significant improvement of the model (objective function value differences [ΔOFV] of -261, -539 and -21.5, respectively). Venous and capillary data were successfully modelled simultaneously using a proportional correction factor for the capillary samples on a population level since no patient contributed with both capillary and venous samples. Capillary concentration samples were estimated to be 11.9% (relative standard error [RSE] of 9.32%) lower compared to venous concentration samples. However, this conversion factor did not improve the model fit significantly.

The following covariates were all selected in the forward covariate search ($p<0.05$); estimated gestational age on bioavailability (exponential relationship) and apparent distribution volume of the peripheral compartment (linear relationship), body temperature on mean transit time (linear relationship) and

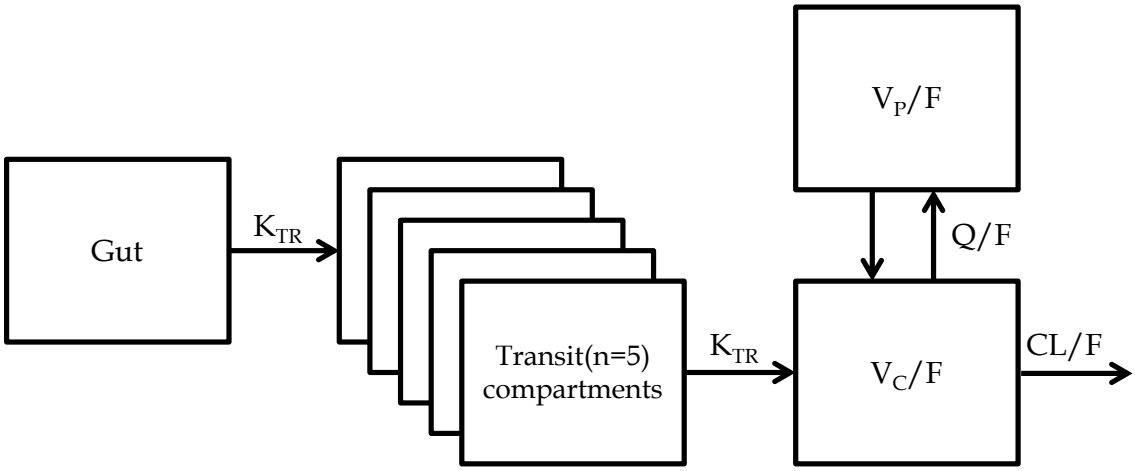

Figure 6.1 Visual representation of the population pharmacokinetic lumefantrine model. K_{TR}: Transit rate constant V_C/F: apparent central volume of distribution V_P/F: apparent peripheral volume of distribution Q/F: inter-compartmental clearance and CL/F: elimination clearance.

pregnancy on inter-compartmental clearance (categorical). However, only body temperature on mean transit time (linear relationship) and pregnancy on inter-compartmental clearance (categorical) could be retained as significant covariates ($p<0.01$) in the backward elimination step. Mean absorption transit time increased with 16.5% with every degree centigrade increase of body temperature between 36.0°C and 39.8°C (*p<0.01*) and inter-compartmental clearance was 36.5% lower in pregnant women compared to non-pregnant women (*p<0.01*). Similar trends of pregnancy-related effects were seen in the full covariate model for pregnancy (Figure 6.2).

Basic goodness-of-fit diagnostics (Figure 6.3) of the final covariate model did not show any trends of model misspecification (20.6% epsilon shrinkage). Additional simulation based diagnostics (i.e. visual predictive checks) indicated high predictive performance of the final model (Figure 6.4). Similarly, the numerical predictive check computed 4.07% (95% CI. 2.56% - 7.87%) and 3.80% (95% CI. 2.35% - 8.29%) of the observed lumefantrine concentrations above and below the 90% prediction interval, respectively. Parameter estimates were robust with reasonably low RSEs (Table 6.2). Eta-shrinkage estimates were relatively high for certain parameters (15.5% to 54.0%) which suggest that post-hoc estimates should be interpreted with caution.

6.3.2 Simulations

Monte Carlo simulations performed with the final population pharmacokinetic model indicated lower day 7 venous plasma concentrations in pregnant women (414 ng/mL) compared with those in non-pregnant women (566 ng/mL) in this

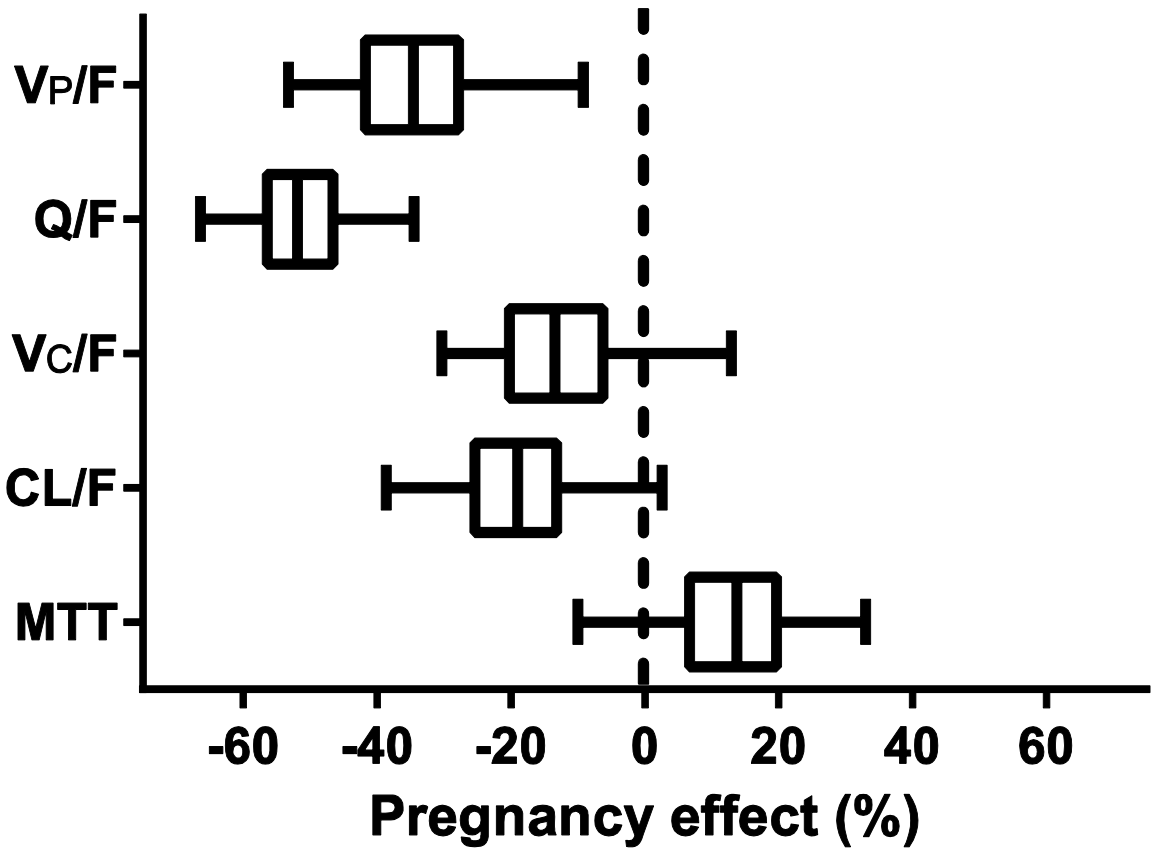

Figure 6.2 Box and whisker plot visualizing the effect of pregnancy on pharmacokinetic parameters from 200 bootstrap runs (boxes represent the 25%-75% percentiles and whiskers represent the 2.5%-97.5% percentiles of the bootstrap estimates). Peripheral distribution volume (V_P/F), inter-compartmental clearance (Q/F), central distribution volume (V_C/F), elimination clearance (CL/F) and mean transit time (MTT).

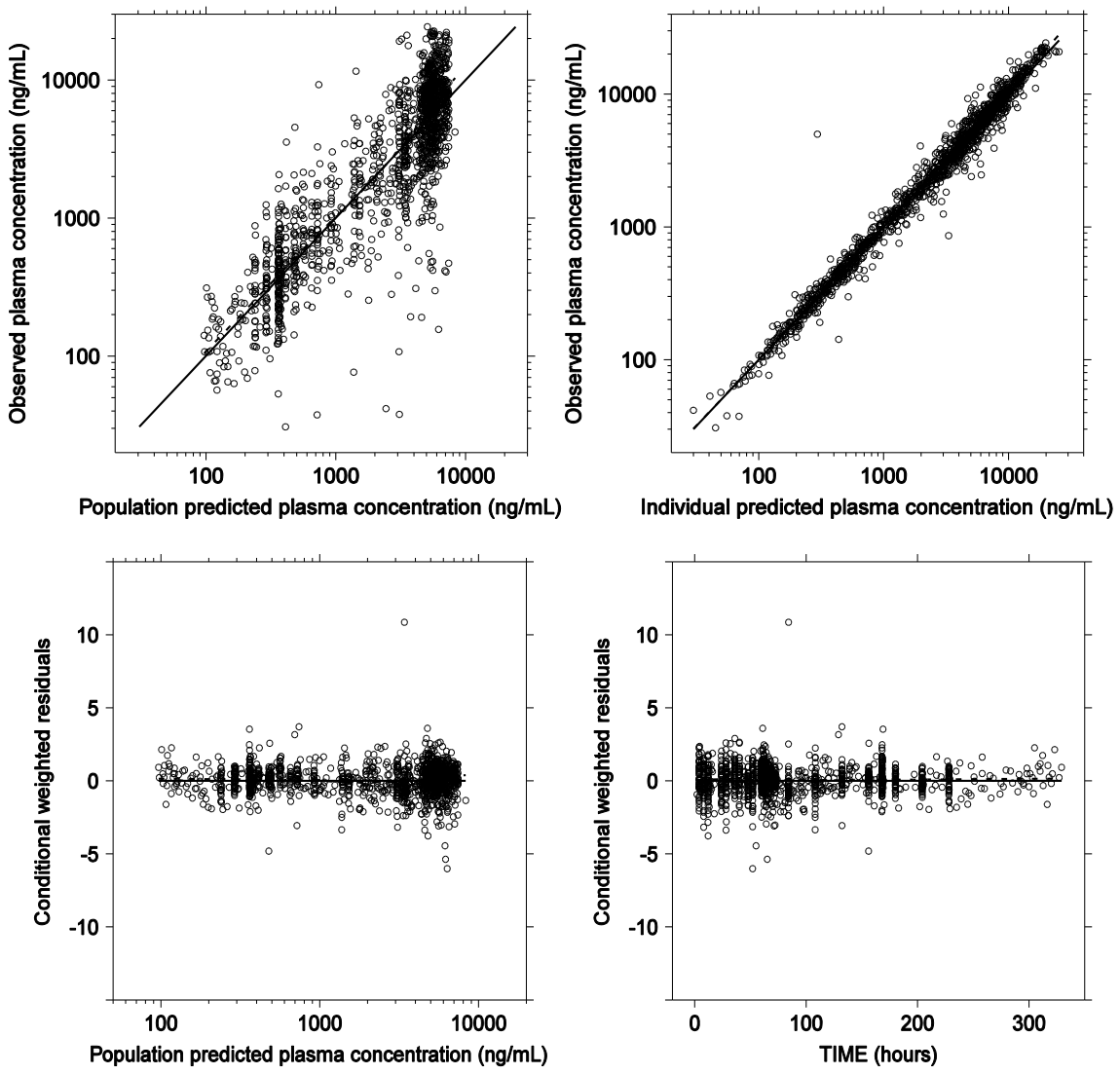

Figure 6.3 Basic goodness-of-fit plots from the final lumefantrine model. The line of identity is represented by the black solid lines and the trend lines (local polynomial regression fitting using 50 evaluations) is represented by the black dashed line.

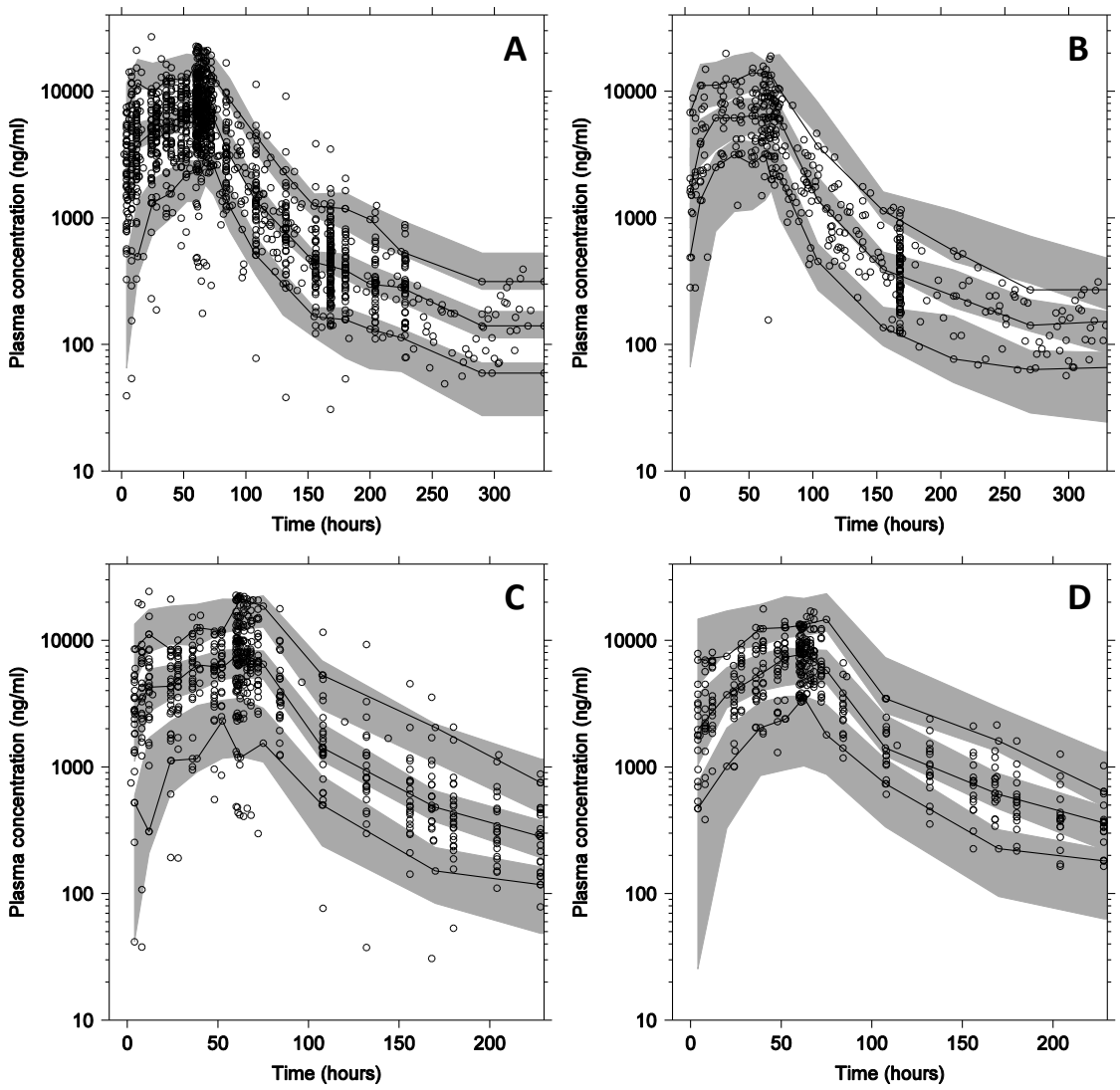

Figure 6.4 Prediction-corrected visual predictive check of the final lumefantrine model for all available data (A) and visual predictive checks of the lumefantrine model stratified for pregnant women with capillary data (B), pregnant women with venous data (C) and non-pregnant women with venous data (D). Open circles represent the observed lumefantrine plasma concentrations. The 5th, 50th and 95th percentiles of the observed data are represented by the solid black lines. The 95% confidence intervals of the 5th, 50th and 95th percentiles of the 2,000 simulations are represented by grey shaded areas.

Table 6.2: Population pharmacokinetic estimates from the final lumefantrine model

Parameter	Fixed effect [a] (%RSE) [b]	95% CI [b]	IIV/IOV† [%CV] [a] (%RSE) [b]	95% CI [b]
CL/F (L/h)	5.09 (7.90)	4.35 - 5.87	17.5 (20.6)	13.8 - 21.0
Vc/F (L)	123 (8.40)	104 -145	-	-
Q/F (L/h)	1.68 (10.2)	1.35 - 2.00	-	-
Vp/F (L)	110 (9.07)	91.7 - 131	21.5 (65.2)	0.213 - 40.0
MTT (h)	4.09 (5.22)	3.70 - 4.55	36.6 (32.0)	22.9 - 47.5
F	1 *fixed*	-	44.8 (31.2)/104 (12.2)†	29.0 - 57.8/87.74 - 125
Box-Cox shape parameter of F	-0.376 (21.7)	-0.516 - -0.227	-	-
Transit compartments (n)	5 *fixed*	-	-	-
Temperature on MTT	0.165 (44.1)	0.0328 - 0.329	-	-
Pregnancy on Q	-0.365 (14.3)	-0.455 - -0.259	-	-
Matrix conversion factor	0.881 (9.32)	0.733 - 1.05	-	-
σ venous	0.0595 (15.3)	0.0382 - 0.0914	-	-
σ capillary	0.0207 (11.8)	0.00957 - 0.0343	-	-
Post-hoc estimates [c]	All women	Non-pregnant women	Pregnant women	
$AUC_{0-\infty}$ (hr*µg/mL)	594 (76.4-1850)	630 (285-1240)	570 (76.4-1850)	
C_{MAX} (µg/mL)	8.37 (0.722-25.6)	8.33 (4.36-15.0)	8.40 (0.722-25.6)	
$T_{1/2}$ (hours)	89.5 (54.3-121)	69.8 (54.3-78.3)	90.3 (64.3-121)	
Day 7 concentration (µg/mL)	0.454 (0.045-2.61)	0.592 (0.258-1.67)	0.423 (0.045-2.61)	

[a] Population mean values, inter-individual variability (IIV) and inter-occasion variability (IOV) estimated by NONMEM. IIV and IOV is presented as the coefficient of variation (CV) and was calculated as $100*\sqrt{e^{\text{mean estimate}}-1}$

[b] Relative Standard Errors (RSEs) are calculated as 100*(standard error/mean value) from 1,000 iterations of a non-parametric bootstrap. The 95% confidence interval (95% CI) is displayed as the 2.5 to 97.5 percentiles of the bootstrap estimates.

[c] Post-hoc estimates were calculated as the median and ranges of the empirical Bayes estimates.

CL/F: elimination clearance, V_C/F: central apparent volume of distribution, V_P/F: peripheral apparent volume of distribution, Q/F: inter-compartmental clearance, MTT: mean transit time, F: relative bioavailability, σ: residual variability for capillary and venous data, AUC: area under the plasma concentration-time curve, C_{MAX}: maximum lumefantrine concentration and $T_{1/2}$: elimination half-life. All parameters are represented as venous matrix.

study (Figure 6.5). This produced a decreased median time of 0.92 days and 0.42 days over the 280 ng/mL and 175 ng/mL targets, respectively, in pregnant women compared to non-pregnant women (Figure 6.5B). This translates into an 7%, 16%, 20%, 20% and 18% lower exposure for pregnant women compared to non-pregnant women when calculating the post-treatment exposures from day 3 to 14, day 4 to 14, day 5 to 14, day 6 to 14 and day 7 to 14, respectively. However, the total exposure was not affected by pregnancy, and lumefantrine plasma concentrations from day 12 onwards were slightly higher in pregnant women compared with those in non-pregnant women. Monte Carlo simulations were also performed to compare results from this study with those previously published for pregnant women in Thailand [83] (Figure 6.5D). This resulted in a similar median day 7 capillary concentration of 370 ng/mL in this study compared to 392 ng/mL in the pregnant women in Thailand.

6.4 Discussion

No comparative pharmacokinetic analyses have been performed previously for lumefantrine in pregnant and non-pregnant women, despite intensive use of this antimalarial drug in the second and third trimesters of pregnancy and poor cure rates in pregnant women in Thailand [66]. An analysis to assess potential effects of pregnancy on lumefantrine pharmacokinetics using a comparable non-pregnant control group was therefore needed.

A transit-compartment absorption model followed by a two-compartment disposition model described the data well in this study. This is in good agreement

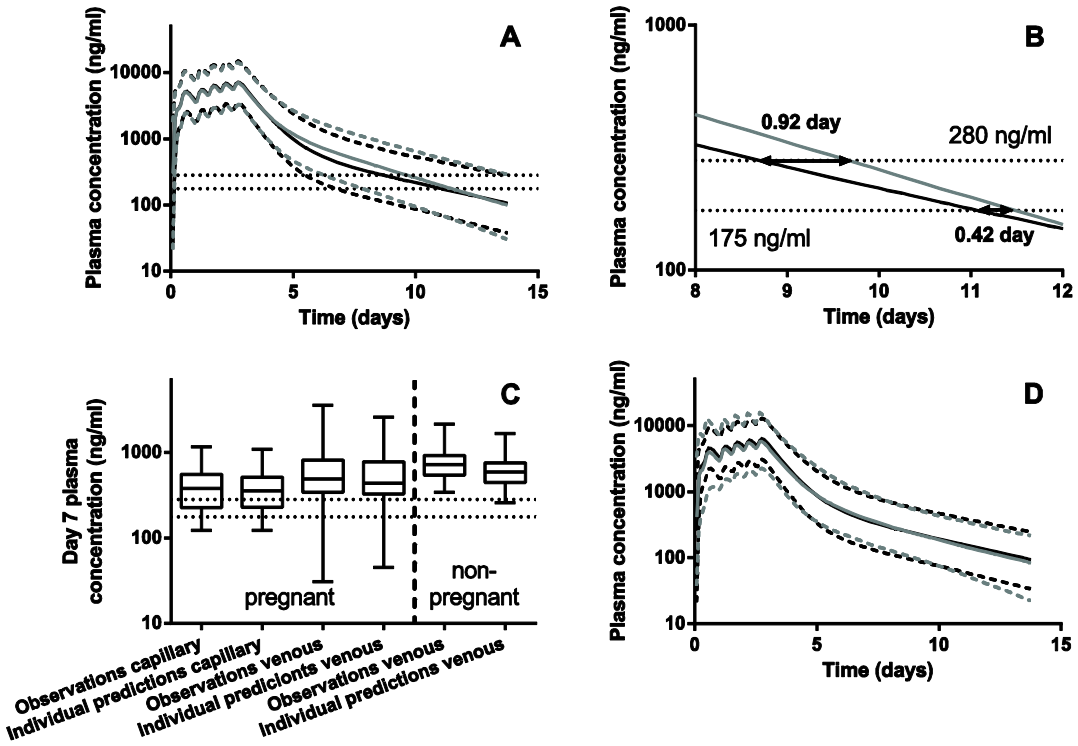

Figure 6.5 An overview of the pregnancy effect on lumefantrine pharmacokinetics. Population predicted concentration-time profiles of lumefantrine venous plasma concentrations in pregnant (black) and non-pregnant (grey) women based on 2,000 simulations from time 0 to day 14 (A) and zoomed in from day 8 to day 12 (B). Panel C show observed and individually predicted day 7 lumefantrine concentrations using the final population pharmacokinetic model. Panel D displays the simulated profiles for lumefantrine capillary plasma concentrations in Uganda (black) and Thailand (grey). Solid lines represent population means and dashed lines represents the 95th and 5th percentiles. The upper and lower horizontal dashed lines in panel A, B and C represent the 280 ng/mL and 175 ng/mL day 7 plasma concentration thresholds, respectively.

with the disposition model presented for sparsely sampled pregnant women in Thailand [83]. However, a three-compartment model was used to describe the disposition pharmacokinetics of lumefantrine in Papua New Guinean children [194]. The extended duration of sampling is likely to explain why a second peripheral compartment was supported by those data. The developed model allowed for a difference in biological matrices (e.g. capillary vs venous plasma) but the 95% confidence interval for the conversion factor ranged from below 1 to above 1 (Table 6.2). This indicated that there was no significant difference between venous and capillary plasma concentrations on a population level, which was also confirmed by backward deletion of the conversion factor parameter (ΔOFV=2.369). Similar findings have been reported previously using a linear regression model to compare capillary and venous lumefantrine plasma concentrations [208].

Shrinkage estimates were relatively high due to the sparse sampling in the capillary arm. For the purpose of this analysis, the shrinkage is acceptable but potential future simulations on an individual level for dose optimization using this model should be treated with caution. The visual predictive check indicates adequate overall predictive power of the model (Figure 6.4). However, confidence intervals in the visual predictive checks stratified for pregnant women with capillary data, venous data, or non-pregnant women with venous data were wider compared to the combined prediction corrected visual predictive check. This is a common phenomenon driven by the smaller sample size in the strata.

Body temperature was a significant covariate on mean absorption transit time. With every degree Celsius increase in body temperature the mean absorption transit time increased by 16.5%. This resulted in a mean transit time of 3.48 hours and 6.05 hours for a patient with a 36.0°C and 39.8°C admission body temperature, respectively. Lumefantrine is poorly absorbed from the gastrointestinal tract into the systemic circulation with an absolute bioavailability of 5% to 12% in rats [202]. Patients with higher fever might have reduced gut motility and prolonged lumefantrine absorption into the systemic circulation. However, this covariate relationship did not affect the systemic lumefantrine exposure in the patients studied here.

Geometric mean values of parasitaemia at admission differed between the three study arms (Table 6.1). However, parasitaemia was tried in the model and did not significantly influence the pharmacokinetics of the drug. This may be explained by similar ranges for the pregnant and non-pregnant group. Furthermore, it has not been shown in previous literature that parasitaemia influences the pharmacokinetics of lumefantrine [83, 194].

Lumefantrine plasma concentration at day 7 has previously been used as a readily measurable simple pharmacokinetic endpoint to predict treatment failure. Simulations using the final population pharmacokinetic model showed lower venous plasma lumefantrine concentrations at day 7 in pregnant women compared to those in non-pregnant women (Figure 6.5). Confidence intervals from the simulations should be interpreted with caution due to relatively large shrinkage values. The lower lumefantrine day 7 plasma concentrations during

pregnancy were caused by a decrease of 36.5% in the inter-compartmental clearance in pregnant women. Due to changes in body composition (increased plasma volume, water and fat content) during pregnancy [90] the distribution of the lipophilic lumefantrine through the body might be altered substantially, which would explain this finding. Total lumefantrine exposure was not affected by pregnancy in this study. However, exposures were higher in non-pregnant women compared with those in pregnant women in the post-treatment phase (area under the plasma concentration–time curve $(AUC)_{day\ 3\text{-}14}$, $AUC_{day\ 4\text{-}14}$, $AUC_{day\ 5\text{-}14}$, $AUC_{day\ 6\text{-}14}$ and $AUC_{day\ 7\text{-}14}$). This might have consequences in terms of efficacy since residual parasites will be eliminated during this phase, preventing recrudescent malaria. Pregnant women displayed higher plasma concentrations from day 12 onwards compared to non-pregnant patients but this is not expected to have a major clinical impact as plasma concentrations were very low by this time. These findings should be interpreted with caution as the control group was not equally sized compared to the arm with pregnant women and this covariate effect may be confounded by the high between-patient variability and between-dose occasion variability on bioavailability. A larger study with a control group would therefore be necessary to confirm the current findings and the potential impact of different pharmacokinetic endpoints (i.e. exposure vs day 7 levels). The bootstrap diagnostics of the full covariate model (Figure 6.2) showed a trend towards lower peripheral volume of distribution during pregnancy, but this covariate did not contribute to a significant improvement of the model. This might be because of the small non-pregnant control group

studied here. Simulated capillary lumefantrine pharmacokinetic profiles indicated similar day 7 concentrations in Thailand compared to Uganda (Figure 6.5D). Both these efficacy studies also reported low observed day 7 lumefantrine concentrations; 35% and 32%, respectively, below the previously defined target concentration of 280 ng/mL [64, 66]. However, low cure rates were reported only in Thailand [66]. The most likely explanation for this difference in efficacy is the substantially higher background immunity in Uganda compared to in Thailand, which would compensate for the underexposure of lumefantrine. More speculative contributors might be altered lumefantrine susceptibility or emerging artemisinin resistance in Southeast Asia [209]. Patients infected with artemisinin resistant parasites would have more residual parasites needing to be cleared by lumefantrine, which could lead to increased failure rates. Lower lumefantrine day 7 concentrations in pregnant patients compared to non-pregnant patients might also accelerate the development of resistance since sub-therapeutic drug exposures may select for parasites with low drug susceptibility [210].

The main metabolite of lumefantrine, desbutyl-lumefantrine, has been reported to have substantial antimalarial activity [211, 212]. It has been suggested that future efficacy and pharmacokinetic studies should include measurement of both lumefantrine and desbutyl-lumefantrine to enable the assessment of a weighted lumefantrine/desbutyl-lumefantrine drug effect [194]. In the current study it was not possible to combine the pharmacokinetic model with a pharmacodynamic model as cure-rates were high. Recently, model efforts have been made to describe the pharmacodynamics of malaria with a time-to-event approach [213].

This type of modelling would be particularly suitable for assessing the individual contributions of lumefantrine and desbutyl-lumefantrine on treatment outcome. Results presented here and model parameters could be used for power calculations and optimal design theory to design an appropriate follow-up study.

6.5 Conclusion

In conclusion, lumefantrine pharmacokinetics was well described using a transit compartment absorption model followed by two disposition compartments. The pharmacokinetic endpoint, day 7 lumefantrine plasma concentration, was 27% lower in pregnant women compared to non-pregnant women and the median times above previously defined target concentrations of 280 ng/mL and 175 ng/mL were decreased by 0.92 days and 0.42 days, respectively. Simulations of capillary plasma concentrations showed similar exposures compared to a previous study in pregnant women in Thailand. However, a high cure rate was seen in this study, most likely because of higher background immunity or increased drug susceptibility to lumefantrine and/or artemether. To avoid the development of resistance and to improve the cure rates of artemether-lumefantrine in other geographical regions, more studies and modelling work have to be performed to support dose optimization, in combination with a confirmatory pharmacokinetic study using an equal sized control group.

7.0 Lumefantrine/desbutyl-lumefantrine

7.1 Background

Artemether-lumefantrine has been reported to be safe to use during the second and third trimester of pregnancy although variable cure rates have been reported in this population [64, 66]. High cure rates were seen in pregnant women in Uganda (98.2%; range 93.5–99.7% at delivery or day 42 if later) but considerably lower cure rates were reported in pregnant women in Thailand (82.0%; range 74.8–89.3% at delivery or day 42 if later) [64, 66]. More than 30% of the patients had day 7 lumefantrine plasma concentrations below the target concentration of 280 ng/mL in both studies [64, 66]. A speculative reason for the lower cure rates in Thailand might be higher background immunity in Africa compared to Thailand or different drug susceptibility in the different regions [214].

Desbutyl-lumefantrine, the main metabolite of lumefantrine, has been reported to have substantial antimalarial activity [211, 212]. Half maximal inhibitory concentrations (IC_{50}) of desbutyl-lumefantrine against clinical isolates of *Plasmodium falciparum* from Mae Hong Son 1997, 1998 and Mae Sot 1998 were 4.38, 6.54 and 8.94 nM, respectively [212]. *In-vitro* IC_{50} values of desbutyl-lumefantrine to laboratory adapted *Plasmodium falciparum* parasites were 9.0 nM and 9.5 nM for chloroquine sensitive (3D7) and chloroquine resistant (W2mef) cultures, respectively [211]. IC_{50} values for lumefantrine in the same *in-vitro* experiments were 65.2 nM and 55.5 nM for 3D7 and W2mef cultures, respectively [211]. These results suggest a much higher antimalarial activity of desbutyl-lumefantrine compared to that of lumefantrine. However, the *in-vivo* ratio of lumefantrine to desbutyl-lumefantrine exposure was 27.4 (7.0-123) in

Papua New Guinean children [211] and the ratio of desbutyl-lumefantrine to lumefantrine concentrations was lower than 5% in the majority of samples in pregnant women in Thailand [80]. Nevertheless, it has been suggested that future efficacy and pharmacokinetic studies should include measurements of both lumefantrine and desbutyl-lumefantrine to enable the assessment of a weighted lumefantrine/desbutyl-lumefantrine drug effect [194].

7.1.1 Study aim

The aim of this study was to assess the population pharmacokinetics and pharmacodynamics of lumefantrine and desbutyl-lumefantrine using a simultaneous drug-metabolite model in pregnant women in the second and third trimester with uncomplicated *Plasmodium falciparum* malaria in Thailand.

7.1.2 Absorption

The time to reach the lumefantrine maximum plasma concentration is 4.0 (4.5-6.0) hours [80, 184-186]. Lumefantrine's main metabolite, desbutyl-lumefantrine, reaches the maximum plasma concentration later compared to lumefantrine at approximately 8 (0.5-12) hours after dosing [80].

7.1.3 Distribution

Only one simultaneous lumefantrine/desbutyl-lumefantrine population pharmacokinetic model has been described and used three and two distribution compartments in children [194].

7.1.4 Metabolism and elimination

There is no information available in literature regarding desbutyl-lumefantrine metabolism in human or in animals. However, one study in Papua New Genuan children indicated a median (interquartile range) terminal elimination half-life for desbutyl-lumefantrine of 141 (135-150) hour [194].

7.2 Study design

Data from two previously published studies, conducted at the north western border of Thailand with Myanmar, was pooled for the current analysis [80, 83]. In both studies, patients were in their second or third trimester of pregnancy and had uncomplicated *Plasmodium falciparum* malaria. Women in the first study (n=13) [80] were enrolled as recrudescent patients with uncomplicated *Plasmodium falciparum* malaria after a supervised quinine treatment of 7 days. Inclusion criteria were second or third pregnancy trimester, ability to understand and adhere to the protocol of the study and haematocrit of 25% or greater. Pregnant patients in the second study (n=103) [83] were enrolled through weekly screening visits at the antenatal clinic (Shoklo Malaria Research Unit) [215]. Inclusion criteria were second or third pregnancy trimester, slide-positive *Plasmodium falciparum* malaria infections between 6 parasites per 500 leukocytes and 40 parasites per 1,000 erythrocytes and the absence of signs of severe malaria. Exclusion criteria for both studies were an inability to follow the antenatal clinic consultation, known chronic disease (cardiac, renal, or hepatic disease or haemoglobinopathy), a history of alcohol or narcotic abuse, signs of

severe malaria, imminent delivery, allergy to artemisinin derivatives or lumefantrine or an inability to tolerate oral treatment. Patients were asked to sign a form of consent if all inclusion criteria and none of the exclusion criteria were fulfilled.

7.2.1 Dosing regimen and blood sampling

Patients in both studies received an identical standard treatment consisting of 80 mg artemether and 480 mg lumefantrine (Coartem, Novartis, Basel, Switzerland) administered as fixed oral treatment twice daily for three days. However, sampling procedures were different between the studies. In study one, venous blood samples (2 mL) were drawn before the last dose and 0.5, 1, 2, 4, 6, 8, 12, 24, 48, 72, 96, 120, 144 and 168 hours after the last dose [80]. In study two, capillary blood from a finger prick was collected randomly in the time windows 0-72 hour, 72-96 hour, 96-144 hour and 144-336 hour after the first dose [83].

7.2.2 Drug analysis

Both lumefantrine and desbutyl-lumefantrine venous plasma concentrations were initially quantified in study one, by using liquid chromatography with UV detection [216]. Capillary lumefantrine plasma concentrations were initially quantified in study two, by using liquid chromatography with UV detection [216]. All capillary samples were reanalysed 5 years later, by using a liquid chromatography-mass spectrometry, for desbutyl-lumefantrine quantification. The lower limit of quantifications for lumefantrine and desbutyl-lumefantrine were 24 ng/mL and 21 ng/mL, respectively, using liquid chromatography with UV detection. The lower limit of quantification for desbutyl-lumefantrine was 10 ng/mL using liquid

chromatography with mass spectrometry detection. The coefficients of variation (%CV) were lower than 8.2% and 7.9% for all quality control samples using UV-detection and mass spectrometric detection, respectively.

7.3 Results

This pooled analysis was conducted using data from two previously published studies. A total number of 13 and 103 patients were enrolled in the dense venous sampled study and in the sparse capillary sampled study, respectively (Table 7.1) [80, 83]. Seventeen out of these 116 patients had recrudescent infections; 22 patients had a novel infection and 77 patients had no parasite reappearance during the 42 days of follow-up in study one [80] and the follow up until delivery or day 42 if later in study two [83] (Table 7.1). The time to recrudescent malaria was 23 (14-63) days. The median time to novel malaria infection was 35 (15-140) days (Table 7.1).

7.3.1 Population pharmacokinetic lumefantrine/desbutyl-lumefantrine model

A two-compartment drug-metabolite model using first-order absorption with lag time was used to simultaneously describe the lumefantrine and desbutyl-lumefantrine pharmacokinetic data (Figure 7.1). Implementation of relative bioavailability significantly (ΔOFV = -284) improved the model fit and a box-cox transformation on relative bioavailability (ΔOFV = -4.86) was needed to correct for model miss-specification in the diagnostic plots (Figure 7.2).

Table 7.1: Demographic summary of the study population.

	Dense sampled [80]	Sparse sampled [83]
Study size	13	103
PK sample size (LF/DLF)	207/175	481/342
PK sample size/patient (LF/DLF)	16 (15-16)/16 (15-16)	5 (1-5)/4 (1-5)
PD sample size (LF/DLF)	13	103
PD sample size/patient (LF/DLF)	1	1
Age (year)	20 (14–42)	24 (15–42)
Body weight (kg)	47 (41–57)	49 (35–65)
Body temperature (°C)	36.0 (35.0–38.5)	36.7 (35.0–39.3)
Estimated gestational age (weeks)	23 (13.1–38.0)	22.6 (13.1–39.0)
Primiparity (%)	31	22.3
Parasitaemia(/µL)	837 (91–25,704)	4,400 (57–153,734)
No parasite reappearance (%)	92.3	63.1
New infections (%)	7.69	20.4
Time to new infection (days)	21	35 (15-140)
Recrudescent infections (%)	0	16.5
Time to recrudescent infection (days)	-	23 (14-63)

LF: lumefantrine DLF: desbutyl-lumefantrine

Values are reported as median (range)

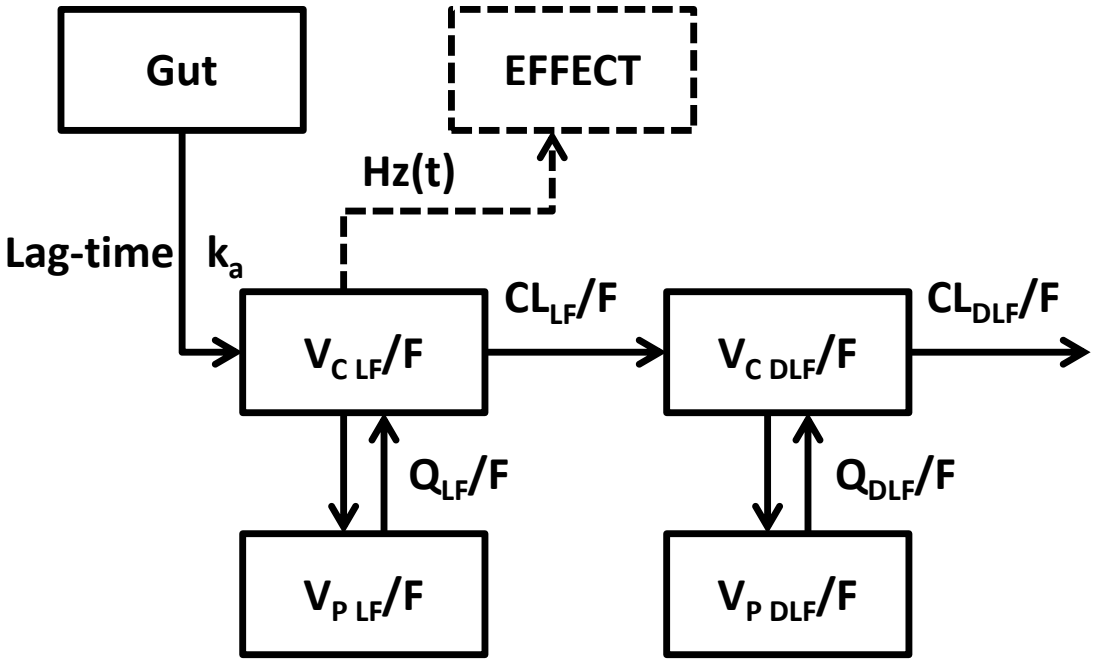

Figure 7.1 Visual representation of the structural population pharmacokinetic drug-metabolite model for lumefantrine and desbutyl-lumefantrine. k_a: absorption rate constant, $V_{C\ LF}/F$: apparent central volume of lumefantrine distribution, $V_{P\ LF}/F$: apparent peripheral volume of lumefantrine distribution, Q_{LF}/F: inter-compartmental clearance lumefantrine, CL_{LF}/F: elimination clearance lumefantrine, $V_{C\ DLF}/F$: apparent central volume of desbutyl-lumefantrine distribution, $V_{P\ DLF}/F$: apparent peripheral volume of desbutyl-lumefantrine distribution, Q_{DLF}/F: inter-compartmental clearance desbutyl-lumefantrine, CL_{DLF}/F: elimination clearance desbutyl-lumefantrine and Hz(t): hazard function.

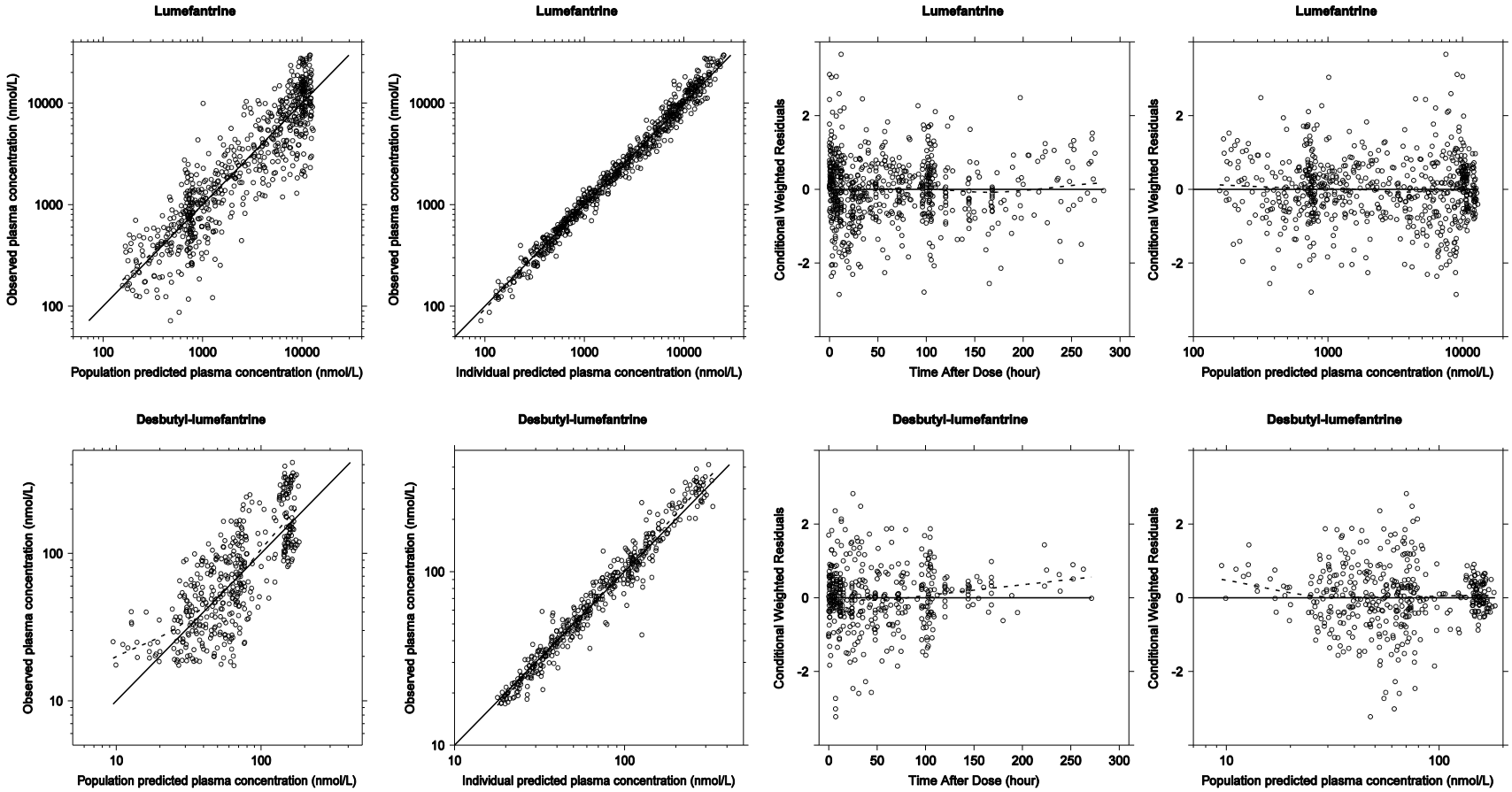

Figure 7.2 Goodness-of-fit plots from the simultaneous pharmacokinetic lumefantrine-desbutyl-lumefantrine model. The black solid line, black dashed line and open circles represent the line of identity, trend-line and observations respectively. Two lumefantrine and desbutyl-lumefantrine baseline values were excluded for the diagnostic plots as they were considered as outliers.

A correction factor was implemented on a population level to correct for differences between the biological matrices (i.e. venous vs capillary plasma) (Table 7.2). Different random residual variability was implemented for venous and capillary samples for both lumefantrine and desbutyl-lumefantrine (Table 7.2).

The covariates parasitaemia (linear on lumefantrine elimination clearance, exponential on desbutyl-lumefantrine elimination clearance and exponential on desbutyl-lumefantrine central apparent volume of distribution) and estimated gestational age (power relationship on the absorption rate constant, linear on lumefantrine inter-compartmental clearance, exponential on lumefantrine peripheral apparent volume of distribution, exponential on desbutyl-lumefantrine central apparent volume of distribution, exponential on lumefantrine elimination clearance, linear on desbutyl-lumefantrine elimination clearance and exponential on desbutyl-lumefantrine inter-compartmental clearance) were selected during the forward step of the stepwise covariate modelling. However, only parasitaemia on desbutyl-lumefantrine elimination clearance and estimated gestational age on the absorption rate constant and lumefantrine inter-compartmental clearance could be retained after the backward step of the stepwise covariate modelling.

The basic goodness of fit plots show accurate and precise predictions of the lumefantrine and desbutyl-lumefantrine data (Figure 7.2). Desbutyl-lumefantrine plasma concentration data below the limit of quantification in the terminal

Table 7.2: Population pharmacokinetic parameter estimates from the final model.

	Fixed effects [a] (%RSE) [b]	95% CI [b]	IIV [a] (%RSE) [b]	95% CI [b]
CL_{LF}/F (L/h)	5.35 (12.9)	4.11-6.77	11.2% (49.5)	3.20-15.7
$V_{C\ LF}$/F (L)	28.4 (26.8)	17.3-46.8	119% (29.4)	78.1-178
Q_{LF}/F (L/h)	1.55 (13.9)	1.17-2.00	23.9% (45.2)	9.14-33.7
$V_{P\ LF}$/F (L)	147 (13.9)	110-187	-	-
k_a (h^{-1})	0.0577 (7.93)	0.0526-0.0655	-	-
Lag-time (h)	1.31 (43.6)	0.0131-2.05	-	-
CL_{DLF}/F (L/h)	197 (11.5)	156-245	23.2% (59.1)	6.93-36.5
$V_{C\ DLF}$/F (L)	6,490 (21.1)	3,460-8,970	90.5% (93.9)	44.8-181
Q_{DLF}/F (L/h)	250 (19.1)	183-369	-	-
$V_{P\ DLF}$/F (L)	13,200 (12.6)	10,500-16,900	-	-
F (%)	100 (fixed)	-	51.2% (14.3)	42.7-58.3
Shape parameter	-0.394 (48.3)	(-)0.765-(-)0.0279	-	-
LF conversion factor	0.878 (13.2)	0.667-1.12	-	-
DLF conversion factor	0.464 (11.5)	0.371-0.585	-	-
Parasitaemia on CL_{DLF}	0.133 (31.8)	0.0455-0.210	-	-
EGA on k_a	-0.715 (19.1)	(-)0.972-(-)0.474	-	-
EGA on Q_{LF}	-0.0271 (22.8)	(-)0.0359-(-)0.0134	-	-
σ venous LF	0.252 (54.0)	0.0208-0.550	-	-
σ capillary LF	0.0464 (15.4)	0.0332-0.0598	-	-
σ venous DLF	0.335 (52.7)	0.0178-0.639	-	-
σ capillary DLF	0.0326 (18.9)	0.0213-0.0458	-	-
Time to event analysis	LF effect		DBL drug effect	
	Fixed effects [a] (%RSE) [b]	95% CI [b]	Fixed effects [a] (%RSE) [b]	95% CI [b]
Baseline hazard	0.000517 (42.2)	0.000268-0.00129	0.000653 (40.9)	0.000332-0.00151
Hazard half-life	401 (23.1)	226-582	381 (17.8)	259-516
IC_{50} (ng/mL)	144 (43.5)	33.6-262	6.10 (53.9)	1.17-14.0

[a] Population mean values and inter-individual variability (IIV) estimated by NONMEM. IIV is presented as $\sqrt{e^{\text{estimate}-1}}\ \text{x}\ 100$

[b] The Relative Standard Error (RSE) is calculated as $100\ \text{x}\ \frac{\text{standard deviation}}{\text{mean parameter estimate}}$ from 1,000 iterations of a non-parametric bootstrap diagnostics. The 95% confidence interval (95% CI) is displayed as the 2.5 to 97.5 percentile of the bootstrap estimates.

LF: lumefantrine, DLF: desbutyl-lumefantrine, Box-Cox shape parameter: shape parameter on Box-Cox transformation, k_a: absorption rate constant, V_C/F: apparent central volume of distribution, V_P/F: apparent peripheral volume of distribution, Q/F: inter-compartmental clearance, CL/F: elimination clearance and IC_{50}: required concentration to reduce the hazard of getting recrudescent malaria with 50%.

elimination phase did not result in any model misspecification (Figure 7.3). The prediction corrected visual predictive check (n=2,000) indicated accurate predictive power for lumefantrine and desbutyl-lumefantrine plasma concentrations (Figure 7.4). Eta shrinkage was high and ranged between 28.1% and 45.5%. Epsilon shrinkage was 4.76%, 21.0%, 3.90% and 28.8% for the venous lumefantrine, capillary lumefantrine, venous desbutyl-lumefantrine and capillary desbutyl-lumefantrine, respectively.

7.3.2 Population pharmacokinetic-pharmacodynamic lumefantrine/desbutyl-lumefantrine model

Pharmacokinetic parameters were fixed to the final estimates and pharmacokinetic-pharmacodynamic data was fitted simultaneously. Interval censoring for the weekly screening was implemented for recrudescent malaria and a gompertz hazard model (OFV = -703) performed better compared to a constant (OFV = -693) or weibull (OFV = -695) hazard model. Both desbutyl-lumefantrine (ΔOFV = -5.19) and lumefantrine (ΔOFV = -7.17) plasma concentrations had a significant effect on the hazard of recrudescent malaria using an E_{MAX} model. However, lumefantrine realised the largest effect and an additive drug effect of desbutyl-lumefantrine did not further improve the model fit. Estimated gestational age (exponential on baseline hazard and exponential on hazard elimination half-life) and body weight (exponential on baseline hazard) were all selected as significant covariates during the forward addition step of the stepwise covariate modelling. However, none of these covariates could be retained in the backward elimination of selected covariates.

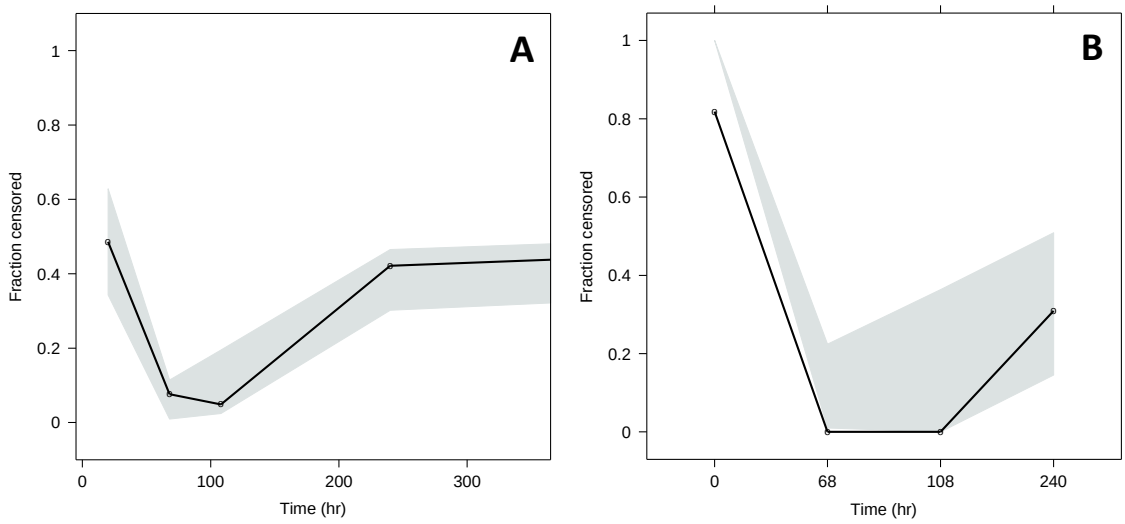

Figure 7.3 Visual predictive check for fraction of censored data. The black solid line represents the observed fraction of plasma samples below quantification limit and the grey shaded area represents the confidence interval of the simulated (n=2,000) fraction plasma samples below quantification limit for the sparse capillary desbutyl-lumefantrine (A) and dense venous desbutyl-lumefantrine (B) data, respectively.

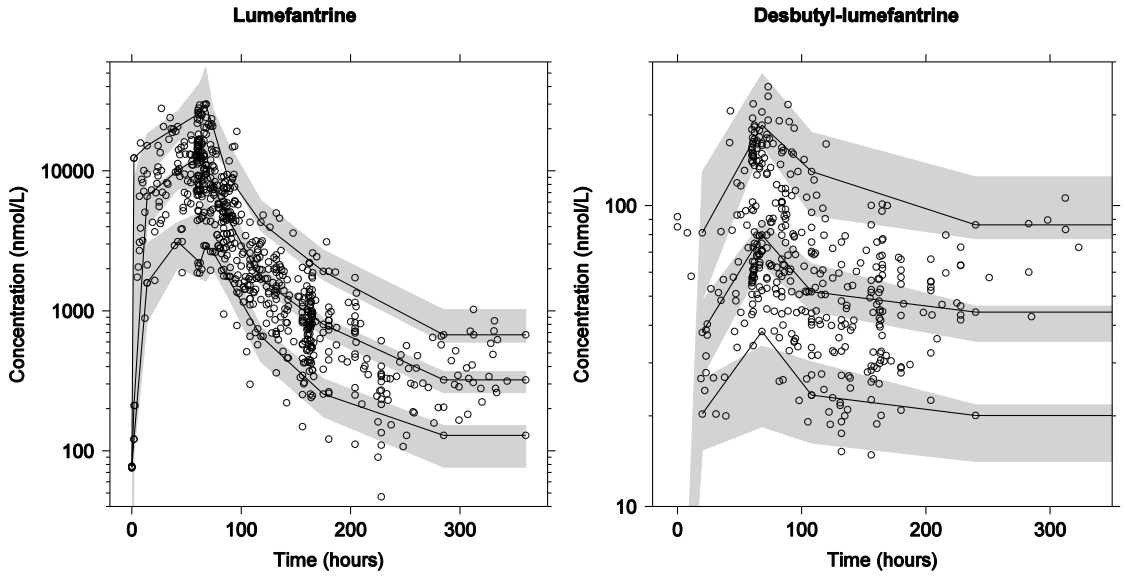

Figure 7.4 Visual predictive check (n=2,000) for lumefantrine and desbutyl-lumefantrine. The black circles represent the observations, the black solid lines represent the 5th, 50th and 95th percentiles of the observed data and the grey shaded areas represent the 90% confidence intervals of the simulated 5th, 50th and 95th percentiles.

Novel infections could be described using a constant hazard model with interval censoring, based on the back-calculated interval time of parasites release from the liver to the blood [217]. The implementation of a lumefantrine or desbutyl-lumefantrine drug effect (E_{MAX} and sigmoidal E_{MAX}) on the constant hazard model did not realise a significant improvement of the model fit.

The 90% confidence interval of 2,000 simulated Kaplan-Meier plots accurately describes the observed recrudescent malaria using either lumefantrine or desbutyl-lumefantrine as drug effect (Figure 7.5A & 7.5B). However, the 90% confidence interval of relative hazard versus plasma concentration indicated a better predictive power for the model using lumefantrine as a predictor of outcome compared to desbutyl-lumefantrine (Figure 7.5C & 7.5D).

7.3.3 Simulations

Monte-Carlo simulations (n=2,000) were performed using the final pharmacokinetic-pharmacodynamic model for a twice daily treatment of three days, five days and ten days. Not surprisingly, simulated lumefantrine and desbutyl-lumefantrine concentrations at day 7 and day 14 increased with extended treatment duration (Figure 7.6E, 7.6F, 7.6G & 7.6H). This resulted in a decreased estimated incidence of recrudescent malaria at day 42 with increasing duration of treatment (Figure 7.6A, 7.6B, 7.6C, & 7.6D).

7.4 Discussion

No population pharmacokinetic-pharmacodynamic analyses for lumefantrine/desbutyl-lumefantrine have been performed in pregnant women,

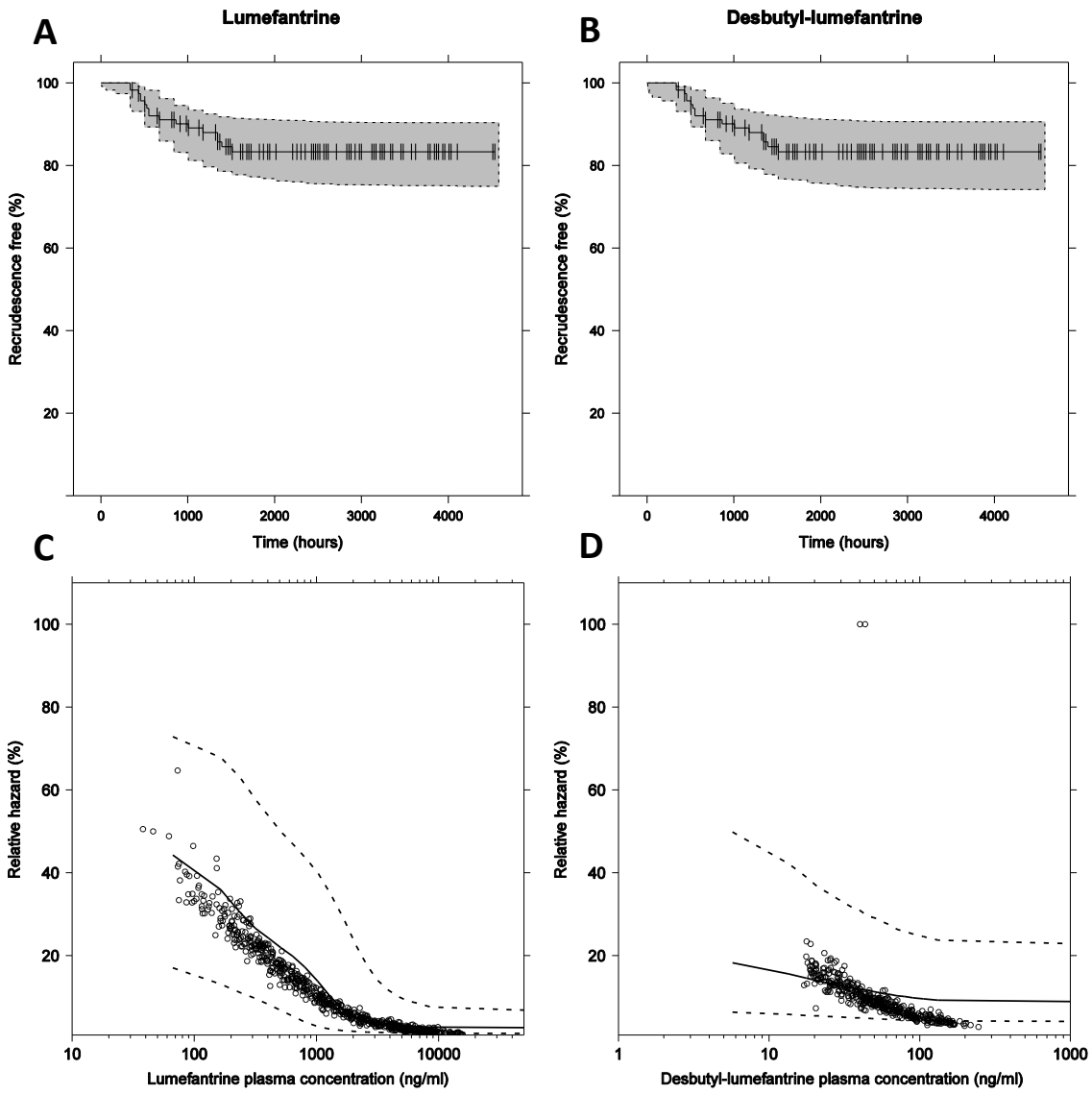

Figure 7.5 Visual predictive check for the time to event Kaplan-Meier analysis with lumefantrine drug effect (A) and desbutyl-lumefantrine drug effect (B), respectively. The gray shaded area represents the 95% confidence interval from 2,000 simulations. A visual predictive check for the relative hazard of recrudescent malaria compared to the baseline hazard versus lumefantrine (C) and desbutyl-lumefantrine (D) plasma concentrations. The dots represent observed concentrations and corresponding estimated relative hazards and the solid and dashed lines represent the median, 5th and 95th percentiles of 2,000 simulations using the final pharmacokinetic-pharmacodynamic model.

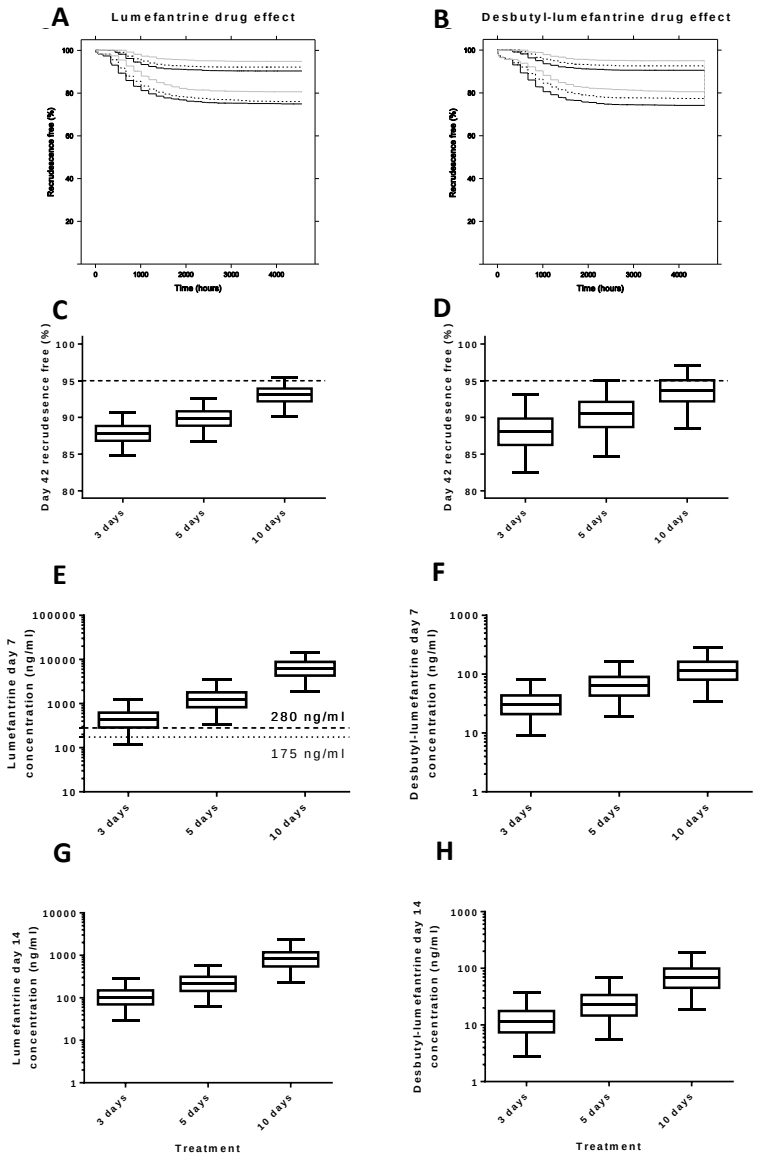

Figure 7.6 The black solid (3 day treatment), black dashed (5 day treatment) and grey solid (10 day treatment) lines represent the 95% confidence intervals of simulated (n=2,000) Kaplan-Meier plots using the final pharmacokinetic-pharmacodynamic model (panel A: using lumefantrine and panel B: using desbutyl-lumefantrine as drug effect). Panel C and D represent the percentage recrudescence free patients at day 42, panel E and F represent plasma concentrations at day 7, and panel G and H represent plasma concentration at day 14. The boxes and whiskers in panel C-H represent the 25%-75% and 2.5%-97.5% of the simulated data. The horizontal dashed line in panel C and D represents the 95% recrudescent malaria free patients. The horizontal dashed line in panel E represents the 280 ng/mL target lumefantrine plasma concentration.

despite the lowered cure rates during pregnancy on the Thai-Myanmar border and the *in-vitro* antimalarial activity of desbutyl-lumefantrine. An analysis to assess potential alterations of lumefantrine and desbutyl-lumefantrine pharmacokinetics and pharmacodynamics during pregnancy using a population approach was therefore urgently needed.

7.4.1 Population pharmacokinetic lumefantrine/desbutyl-lumefantrine model

Lumefantrine absorption and disposition pharmacokinetics were best described using first-order absorption with lag-time followed by a two-compartment distribution model (Figure 7.1). This was identical to the previously performed analysis of the sparsely sampled capillary lumefantrine data [83]. Desbutyl-lumefantrine was best described using two disposition compartments as previously shown in Papua New Guinean children [194]. Estimated gestational age as a covariate on inter-compartmental clearance of lumefantrine corresponds with previously published findings in pregnant and non-pregnant women in Uganda [214]. Estimated gestational age as a covariate on k_a, resulting in a reduced k_a with increasing gestational age, could be explained by decreased gut-motility during pregnancy [90-92]. Parasitaemia correlated significantly with desbutyl-lumefantrine elimination clearance resulting in a higher clearance for patients with higher admission parasitaemia. However, no information is available in literature about the metabolic pathway of desbutyl-lumefantrine, which complicates the interpretation of this covariate relationship. A

speculative explanation might be increasing enzyme activity or decreasing plasma protein binding with increasing parasitaemia. However, altered plasma protein binding is a more likely explanation compared to increased enzyme activity as generally enzymes tend to display lowered activity in more severely sick patients. The final population pharmacokinetic model showed a good predictive performance and goodness-of-fit diagnostics for lumefantrine and desbutyl-lumefantrine.

7.4.2 Population pharmacokinetic-pharmacodynamic lumefantrine/desbutyl-lumefantrine model

Pharmacokinetic parameters were fixed in the pharmacokinetic-pharmacodynamic model and the chosen approach resulted in an adequate fit of observed data for recrudescent malaria (Figure 7.5). A sigmoidal E_{MAX} model for both lumefantrine and desbutyl-lumefantrine realised a significant improvement of the model fit but it was not considered superior over an E_{MAX} model due to the instability of the model (>100% different Hill-factors with different initial estimates). A possible explanation for the poor stability might be the small number of recrudescent malaria episodes (17 out of 116 observations) during the follow-up period. Lumefantrine and desbutyl-lumefantrine plasma concentrations could be used interchangeably as predictors for recrudescent malaria but lumefantrine showed a better predictive power compared to desbutyl-lumefantrine (Figure 7.5C & 7.5D). Neither lumefantrine nor desbutyl-lumefantrine plasma concentrations resulted in a significant prophylactic effect of preventing novel infections in pregnant women on the Thailand-Myanmar border.

Lumefantrine has a relatively short half-life of 3.3 days which is likely to explain the lack of prophylactic efficacy during the follow-up period.

7.4.3 Simulations

Prolonged treatment simulations using the final model assumed time-independent lumefantrine and desbutyl-lumefantrine pharmacokinetics. The simulations showed that an extension of the standard three day treatment with two days (twice daily dosing for five days) or seven days (twice daily dosing for ten days) resulted in improved cure-rates but did not realise cure-rates above 95%. However, the results should be interpreted with caution due to relatively high eta-shrinkage estimates. Furthermore, the model failed to realise a cure-rate close to 100% with a ten day treatment course and the current plasma concentration range although this would not be expected. The sigmoidal E_{MAX} model could not be reliably estimated and a bigger sample size might therefore enable a more precise estimation of the Hill-factor. This may consequently result in a cure-rate close to 100% with a ten day treatment course and plasma concentration within the current range. On the other hand, prolonged treatment will also increase the total artemether/dihydroartemisinin exposure which results in a lower parasite load to be killed by lumefantrine. However, the artemether/dihydroartemisinin effect in the model is included in the current lumefantrine drug effect. Accurate cure rates after prolonged treatment simulated with the current model will therefore be not accurately estimated due to the absence of an artemether/dihydroartemisinin drug-effect. However, the

simulations indicate a relative increase in treatment outcome after prolonged treatment duration compared to that after a standard dosing regimen.

Other factors rather than solely pharmacokinetic exposures might have an impact on the treatment outcome. A residual parasite resistant to lumefantrine might be hard to eliminate from the human body and this might be even more pronounced in pregnant patients due to their modulated immune system. Also, resistance against artemisinin derivatives in South East Asia can contribute to the decreased treatment efficacy due to an increased number of residual parasites which have to be cleared by lumefantrine.

The most important issue at this point is to understand the underlying source of the reduced efficacy of artemether/lumefantrine during pregnancy on the Thailand-Myanmar border, and if adequate dose optimisation can increase the cure-rate. A sufficiently powered study with an equally sized non-pregnant control group, frequent pharmacokinetic (lumefantrine/desbutyl-lumefantrine and artemether/dihydroartemisinin plasma concentration samples), and pharmacodynamic samples (parasite clearance time and treatment outcome) is therefore urgently needed. The continued use of currently recommended doses of this drug combination in pregnant women on the Thailand-Myanmar border might result in increased failure rates and the spread of drug resistant parasites.

7.5 Conclusion

In conclusion, a simultaneous drug-metabolite model was developed which adequately described the pharmacokinetic properties of lumefantrine and

desbutyl-lumefantrine. The pharmacodynamic data was successfully modelled using a time-to-event model linked to the pharmacokinetic model. Lumefantrine and desbutyl-lumefantrine could be used interchangeably as predictors of treatment failure but lumefantrine realised a better predictive power in this model. An additive drug effect of desbutyl-lumefantrine did not further improve the model fit. Simulations showed that the drug combination of artemether/lumefantrine with the standard dosing regimen is not effective on the Thailand-Myanmar border in the treatment of uncomplicated *Plasmodium falciparum* malaria during the second and third trimester of pregnancy and that increased treatment duration results in improved cure rates.

8.0 A power calculation methodology for mixed designs

8.1 Background

Population pharmacokinetic analyses can be performed on datasets consisting of dense, sparse or a combination of dense and sparse sampled data [218]. The random variability in a population pharmacokinetic analysis is preferably explained by physiological covariates (e.g. body weight, sex, body temperature), irrespectively of which sampling design is being analysed. However, both the sampling schedule and number of individuals affects the statistical power for hypothesis testing of these covariates. A dataset consisting of mixed sparse and dense sampled individuals requires a different sample size for hypothesis testing compared to a study design consisting of solely a dense or sparse sampled study design. Furthermore, the ratio of sparse/dense sampled individuals in a combined study design may also contribute to altered precision of the parameter estimates. The impact of (combined) sampling schemes on statistical power to detect covariate effects and precision of the pharmacokinetic parameters should therefore be evaluated during the design phase of the study. This can ensure that the design is sufficient to answer the key research questions of the population pharmacokinetic study. The Monte Carlo Mapped Power calculation method [106] (a simulation based power calculation methodology using the likelihood ratio test) was further developed in the current study to enable the determination of statistical power for varying sample sizes of sparse only, dense only and mixed sparse/dense sampled study designs.

An example for pharmacokinetic studies with mixed designs is a pharmacokinetic study nested within a clinical efficacy study. Typically, these studies include a

relatively densely sampled pharmacokinetic study arm, implemented for a descriptive pharmacokinetic analysis, and a relatively sparse sampled pharmacokinetic study arm, which may have been implemented for hypothesis testing of covariates. Optimal design methods have been used to ensure the design is adequate for the descriptive pharmacokinetic analysis (i.e. good precision for parameter estimates). However, these type of pharmacokinetic studies are rarely designed under the assumption that hypothesis testing of covariate effects can be performed using the sparse and dense sampled study arms simultaneously. Moreover, often no sample size calculations are performed to detect the covariate effects on the full study population which may change the required sample size compared to sample size calculations performed to detect the covariate effects on the sparse or dense sampled design only. The impact of sampling design and number of individuals in mixed study designs should therefore be evaluated during the design phase of the study to avoid unethical situations where either too few or too many patients are enrolled.

Another situation where power calculations for mixed pharmacokinetic study designs could be useful is pooling of individual datasets for a meta-analysis. Power calculations for mixed study designs can confirm if the sample size available for the meta-analysis is sufficient to detect a clinically important effect of the covariate of interest. The calculated statistical power may highlight the need for inclusion of more studies to the pooled dataset and thereby save unnecessary work, notably, pooled population pharmacokinetic analyses are computationally intensive.

8.1.1 Study aim

The aim of this study was to apply a data-dependent approach using the likelihood ratio test to perform statistical power calculations for mixed (sparse and dense sampled) study designs. A workflow which guides an easy and straightforward pharmacokinetic study design, considering the cost efficiency of alternative study designs, was used during this study.

8.2 Methods

The data dependent statistical power calculation methodology using the likelihood ratio test for mixed pharmacokinetic study designs was first assessed through a predefined workflow (Figure 8.1) on a hypothetical drug. The impact of different study designs (i.e. cross-over study design, parallel study design and different sampling schemes) on the required sample size to detect the covariate was evaluated. The power calculation methodology was subsequently used to design a case study. The anti-malarial, dihydroartemisinin, was used for the case study and a pharmacokinetic study was designed to evaluate the effect of the binary covariate, pregnancy, on its pharmacokinetics.

8.2.1 The models

The pharmacokinetic model used for the simulation example followed first order absorption, one compartment disposition pharmacokinetics and first order elimination (Table 8.1) [82]. The model used for the dihydroartemisinin example followed transit absorption, one compartment disposition pharmacokinetics and first order elimination (Table 8.1) [82]. A binary covariate on elimination clearance

Table 8.1: Summary of simulation and dihydroartemisinin example.

	Simulation example		Dihydroartemisinin example	
Pharmacokinetic model				
	fixed effects	IIV/IOV†	fixed effects	IIV/IOV†
Transit compartments (n)	-	-	7	-
MTT (h)	-	-	0.982	0.23†
k_a (h-1)	0.8	0.1	-	-
F (%)	-	-	100 (fixed)	0.0881
CL (L/h)	20	0.08/0.02†	78	-
V (L)	70	0.1	129	0.0162
Covariate on CL (%)	30	-	20	-
Residual error	10% (proportional on arithmetic data)		0.3364 (additive on LN data)	
Dataset				
	Parallel design	Crossover design	Parallel design	
Sampling times sparse (h)	window 1: 0, 0.5, 1, 1.5, 2, 2.5, 3 or 4 window 2: 5, 6, 8, 10, 12, 16, 20 or 24	window 1: 0, 0.5, 1, 1.5, 2, 2.5, 3 or 4 window 2: 5, 6, 8, 10, 12, 16, 20 or 24	pregnant window 1: 0.42-0.48, window2: 1.2-3.4, window3: 3.4-4.9 and window 4: 6.0-8.0 non-pregnant window1: 0.28-0.48, window 2: 0.5-0.95, window3: 2.5-3.7 and window 4: 5.8-6.6 [219]	
Sampling times dense (h)	0, 0.5, 1, 1.5, 2, 2.5, 3, 4, 5, 6, 8, 10, 12, 16, 20 and 24	0, 0.5, 1, 1.5, 2, 2.5, 3, 4, 5, 6, 8, 10, 12, 16, 20 and 24	0, 0.25, 0.5, 1, 2, 3, 4, 6, 8 and 12 [82]	
Number of patients	1,000	500	1,000	
Financial figures				
	Parallel design	Crossover design	Parallel design	
Sparse sampled hospital cost (units)	750	1,500	750	
Dense sampled hospital cost (units)	1,000	2,000	1,000	
Price per analyses sample (units)	50	50	50	

MTT: mean transit time, k_a: absorption rate constant, F: bioavailability, CL: elimination clearance, V: apparent volume of distribution, IIV: inter-individual variability presented as variance and IOV: inter-occasion variability presented as variance.

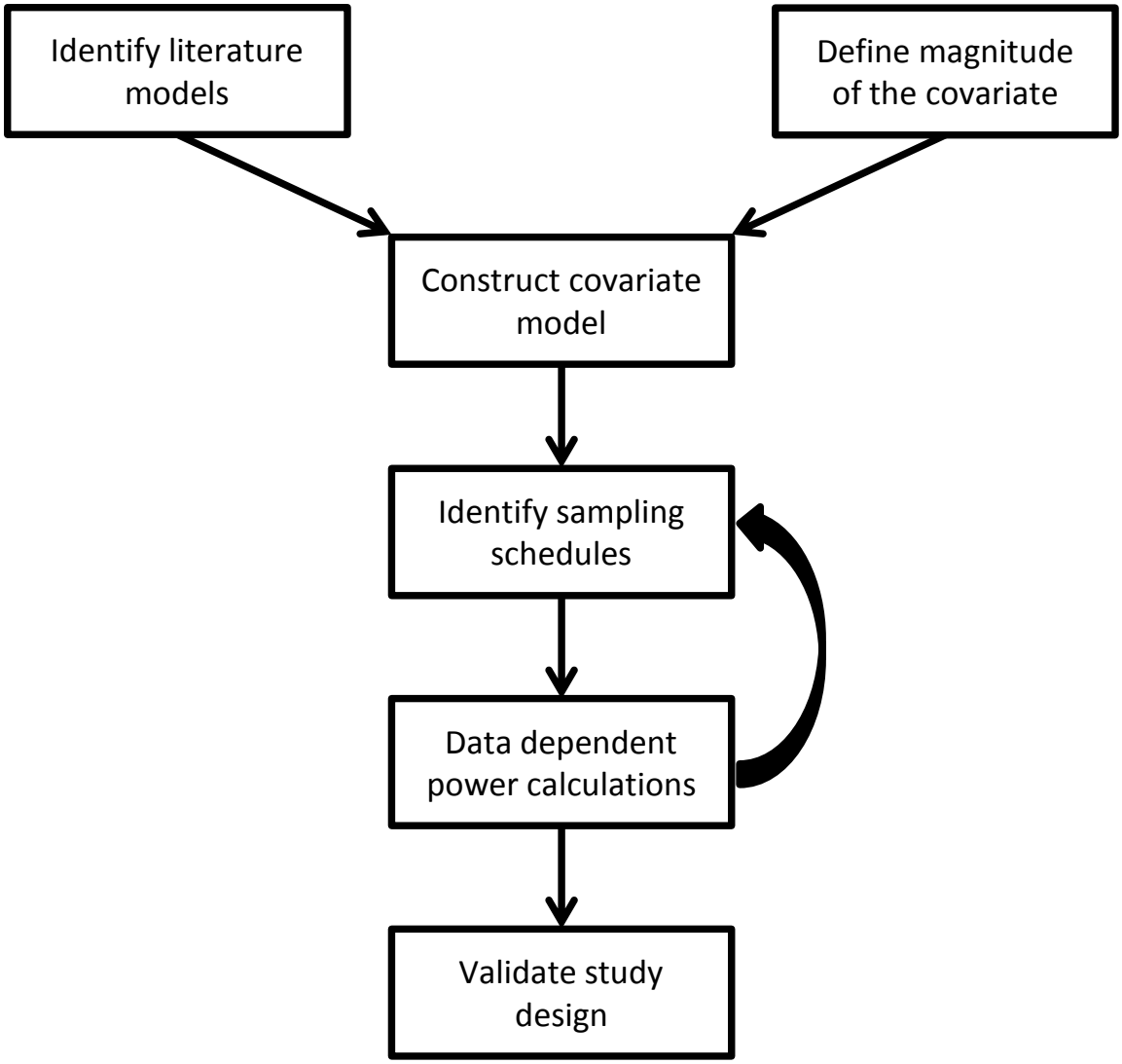

Figure 8.1 Visual representation of the applied workflow. Identify literature models: reference models from literature were collected for the paradigm drugs, define magnitude of the covariate: the magnitude of covariate differences that results in clinically important differences in drug exposure were defined, construct covariate model: a final covariate model to perform the power calculations with was constructed, identify sampling schedules: possible sampling schedules were retrieved from literature or may be obtained with an optimal design method, Data-dependent power calculation: the data-dependent power calculations using the log likelihood ratio test for selected study designs was executed and validate study designs: different study designs were assessed for pharmacological (simulation re-estimation) and economic feasibility (calculating budget).

was implemented in both the simulation (30%) and the dihydroartemisinin (20%) example (Table 8.1).

8.2.2 The datasets

A crossover and parallel study design was evaluated with the simulation example and with the dihydroartemisinin example only a parallel study design was assessed. Datasets for a parallel study design consisted of 1,000 individuals (500 patients displaying the binary covariate and 500 patients not displaying the binary covariate) and datasets for a crossover design consisted of 500 patients (displaying the binary covariate during the first visit and not displaying the binary covariate during the second visit) (Table 8.1). Sampling designs (sparse and dense) were equal for the parallel and crossover study design in the simulation example (Table 8.1). One sample per patient was drawn from the selected sampling times in window 1 and window 2 in the sparse sampled study arm of the simulation study (Table 8.1). For patients in the sparse sampled arm of the dihydroartemisinin example, a sample could be drawn at any time within the specified sampling windows (Table 8.1).

8.2.3 The power calculations

The data dependent power calculation methodology for combined pharmacokinetic study designs that was presented is a further developed version of the Monte Carlo mapped power method [106]. Two datasets with either a dense sampling design (dataset A) or a sparse sampling design (dataset B) were simulated. Simulations were executed using the true population pharmacokinetic model containing the covariate effect of interest in NONMEM

7.2 (ICON Development Solutions, Ellicott City, MD) on a Windows 7 operating system (Microsoft Corporation, Seattle, WA) with a G-Fortran compiler (Free Software Foundation, Boston, MA). The simulated datasets were subsequently re-estimated using 1.) a model including the covariate effect (covariate model) and 2.) a model not including the covariate effect (base model). Re-estimation of a simulated parallel design was performed without inter occasion variability as only one occasion per individual was available.

At random, individuals (from dataset A and dataset B) were drawn to create new design combinations in terms of number of patients with sparse and dense sampling (matrix 1):

MATRIX 1

$$\begin{bmatrix} - & A(0)/B(1) & A(0)/B(2) & \cdots & A(0)/B(n) \\ A(1)/B(0) & A(1)/B(1) & A(1)/B(2) & \cdots & A(1)/B(n) \\ A(2)/B(0) & A(2)/B(1) & A(2)/B(2) & \cdots & A(2)/B(n) \\ \vdots & \vdots & \vdots & \ddots & \vdots \\ A(n)/B(0) & A(n)/B(1) & A(n)/B(2) & \cdots & A(n)/B(n) \end{bmatrix}$$

A(n) and B(n) in matrix 1 represents the number of patients randomly drawn from dataset A and dataset B to create a new study design. The difference in objective function (ΔOFV; calculated as minus twice the natural logarithm of the likelihood of the data) for the newly created datasets was obtained by deducting the OFV obtained with the covariate model from the OFV obtained with the base model (equation 8.1):

EQ 8.1:

$$\Delta OFV = \sum_{i=1}^{n} iOFV_{covariate} - \sum_{i=1}^{n} iOFV_{base}$$

The iOFV in equation 8.1 represents the individual objective function value for individual i. The procedure was repeated 10,000 times for every study design scenario and the power was expressed as the percentage out of 10,000 draws that ΔOFV dropped lower than -3.84 ($p<0.05$). A power of 80% in this study was considered to be the threshold and this means that the covariate can be detected as a statistically significant covariate in 80% of the studies.

8.2.3 Validation of the proposed study designs

A selection of potential study designs (with at least 80% power) was made and subsequently simulated and re-estimated (n=1,000) in order to obtain the percentage relative standard error (RSE) on the estimates of the fixed effects, random effects, and the residual variability (equation 8.2).

EQ 8.2:
$$\mathrm{RSE}(\%) = 100 * \frac{\text{standard error}}{\text{mean parameter estimate}}$$

Financial figures

Moreover, the selection of study designs was evaluated from a cost effective point of view (equation 8.3).

EQ 8.3:
$$\mathrm{Budget}(\text{patient}) = \text{cost(hospitalisation)} * \text{days(n)} + \text{cost(assay)} * \text{samples(n)}$$

Days in equation 8.3 represent the total number of days that patients were hospitalised during the study which may be longer for patients in the dense sampled study arm compared to patients in the sparse sampled study arm. Samples in equation 8.3 represent the total number of samples analysed during the study.

The hospitalisation cost for patients in the dense sampled arm was 1,000 units and 750 units for patients in the sparse sampled arm, respectively. The cost of analysing one sample was 50 units.

8.3 Results

8.3.1 Simulation example

For a cross-over study design, 7 (dense sampling only), 9 (5 assigned to dense sampling/4 assigned to sparse sampling), 10 (3 assigned to dense sampling/7 assigned to sparse sampling) or 13 (sparse sampling only) patients were required to detect a binary covariate (30% increase in elimination clearance) with at least 80% statistical power (Figure 8.2A). For a parallel study design a total (i.e. patients displaying and patients not displaying the covariate) number of 52 (dense sampling only), 58 (34 assigned to dense sampling/24 assigned to sparse sampling), 60 (18 assigned to dense sampling/42 assigned to sparse sampling) or 66 (sparse sampling only) patients were required to detect a binary covariate (30% increase in elimination clearance) with at least 80% power (Figure 8.2B).

The precision on V and k_a was improved by the inclusion of dense sampled patients compared to a study design consisting of solely sparse sampled patients in both the parallel and cross-over settings (Table 8.2). Precision on all parameter

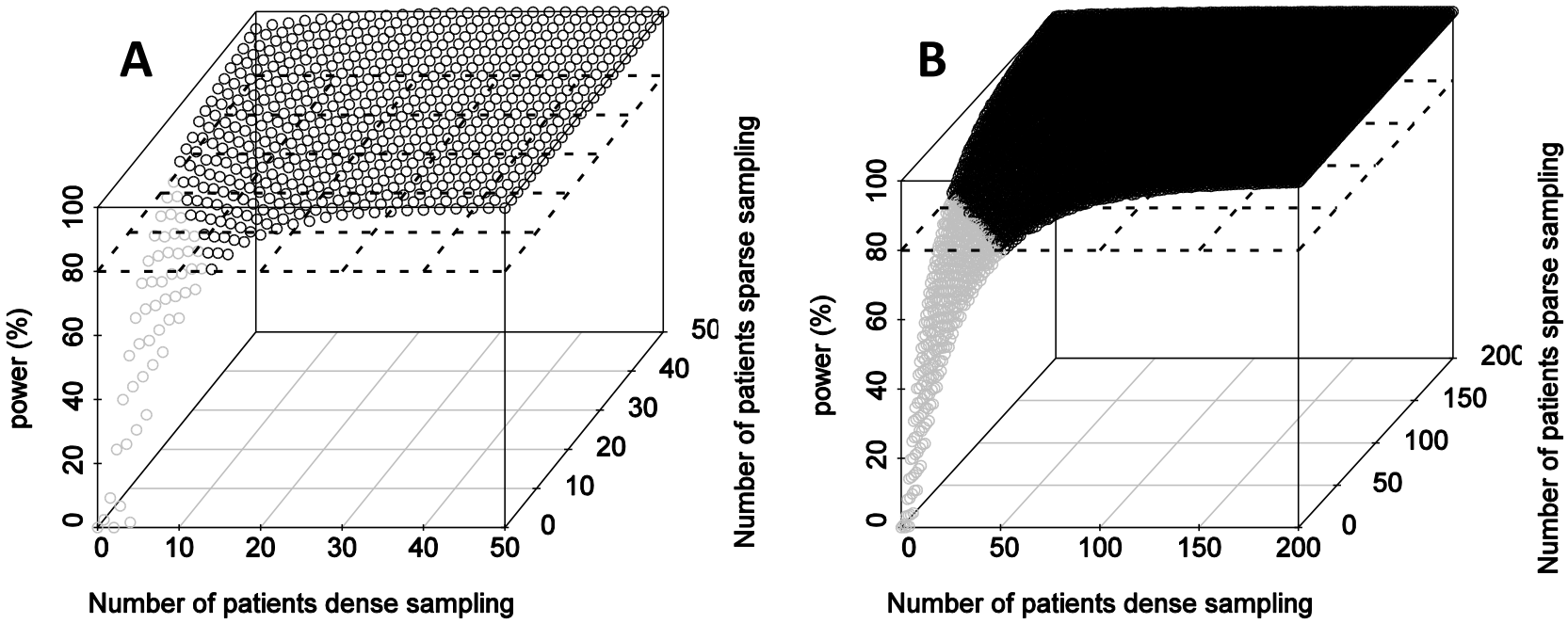

Figure 8.2 Results from power calculations for a cross over design (A) and a parallel design (B), respectively.

Table 8.2: Summary of simulation study results.

Study design	Sampling design (N)			Samples (N)			Parameter precision (% RSE)									Study Cost	Patient cost
	Total	Dense ID's	Sparse ID's	Total	Dense	Sparse	CL	V	k_a	cov	Cl IIV	V IIV	k_a IIV	Cl IOV	Sigma	Hypothetical	Hypothetical
Cross-over	7	7	0	224	224	0	12.4	12.2	13.3	34.4	66.4	62.5	85.3	60.3	11.0	25,200	3,600
	9	5	4	176	160	16	11.5	13.3	16.9	34.3	68.3	68.8	106	68.9	12.5	22,800	2,760
	10	3	7	124	96	28	11.5	13.8	19.7	34.9	68.3	79.4	139	75.5	15.7	19,200	2,270
	13	0	13	52	0	52	11.5	19.0	53.6	37.4	69.4	114	222	106	32.8	15,600	1,700
Parallel	52	52	0	832	832	0	5.71	4.82	5.71	34.0	22.3	23.0	36.6	-	5.93	93,600	1,800
	58	34	24	592	544	48	5.90	5.35	6.74	35.8	24.3	27.7	45.1	-	6.96	75,600	1,410
	60	18	42	372	288	84	6.31	6.30	8.71	36.2	26.0	34.2	63.0	-	9.45	57,600	1,140
	66	0	66	132	0	132	6.83	14.0	22.9	39.5	33.6	62.8	128	-	32.7	39,600	850

The sampling design was expressed as total number of patients (i.e. 50% patient displaying the categorical covariate and 50% patients not displaying the categorical coavariate). Parameter precision was calculated as $100 * \frac{\text{standard error}}{\text{mean parameter estimate}}$ obtained from 1,000 simulated and re-estimated studies. The study cost was calculated as: $\text{cost(hospitalisation)} * \text{days(n)} + \text{cost(assay)} * \text{samples(n)}$ using 1,000 units and 500 units as hospitalisation cost per day for dense and sparse designs, respectively, and an assay cost of 50 units per sample.

estimates was better using a parallel study design compared to a cross-over study design (Table 8.2).

As expected, a cross-over study design is cheaper to conduct compared to a parallel design since less patients and samples are needed to achieve 80% statistical power. Furthermore, sparse sampled study designs are cheaper to conduct compared to dense sampled study designs in both the cross-over and parallel study design.

8.3.2 Dihydroartemisinin example

Using a parallel study design 88 (dense sampling only), 98 (56 assigned to dense sampling/42 assigned to sparse sampling), 108 (28 assigned to dense sampling/80 assigned to sparse sampling) or 120 (sparse sampling only) patients were required to detect the pregnancy effect (20% increase in elimination clearance) with 80% power (Figure 8.3).

Between subject variability on V and the residual error display substantial differences between the different study designs but values of the RSEs do not reach levels higher than 20% (Table 8.3).

The more dense sampled patients included in the study design, the more expensive the total study became. Furthermore, a dense sampled patient is more expensive compared to a sparse sampled patient (Table 8.3).

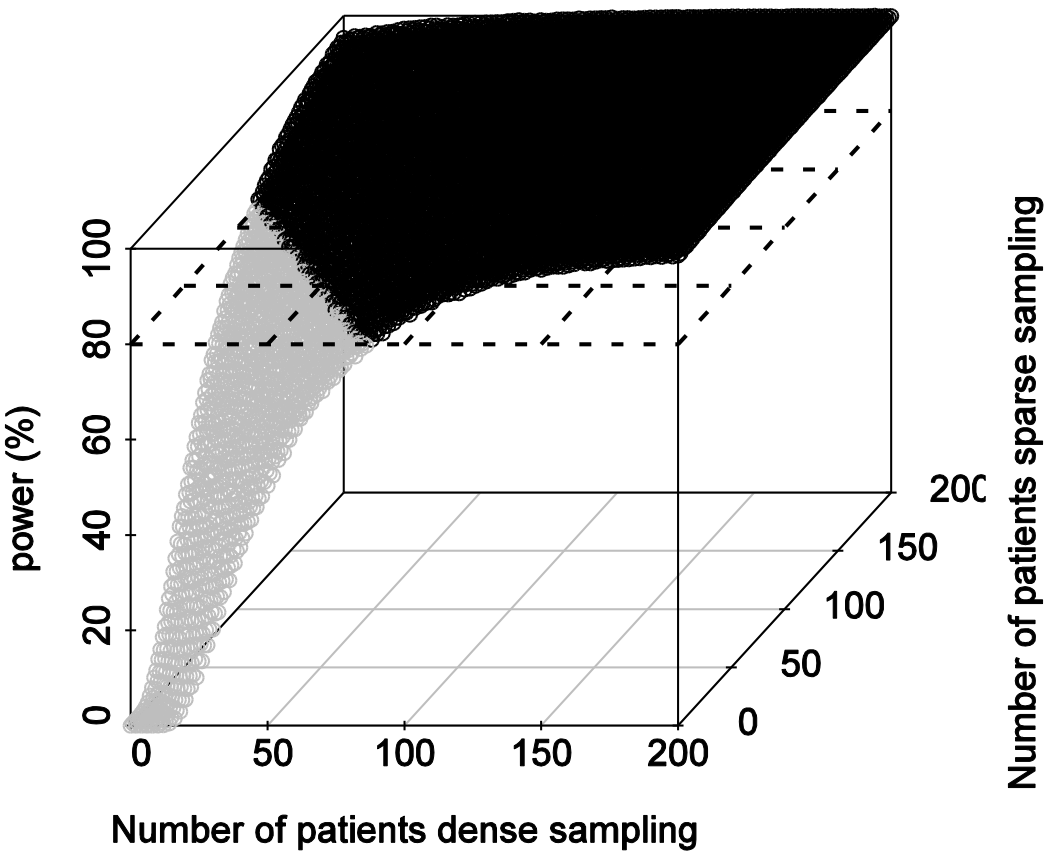

Figure 8.3 Results from power calculations for a dihydroartemisinin study design.

Table 8.3: Summary of dihydroartemisinin case study results.

Sampling design (N)			Samples (N)			Parameter precision (% RSE)								Study Cost	Patient cost
Total	Dense ID's	Sparse ID's	Total	Dense	Sparse	Cl	V	MTT	PREG_Cl	PFC_F	V_IIV	F_IIV	Sigma	Hypothetical	Hypothetical
88	88	0	880	880	0	4.97	5.39	0.98	16.5	5.65	21.9	23.4	2.68	176,000	1,500.0
98	56	42	728	560	168	5.05	5.80	1.16	18.1	5.70	25.8	25.5	3.05	141,000	1,264.3
108	28	80	600	280	320	5.11	6.12	1.39	18.8	5.94	31.5	26.4	3.54	112,000	1,092.6
120	0	120	480	0	480	5.45	7.06	1.79	21.4	5.55	43.4	27.7	4.42	84,000	950.0

The sampling design was expressed as total number of patients (i.e. 50% patient displaying the categorical covariate and 50% patients not displaying the categorical coavariate). Parameter precision was calculated as $100 * \frac{\text{standard error}}{\text{mean parameter estimate}}$ obtained from 1,000 simulated and re-estimated studies. The study cost was calculated as: $\text{cost(hospitalisation)} * \text{days(n)} + \text{cost(assay)} * \text{samples(n)}$ using 1,000 units and 500 units as hospitalisation cost per day for dense and sparse designs, respectively, and an assay cost of 50 units per sample.

8.4 Discussion

8.4.1 Characteristics of the study design matrix

If a diagonal is drawn in the matrix between two study designs consisting of solely sparse and solely dense sampled data, both reaching 80% power, also all combined study designs around this diagonal reach approximately 80% power. This phenomenon can be explained by the power relationship between the power of the study design (only sparse or only dense sampled patients) and number of patients.

8.4.2 Dihydroartemisinin example

The pregnancy covariate effect on dihydroartemisinin elimination clearance was implemented as a 20% categorical increase for simulation purposes. This has a smaller impact on dihydroartemisinin exposure compared to the actual 37.5% decrease in dihydroartemisinin bioavailability found in the pharmacokinetic study [82]. The proposed study design would therefore be sufficient to detect the actual 37.5% decrease in dihydroartemisinin bioavailability in a clinical setting.

8.4.3 Cross-over vs parallel design

The simulation example indicated that a cross-over design requires substantially fewer patients and plasma concentration samples to statistically detect the covariate effect compared to a parallel study design. However, a cross-over study design is not always feasible in the clinical setting. For example, a cross-over study design for dihydroartemisinin would not work in South East Asia due

to the relatively low malaria incidence rates. It is unlikely that a pregnant patient can attend the second visit within a reasonable time frame as non-pregnant malaria patient. An alternative would then be to include the non-pregnant women during the second visit as healthy volunteers but this would confound the results as a disease effect for dihydroartemisinin has previously been described [82]. Furthermore, studying post-partum women as healthy volunteers may be seen as unethical. Moreover, clinical studies for antimalarial compounds can only be performed during the malaria seasons and a parallel study design in such cases deserves the preference due to the reduced length of the study compared to the cross-over design.

8.4.4 Dense vs sparse

In both the simulation examples (cross-over and parallel study design) and in the dihydroartemisinin case study, similar or better precision on all parameter estimates was obtained using the dense sampling design compared to the sparse sampling design. Considering the results obtained with the partly dense and sparse sampled study design, it can be stated that parameter precision gets generally better with an increasing number of plasma concentration samples in the study. However, regarding the hypothesis testing of the covariate, there is always more to be gained from including more patients with fewer samples than fewer patients with more samples. On the other hand, a (partly) dense sampled study design may be preferred because it is more likely to be executable in certain circumstances. Fewer patients are required in a (partly) dense sampled

study design compared to a study design consisting of solely sparse sampled individuals. This could be of particular interest for orphan diseases.

For certain drugs optimal sampling schedules for sparse and dense sampling may not be available. In those cases sampling designs can be adjusted and the data dependent power calculations can be redone until the outcome is clinically feasible and expected residual errors on parameter estimates are acceptable. Combining a data dependent power calculation method with optimal design methods for determining the sampling schedules and sample sizes can be highly useful.

8.4.5 Financial aspects

Except of clinical feasibility (probability that the required number of patients can be included) and expected optimal precision of parameter estimates also the financial aspects of a study design be should evaluated. For example, there are no major differences in the parameter estimate precision for dihydroartemisinin pharmacokinetics between the four proposed study designs but the study costs vary tremendously. If there is no relevant benefit in precision of parameter estimates when choosing for an expensive dense sampled design, one could also execute the cheaper sparse sampled design. On the other hand, in case of malaria in areas with low incidence rates it may be better to choose the more expensive dense sampled or mixed dense and sparse sampled design as it may not be feasible to fulfil the required sample size for the sparse sampled design.

The difference in study costs in the simulated study example and the selected dihydroartemisinin example is mainly on account of the number of samples to be analysed. There is only a small difference in hospitalisation costs as all samples were drawn on the same day (1,000 units for a dense sample study design and 750 units for a sparse sampled study design). However, the hospitalisation costs can have a bigger influence on pharmacokinetic study cost when looking at drugs with a long elimination half-life's where multiple hospital visits are required for a dense study design compared to fewer hospital visits for a sparse study design.

8.5 Conclusion

In conclusion, the data-depentent power calculation methodology using the log likelihood ratio test which enables the evaluation of mixed (sparse and dense sampled) study designs was successfully assessed. A workflow which guides an easy and straightforward pharmacokinetic study design considering the cost-efficacy of the study was effectively used. The results show that prior knowledge can have a major contribution to a pharmacokinetic trial design and this encourages the collaboration between clinical pharmacologists, pharmacometricians and clinicians.

9.0 Summary

9.1 Quinine pharmacokinetics

In chapter 3, it was shown that pregnancy related covariates (i.e. estimated gestational age or trimester) did not significantly affect quinine pharmacokinetics in (22) pregnant women (second and third trimester) with uncomplicated *Plasmodium falciparum* malaria in Uganda. However, a non-significant trend of increased elimination clearance with increasing estimated gestational age was observed. This might indicate a lower quinine exposure in pregnant women later in their pregnancy compared to pregnant women earlier in their pregnancy. A comparison of the current findings to quinine pharmacokinetic parameter estimates in non-pregnant women from literature was not possible due to the different routes of administration (oral vs intravenous) and the different analysis methodologies (non-compartmental analysis vs population approach). A new study using a non-pregnant control group is needed to study quinine pharmacokinetics in pregnant patients.

The developed population pharmacokinetic model for quinine also described an increased (50.7%) quinine exposure in a typical patient with a total parasite biomass of 10^{11} compared to a typical patient with a total parasite biomass of 10^{7}. Moreover, the quinine exposure during the first 8 hours of treatment was 15% higher in patients with admission body temperature of 39°C compared to patients with admission body temperature of 36°C. The disease effect during the acute phase compared to the convalescence phase has been reported previously in literature and is most likely caused by increased alpha-1-acid-glycoprotein concentrations. However, this disease effect has never been

implemented in a population pharmacokinetic model for quinine which makes the presented work unique.

9.2 Artesunate/dihydroartemisinin pharmacokinetics

In chapter 4, it was shown that dihydroartemisinin elimination clearance was 27.2% higher in pregnant women (on the Thai-Myanmar border) with uncomplicated *Plasmodium falciparum* malaria (second and third trimester) compared to the same women 3 months post-partum without malaria. This resulted in a lowered dihydroartemisinin exposure which was also observed in a study with pregnant women in Congo using non-pregnant women and post-partum women as a control group. Furthermore, a disease effect was seen in this study resulting in a higher (90.3%) artesunate and dihydroartemisinin exposure during the acute malaria phase compared to the convalescence phase and healthy post-partum status. The developed population pharmacokinetic model is unique in the sense that it is the first drug-metabolite model that describes absolute oral bioavailability, disease effect and pregnancy effect simultaneously.

Even though a clear decrease in dihydroartemisinin exposure was seen during pregnancy, more modelling work (pooled pharmacokinetic analyses) and confirming clinical studies (pregnant women with a matching non-pregnant control group) have to be done to support (and modify if required) evidence-based dose optimisations.

9.3 Artemether/dihydroartemisinin pharmacokinetics

In chapter 5, it was shown that estimated gestational age did not affect artemether and dihydroartemisinin pharmacokinetics in pregnant women (in the second and third trimester) with uncomplicated *Plasmodium falciparum* malaria in Uganda. However, overall plasma concentrations tend to be lower compared to non-pregnant patients from the literature. Furthermore, studies in pregnant and non-pregnant women receiving oral dihydroartemisinin or oral artesunate indicate increased dihydroartemisinin exposure during pregnancy. Comparisons to literature have to be interpreted with caution because of differences in assays, study populations and parental administration. Nevertheless, the finding is a worrisome and indicates an urgent need for a study with an equally sized non-pregnant control group. Such a study would enable the quantification of the pregnancy effect and can support dose optimisation if this appears to be required.

9.4 Lumefantrine pharmacokinetics

In chapter 6, it was shown that day 7 lumefantrine plasma concentration were 27% lower in pregnant women (in the second and third trimester) with uncomplicated *Plasmodium falciparum* malaria compared to non-pregnant women with uncomplicated *Plasmodium falciparum* malaria in Uganda. This resulted in a median reduction of 0.92 and 0.42 days above the target plasma concentrations of 280 ng/mL and 175 ng/mL, respectively. A confirming study

using an equally sized non-pregnant control group is needed due to the unequal control group in the current study.

9.5 Lumefantrine/desbutyl-lumefantrine pharmacokinetics-pharmacodynamics

In chapter 7, it was shown that lumefantrine and desbutyl-lumefantrine had a similar drug effect on recrudescent malaria but an additive drug effect of both compounds did not further improve the model. However, desbutyl-lumefantrine did not have an improved prognostic effect compared to lumefantrine as stipulated in recent literature. Simulations using the simultaneous population pharmacokinetic-pharmacodynamic lumefantrine/desbutyl-lumefantrine model showed increased cure rates after treatment prolongation with two days (five day treatment) and seven days (ten day treatment). A study with prolonged artemether-lumefantrine treatment at the Thai-Myanmar border is therefore needed to assess dose optimisations, increase the cure rates, and stop the spread of resistance.

9.6 Optimal pharmacokinetic study design

In chapter 8, it was shown that the data dependent power calculation methodology using the log likelihood ratio test was successful for the evaluation of mixed (sparse and dense sampled) pharmacokinetic study designs. A workflow which guides an easy and straightforward pharmacokinetic study design, including the cost-efficacy of the study, was effectively used. From the

results it was concluded that prior pharmacometric knowledge can have a major contribution to a pharmacokinetic trial design. The collaboration between clinical pharmacologists, pharmacometricians and clinicians should therefore be encouraged during the design phase of pharmacokinetic studies.

9.7 General conclusion

In conclusion, the aim of this thesis “to study the pharmacokinetics and pharmacodynamics of the most commonly used drugs for the treatment of uncomplicated *Plasmodium falciparum* malaria during the second and third trimester of pregnancy using a pharmacometric approach” was successfully executed. More studies are needed for quinine and artemether-dihydroartemisinin in order to quantify the effect of pregnancy on pharmacokinetics using a non-pregnant control group. However, trends of artemether-dihydroartemisinin underexposure have been observed based on literature comparisons. The effect of pregnancy could on the other hand be quantified on artesunate-dihydroartemisin and lumefantrine pharmacokinetics. Confirming studies for artesunate-dihydroartemisinin and lumefantrine/desbutyl-lumefantrine are needed to further support evidence-based dose optimisation. Pharmacokinetic studies are often nested in efficacy studies with sometimes densely and sparsely sampled patients. A data-dependent power calculation method using the log likelihood ratio test was therefore used to calculate a sufficient sample size for mixed (sparse and dense sampled) pharmacokinetic

study designs. The evaluated sample size calculation methodology can contribute to an effective design of future pharmacokinetic studies.

10.0 Related publications

Various parts of this thesis have been published and with permission of the journals (Malaria journal, Antimicrobial agents and chemotherapy and CPT: Pharmacometrics & Systems Pharmacology) results were processed in this thesis.

Tarning J, **Kloprogge F**, et al. *Population pharmacokinetics of Artemether and dihydroartemisinin in pregnant women with uncomplicated Plasmodium falciparum malaria in Uganda.* Malaria journal, 2012. 11(1): p. 293

Tarning J, **Kloprogge F**, et al. *Pharmacokinetic properties of artemether, dihydroartemisinin, lumefantrine and quinine in pregnant women with uncomplicated falciparum malaria in Uganda.* Antimicrob Agents Chemother, 2013

Kloprogge F, Piola P, et al. *Population Pharmacokinetics of Lumefantrine in Pregnant and Nonpregnant Women With Uncomplicated Plasmodium falciparum Malaria in Uganda.* CPT: Pharmacometrics & Systems Pharmacology. 2013

Kloprogge F, Jullien V, et al. *Population pharmacokinetics of quinine in pregnant women with uncomplicated Plasmodium falciparum malaria in Uganda.* Journal of Antimicrobial Chemotherapy. 2013 (submitted)

Furthermore, proportions of this thesis have been presented at conferences by oral presentation or posters.

Frank Kloprogge, Philippe Guerin et al. *Population pharmacokinetics of lumefantrine, artemether and dihydroartemisinin in pregnant and non-pregnant women in Uganda.* Joint International Tropical Medicine Meeting, 1-2 December 2011, Bangkok, Thailand. (oral presentation)

Frank Kloprogge, Rose McGready et al. *Pharmacokinetic properties of artesunate in pregnant women with falciparum malaria.* Joint International Tropical Medicine Meeting, 11-13 December 2013, Bangkok, Thailand. (oral presentation)

Joel Tarning, **Frank Kloprogge**, et al. *Population pharmacokinetics of artemether and dihydroartemisinin in pregnant women with uncomplicated Plasmodium falciparum malaria in Uganda.* ASTMH-meeting, 4-8 December 2011, Philadelphia, USA. (poster)

Frank Kloprogge, Philippe Guerin et al. *Population pharmacokinetics of lumefantrine in pregnant and non-pregnant women with uncomplicated Plasmodium falciparum malaria in Uganda.* PAGE-meeting, 5-8 June, 2012, Venice, Italy. (poster)

Frank Kloprogge, Rose McGready, et al. *Population pharmacokinetics and pharmacodynamics of lumefantrine in pregnant women with uncomplicated P. falciparum malaria in Thailand.* PAGE-meeting, 11-14 June, 2013, Glasgow, Scotland. (poster)

Acknowledgements

This thesis is supported and endorsed by the Malaria in Pregnancy Consortium, which is funded through a grant from the Bill & Melinda Gates Foundation (grant number: 46099). A great number of people have supported me in different ways during the research presented in this thesis and I would like to thank them all for their support, especially:

Joel Tärning, thank you for supporting me in following my curiosity. You have provided me with in-depth understanding of the projects and critical and inspirational discussions. Equally important were your constant support on pharmacokinetics and pharmacodynamics and introducing me into the newest pharmacometric techniques.

Nick White, thank you for taking me away from models, and forcing me to think about the clinical implications of the findings. Your lectures were a source of inspiration.

Francois Nosten, thank you for your valuable contributions regarding the causes and clinical consequences of the presented findings.

Niklas Lindegårdh, for introducing me into the world of analytical chemistry. I also adopted a fraction of his fanatic exercise schedule, which often helped me as distraction.

Patrice Piola, Philippe Guerin and all involved staff at the study site in Kampala, Uganda, thank you for planning and conducting the pharmacokinetic studies. Without these studies chapter 3, 5 and 6 of this thesis would not have existed.

Rose McGready, Francois Nosten and all involved staff at the SMRU, Mae Sot, Thailand, thank you for planning and conducting the pharmacokinetic studies. Without these studies chapter 4 and 7 would not have existed.

All patients who participated in the pharmacokinetic studies in Uganda and Thailand/Myanmar.

All collaborators (Nicholas P. J. Day, Mehul Dhorda, Warunee Hanpithakpon, Nathar Hlaing, Vincent Jullien, Sulaiman Muwanga, Nitra Nuengchamnong, Aung Pyae Phyo, Marcus J. Rijken, Julie Simpson, Hla Hla Than, Naw Thida Zin, Eleano Turyakira) thank you for your valuable scientific input.

My roommates, Kalayanee Chairat, Praiya Thana, Palang Chotsiri, Instiati, Thanaporn Wattanakul, Natthida Sriboonvorakul, Martin Bergstrand, Joe Illingworth and Richard Höglund for all scientific input and discussions, none scientific discussions, and fun we had outside office hours. Dam, Oam, Palang, Pum and Toto, thank you for helping me out with daily life in Thailand.

Daniel Blessborn and Thomas Pouplin, thank you for answering bio-analytical related questions and thank you to all other lab staff for performing the bio-analytical analyses.

Sompob Saralamba and Mongkol Fungprasertkul, thank you for your help in keeping all hardware and software running.

Furthermore, I would like to thank all people I have met at MORU in Bangkok and the Green Templeton College in Oxford for their warm welcome and great company.

To my parents, thank you for the constant support and encouragement throughout all the different stages of my life and education.

Els, thank you for the great times we always have! The fun we have when I am with you has helped me to get energy and inspiration in order to focus and deliver when I needed to work on the projects.

Appendix A

```
$PROBLEM    ...

$ABBREVIATED
            COMRES=2                ;define number of common reserves

$INPUT      ...

$DATA       ...

$SUBROUTINE
            ADVAN6                  ;open ADVAN
            TOL=5                   ;tolerance

$MODEL
            COMP=(n)                ;sampling compartment
            COMP=(n+1)              ;AUC compartment

$PK
            S2=V                    ;scaling factor compartment

            IF (NEWIND.LE.1) THEN   ;assign negative Cmax Tmax for ID
            COM(1)=-1               ;holder of Cmax
            COM(2)=-1               ;holder of Tmax
            ENDIF

$DES
            DADT(n)  = ...          ;DE sampling compartment
            DADT(n+1)= A(n)         ;integral sampling compartment
            AUC      = A(n+1)/S2    ;area under the curve

            CTD      = A(n+1)/S2    ;concentration sampling compartment
            IF (CTD.GT.COM(1)) THEN ;if CTD is bigger than previous
            COM(1)   = CTD          ;Cmax is concentration
            COM(2)   = T            ;Tmax is time
            ENDIF

$ERROR
            CMAX = COM(1)           ;define CMAX variabile
            TMAX = COM(2)           ;define TMAX variabile

$TABLE ID AUC CMAX TMAX             ;define variables to export
NOAPPEND NOPRINT ONEHEADER FILE=... ;define format and name export file
```

Appendix B

```
$PK
;Half-life calculation 1-compartment model
      t12   = log(2)/(CL/V)         ;calculation elimination half-life

;Half-life calculation 2-compartment model

      SUM   = K20+K23+K32

      ROOT  = SQRT(SUM*SUM-4*K32*K20)

      ALPHA = 0.5*(SUM+ROOT)

      BETA  = 0.5*(SUM-ROOT)

      t12_A = 0.693/(ALPHA)         ;distribution phase half-life

      t12_B = 0.693/(BETA)          ;elimination phase half-life
```

References

1. WHO, *World malaria report 2012.* 2012.
2. Griffith, K.S., et al., *Treatment of malaria in the United States: a systematic review.* Jama, 2007. **297**(20): p. 2264-77.
3. White, N.J., *Malaria*, in *Manson's Tropical Diseases*, G.C. Cook and A.I. Zumla, Editors. 2009. p. 1201-1300.
4. Brabin, B., *Analysis of malaria in pregnancy in Africa.* Bull World Health Organ, 1983. **61**: p. 1005-1016.
5. Dellicour, S., et al., *Quantifying the number of pregnancies at risk of malaria in 2007: a demographic study.* PLoS Med, 2010. **7**(1): p. e1000221.
6. Warhust, D.C., *The parasite*, in *Travelers' Malaria*, P.e. Schlagenhauf-Lawlor, Editor 2008, BC Decker Inc.: Hamilton, Ont. p. 70-80.
7. Ponnudurai, T., et al., *Feeding behaviour and sporozoite ejection by infected Anopheles stephensi.* Transactions of the Royal Society of Tropical Medicine and Hygiene, 1991. **85**(2): p. 175-80.
8. Rosenberg, R., et al., *An estimation of the number of malaria sporozoites ejected by a feeding mosquito.* Transactions of the Royal Society of Tropical Medicine and Hygiene, 1990. **84**(2): p. 209-12.
9. Miller, L.H., et al., *Malaria biology and disease pathogenesis: insights for new treatments.* Nature medicine, 2013. **19**(2): p. 156-67.
10. WHO, *World health organization Guidelines for the treatment of malaria*2010.
11. Ponsford, M.J., et al., *Sequestration and microvascular congestion are associated with coma in human cerebral malaria.* The Journal of infectious diseases, 2012. **205**(4): p. 663-71.
12. Poespoprodjo, J.R., et al., *Adverse pregnancy outcomes in an area where multidrug-resistant plasmodium vivax and Plasmodium falciparum infections are endemic.* Clin Infect Dis, 2008. **46**(9): p. 1374-81.
13. Viebig, N.K., et al., *A single member of the Plasmodium falciparum var multigene family determines cytoadhesion to the placental receptor chondroitin sulphate A.* EMBO reports, 2005. **6**(8): p. 775-81.
14. Chotivanich, K., et al., *Plasmodium vivax adherence to placental glycosaminoglycans.* PloS one, 2012. **7**(4): p. e34509.
15. Agbor-Enoh, S.T., et al., *Chondroitin sulfate proteoglycan expression and binding of Plasmodium falciparum-infected erythrocytes in the human placenta during pregnancy.* Infection and immunity, 2003. **71**(5): p. 2455-61.
16. Carvalho, B.O., et al., *On the cytoadhesion of Plasmodium vivax-infected erythrocytes.* J Infect Dis, 2010. **202**(4): p. 638-47.
17. Jansen, F.H. and S.A. Soomro, *Chemical instability determines the biological action of the artemisinins.* Curr Med Chem, 2007. **14**(30): p. 3243-59.
18. Krishna, S., et al., *Re-evaluation of how artemisinins work in light of emerging evidence of in vitro resistance.* Trends Mol Med, 2006. **12**(5): p. 200-5.
19. Eckstein-Ludwig, U., et al., *Artemisinins target the SERCA of Plasmodium falciparum.* Nature, 2003. **424**(6951): p. 957-61.
20. Klayman, D.L., *Qinghaosu (artemisinin): an antimalarial drug from China.* Science, 1985. **228**(4703): p. 1049-55.

21. Ding, X.C., H.P. Beck, and G. Raso, *Plasmodium sensitivity to artemisinins: magic bullets hit elusive targets.* Trends Parasitol, 2011. **27**(2): p. 73-81.
22. Haynes, R.K., et al., *Reactions of antimalarial peroxides with each of leucomethylene blue and dihydroflavins: flavin reductase and the cofactor model exemplified.* ChemMedChem, 2011. **6**(2): p. 279-91.
23. Haynes, R.K., et al., *Facile oxidation of leucomethylene blue and dihydroflavins by artemisinins: relationship with flavoenzyme function and antimalarial mechanism of action.* ChemMedChem, 2010. **5**(8): p. 1282-99.
24. Delves, M., et al., *The activities of current antimalarial drugs on the life cycle stages of Plasmodium: a comparative study with human and rodent parasites.* PLoS medicine, 2012. **9**(2): p. e1001169.
25. ter Kuile, F., et al., *Plasmodium falciparum: in vitro studies of the pharmacodynamic properties of drugs used for the treatment of severe malaria.* Exp Parasitol, 1993. **76**(1): p. 85-95.
26. Geary, T.G., A.A. Divo, and J.B. Jensen, *Stage specific actions of antimalarial drugs on Plasmodium falciparum in culture.* The American journal of tropical medicine and hygiene, 1989. **40**(3): p. 240-4.
27. Price, R.N., et al., *Effects of artemisinin derivatives on malaria transmissibility.* Lancet, 1996. **347**(9016): p. 1654-8.
28. Pukrittayakamee, S., et al., *Activities of artesunate and primaquine against asexual- and sexual-stage parasites in falciparum malaria.* Antimicrobial agents and chemotherapy, 2004. **48**(4): p. 1329-34.
29. Wilairatana, P., N. Tangpukdee, and S. Krudsood, *Long term primaquine administration to reduce Plasmodium falciparum gametocyte transmission in hypoendemic areas.* Southeast Asian J Trop Med Public Health, 2010. **41**(6): p. 1306-11.
30. Chou, A.C., R. Chevli, and C.D. Fitch, *Ferriprotoporphyrin IX fulfills the criteria for identification as the chloroquine receptor of malaria parasites.* Biochemistry, 1980. **19**(8): p. 1543-9.
31. Bray, P.G., S.A. Ward, and P.M. O'Neill, *Quinolines and artemisinin: chemistry, biology and history.* Current topics in microbiology and immunology, 2005. **295**: p. 3-38.
32. John, G.K., et al., *Primaquine radical cure of Plasmodium vivax: a critical review of the literature.* Malaria journal, 2012. **11**: p. 280.
33. Dondorp, A.M., et al., *Artesunate versus quinine in the treatment of severe falciparum malaria in African children (AQUAMAT): an open-label, randomised trial.* Lancet, 2010. **376**(9753): p. 1647-1657.
34. Dondorp, A., et al., *Artesunate versus quinine for treatment of severe falciparum malaria: a randomised trial.* Lancet, 2005. **366**(9487): p. 717-25.
35. White, N.J., *Delaying antimalarial drug resistance with combination chemotherapy.* Parassitologia, 1999. **41**(1-3): p. 301-8.
36. White, N., *Antimalarial drug resistance and combination chemotherapy.* Philos Trans R Soc Lond B Biol Sci, 1999. **354**(1384): p. 739-49.
37. Alin, M.H., et al., *Clinical efficacy and pharmacokinetics of artemisinin monotherapy and in combination with mefloquine in patients with falciparum malaria.* Br J Clin Pharmacol, 1996. **41**(6): p. 587-92.
38. Krudsood, S., et al., *Dose ranging studies of new artemisinin-piperaquine fixed combinations compared to standard regimens of artemisisnin combination therapies for acute uncomplicated falciparum malaria.* Southeast Asian J Trop Med Public Health, 2007. **38**(6): p. 971-8.

39. Tangpukdee, N., et al., *Efficacy of Artequick versus artesunate-mefloquine in the treatment of acute uncomplicated falciparum malaria in Thailand.* Southeast Asian J Trop Med Public Health, 2008. **39**(1): p. 1-8.
40. Trung, T.N., et al., *A randomized, controlled trial of artemisinin-piperaquine vs dihydroartemisinin-piperaquine phosphate in treatment of falciparum malaria.* Chin J Integr Med, 2009. **15**(3): p. 189-92.
41. WHO, *World health organization Guidelines for the treatment of malaria.* 2010(Second edition).
42. Ashley, E.A., et al., *Randomized, controlled dose-optimization studies of dihydroartemisinin-piperaquine for the treatment of uncomplicated multidrug-resistant falciparum malaria in Thailand.* J Infect Dis, 2004. **190**(10): p. 1773-82.
43. Ashley, E.A., et al., *A randomized, controlled study of a simple, once-daily regimen of dihydroartemisinin-piperaquine for the treatment of uncomplicated, multidrug-resistant falciparum malaria.* Clin Infect Dis, 2005. **41**(4): p. 425-32.
44. Awab, G.R., et al., *Dihydroartemisinin-piperaquine versus chloroquine to treat vivax malaria in Afghanistan: an open randomized, non-inferiority, trial.* Malar J, 2010. **9**: p. 105.
45. Grande, T., et al., *A randomised controlled trial to assess the efficacy of dihydroartemisinin-piperaquine for the treatment of uncomplicated falciparum malaria in Peru.* PLoS ONE, 2007. **2**(10): p. e1101.
46. Janssens, B., et al., *A randomized open study to assess the efficacy and tolerability of dihydroartemisinin-piperaquine for the treatment of uncomplicated falciparum malaria in Cambodia.* Trop Med Int Health, 2007. **12**(2): p. 251-9.
47. Karema, C., et al., *Safety and efficacy of dihydroartemisinin/piperaquine (Artekin) for the treatment of uncomplicated Plasmodium falciparum malaria in Rwandan children.* Trans R Soc Trop Med Hyg, 2006. **100**(12): p. 1105-11.
48. Mayxay, M., et al., *An open, randomized comparison of artesunate plus mefloquine vs. dihydroartemisinin-piperaquine for the treatment of uncomplicated Plasmodium falciparum malaria in the Lao People's Democratic Republic (Laos).* Trop Med Int Health, 2006. **11**(8): p. 1157-65.
49. Tran, T.H., et al., *Dihydroartemisinin-piperaquine against multidrug-resistant Plasmodium falciparum malaria in Vietnam: randomised clinical trial.* Lancet, 2004. **363**(9402): p. 18-22.
50. Zwang, J., et al., *Safety and efficacy of dihydroartemisinin-piperaquine in falciparum malaria: a prospective multi-centre individual patient data analysis.* PLoS One, 2009. **4**(7): p. e6358.
51. Tarning, J., et al., *Population Pharmacokinetics and Pharmacodynamics of Piperaquine in Children With Uncomplicated Falciparum Malaria.* Clinical pharmacology and therapeutics, 2012.
52. Tangpukdee, N., et al., *An open randomized clinical trial of Artekin vs artesunate-mefloquine in the treatment of acute uncomplicated falciparum malaria.* Southeast Asian J Trop Med Public Health, 2005. **36**(5): p. 1085-91.
53. van Vugt, M., et al., *Randomized comparison of artemether-benflumetol and artesunate-mefloquine in treatment of multidrug-resistant falciparum malaria.* Antimicrob Agents Chemother, 1998. **42**(1): p. 135-9.
54. Zwang, J., et al., *Efficacy of artesunate-amodiaquine for treating uncomplicated falciparum malaria in sub-Saharan Africa: a multi-centre analysis.* Malar J, 2009. **8**: p. 203.

55. Sagara, I., et al., *Efficacy and safety of a fixed dose artesunate-sulphamethoxypyrazine-pyrimethamine compared to artemether-lumefantrine for the treatment of uncomplicated falciparum malaria across Africa: a randomized multi-centre trial.* Malar J, 2009. **8**: p. 63.
56. Hatz, C., et al., *Treatment of acute uncomplicated falciparum malaria with artemether-lumefantrine in nonimmune populations: a safety, efficacy, and pharmacokinetic study.* Am J Trop Med Hyg, 2008. **78**(2): p. 241-7.
57. WHO, *Global report on antimalarial drug efficacy and drug resistance: 2000-2010*2010.
58. Pukrittayakamee, S., et al., *Therapeutic responses to quinine and clindamycin in multidrug-resistant falciparum malaria.* Antimicrobial agents and chemotherapy, 2000. **44**(9): p. 2395-8.
59. Looareesuwan, S., et al., *Randomised trial of mefloquine-tetracycline and quinine-tetracycline for acute uncomplicated falciparum malaria.* Acta tropica, 1994. **57**(1): p. 47-53.
60. Meek, S.R., et al., *Treatment of falciparum malaria with quinne and tetracycline or combined mefloquine/sulfadoxine/pyrimethamine on the Thai-Kampuchean border.* The American journal of tropical medicine and hygiene, 1986. **35**(2): p. 246-50.
61. Metzger, W., et al., *High efficacy of short-term quinine-antibiotic combinations for treating adult malaria patients in an area in which malaria is hyperendemic.* Antimicrobial agents and chemotherapy, 1995. **39**(1): p. 245-6.
62. de Souza, J.M., et al., *An open, randomized, phase III clinical trial of mefloquine and of quinine plus sulfadoxine-pyrimethamine in the treatment of symptomatic falciparum malaria in Brazil.* Bulletin of the World Health Organization, 1985. **63**(3): p. 603-9.
63. McGready, R., et al., *Adverse effects of falciparum and vivax malaria and the safety of antimalarial treatment in early pregnancy: a population-based study.* The Lancet infectious diseases, 2012. **12**(5): p. 388-96.
64. Piola, P., et al., *Efficacy and safety of artemether-lumefantrine compared with quinine in pregnant women with uncomplicated Plasmodium falciparum malaria: an open-label, randomised, non-inferiority trial.* Lancet Infect Dis, 2010. **10**(11): p. 762-9.
65. Abdulla, S., et al., *Efficacy and safety of artemether-lumefantrine dispersible tablets compared with crushed commercial tablets in African infants and children with uncomplicated malaria: a randomised, single-blind, multicentre trial.* Lancet, 2008. **372**(9652): p. 1819-27.
66. McGready, R., et al., *A randomised controlled trial of artemether-lumefantrine versus artesunate for uncomplicated plasmodium falciparum treatment in pregnancy.* PLoS Med, 2008. **5**(12): p. e253.
67. Kaye, D.K., et al., *A randomized clinical trial comparing safety, clinical and parasitological response to artemether-lumefantrine and chlorproguanil-dapsone in treatment of uncomplicated malaria in pregnancy in Mulago hospital, Uganda.* J Infect Dev Ctries, 2008. **2**(2): p. 135-9.
68. McGready, R., et al., *Randomized comparison of quinine-clindamycin versus artesunate in the treatment of falciparum malaria in pregnancy.* Trans R Soc Trop Med Hyg, 2001. **95**(6): p. 651-6.
69. Mutabingwa, T.K., et al., *Randomized trial of artesunate+amodiaquine, sulfadoxine-pyrimethamine+amodiaquine, chlorproguanal-dapsone and SP for malaria in pregnancy in Tanzania.* PLoS One, 2009. **4**(4): p. e5138.

70. McGready, R., et al., *Randomized comparison of mefloquine-artesunate versus quinine in the treatment of multidrug-resistant falciparum malaria in pregnancy.* Trans R Soc Trop Med Hyg, 2000. **94**(6): p. 689-93.
71. McGready, R., et al., *A randomized comparison of artesunate-atovaquone-proguanil versus quinine in treatment for uncomplicated falciparum malaria during pregnancy.* J Infect Dis, 2005. **192**(5): p. 846-53.
72. Bardaji, A., et al., *Intermittent preventive treatment of malaria in pregnant women and infants: making best use of the available evidence.* Expert opinion on pharmacotherapy, 2012. **13**(12): p. 1719-36.
73. Karunajeewa, H.A., et al., *Pharmacokinetic properties of sulfadoxine-pyrimethamine in pregnant women.* Antimicrob Agents Chemother, 2009. **53**(10): p. 4368-76.
74. Green, M.D., et al., *Pharmacokinetics of sulfadoxine-pyrimethamine in HIV-infected and uninfected pregnant women in Western Kenya.* J Infect Dis, 2007. **196**(9): p. 1403-8.
75. Nyunt, M.M., et al., *Pharmacokinetics of sulfadoxine and pyrimethamine in intermittent preventive treatment of malaria in pregnancy.* Clin Pharmacol Ther, 2010. **87**(2): p. 226-34.
76. Okoko, B.J., G. Enwere, and M.O. Ota, *The epidemiology and consequences of maternal malaria: a review of immunological basis.* Acta Trop, 2003. **87**(2): p. 193-205.
77. Jamieson, D.J., R.N. Theiler, and S.A. Rasmussen, *Emerging infections and pregnancy.* Emerging infectious diseases, 2006. **12**(11): p. 1638-43.
78. Mor, G. and I. Cardenas, *The immune system in pregnancy: a unique complexity.* American journal of reproductive immunology, 2010. **63**(6): p. 425-33.
79. Diagne, N., et al., *Increased susceptibility to malaria during the early postpartum period.* The New England journal of medicine, 2000. **343**(9): p. 598-603.
80. McGready, R., et al., *The pharmacokinetics of artemether and lumefantrine in pregnant women with uncomplicated falciparum malaria.* Eur J Clin Pharmacol, 2006. **62**(12): p. 1021-31.
81. McGready, R., et al., *Pharmacokinetics of dihydroartemisinin following oral artesunate treatment of pregnant women with acute uncomplicated falciparum malaria.* Eur J Clin Pharmacol, 2006. **62**(5): p. 367-71.
82. Tarning, J., et al., *Population pharmacokinetics of dihydroartemisinin and piperaquine in pregnant and non-pregnant women with uncomplicated malaria.* Antimicrobial agents and chemotherapy, 2012.
83. Tarning, J., et al., *Population pharmacokinetics of lumefantrine in pregnant women treated with artemether-lumefantrine for uncomplicated Plasmodium falciparum malaria.* Antimicrob Agents Chemother, 2009. **53**(9): p. 3837-46.
84. McGready, R., et al., *The pharmacokinetics of atovaquone and proguanil in pregnant women with acute falciparum malaria.* Eur J Clin Pharmacol, 2003. **59**(7): p. 545-52.
85. Rijken, M.J., et al., *Pharmacokinetics of dihydroartemisinin and piperaquine in pregnant and nonpregnant women with uncomplicated falciparum malaria.* Antimicrobial agents and chemotherapy, 2011. **55**(12): p. 5500-6.
86. Adam, I., et al., *Pharmacokinetics of piperaquine in pregnant women in Sudan with uncomplicated Plasmodium falciparum malaria.* The American journal of tropical medicine and hygiene, 2012. **87**(1): p. 35-40.
87. Hoglund, R.M., et al., *A population pharmacokinetic model of piperaquine in pregnant and non-pregnant women with uncomplicated Plasmodium falciparum malaria in Sudan.* Malaria journal, 2012. **11**: p. 398.

88. Rijken, M.J., et al., *Pharmacokinetics of amodiaquine and desethylamodiaquine in pregnant and post-partum women with Plasmodium vivax malaria.* Antimicrobial agents and chemotherapy, 2011.
89. Tarning, J., et al., *Population Pharmacokinetic and Pharmacodynamic Modeling of Amodiaquine and Desethylamodiaquine in Women with Plasmodium vivax Malaria during and after Pregnancy.* Antimicrobial agents and chemotherapy, 2012. **56**(11): p. 5764-73.
90. Dawes, M. and P.J. Chowienczyk, *Drugs in pregnancy. Pharmacokinetics in pregnancy.* Best Pract Res Clin Obstet Gynaecol, 2001. **15**(6): p. 819-26.
91. Anderson, G.D., *Pregnancy-induced changes in pharmacokinetics: a mechanistic-based approach.* Clin Pharmacokinet, 2005. **44**(10): p. 989-1008.
92. Anderson, G.D., *Using pharmacokinetics to predict the effects of pregnancy and maternal-infant transfer of drugs during lactation.* Expert Opin Drug Metab Toxicol, 2006. **2**(6): p. 947-60.
93. Malcolm, R. and T.T. N., *CLINICAL PHARMACOKINETICS AND PHARMACODYNAMICS CONCEPTS AND APPLICATIONS*. Fourth ed2011.
94. P., K.J. and M.M. L., *SURVIVAL ANALYSIS Techniques for Censored and Truncated Data*. Second ed2003.
95. Petersson, K.J., et al., *Semiparametric distributions with estimated shape parameters.* Pharmaceutical research, 2009. **26**(9): p. 2174-85.
96. Ahn, J.E., et al., *Likelihood based approaches to handling data below the quantification limit using NONMEM VI.* J Pharmacokinet Pharmacodyn, 2008. **35**(4): p. 401-21.
97. Beal, S.L., *Ways to fit a PK model with some data below the quantification limit.* J Pharmacokinet Pharmacodyn, 2001. **28**(5): p. 481-504.
98. Savic, R.M., et al., *Implementation of a transit compartment model for describing drug absorption in pharmacokinetic studies.* J Pharmacokinet Pharmacodyn, 2007. **34**(5): p. 711-26.
99. McLeay, S.C., et al., *The relationship between drug clearance and body size: systematic review and meta-analysis of the literature published from 2000 to 2007.* Clinical pharmacokinetics, 2012. **51**(5): p. 319-30.
100. Lindbom, L., P. Pihlgren, and E.N. Jonsson, *PsN-Toolkit--a collection of computer intensive statistical methods for non-linear mixed effect modeling using NONMEM.* Comput Methods Programs Biomed, 2005. **79**(3): p. 241-57.
101. Jonsson, E.N. and M.O. Karlsson, *Automated covariate model building within NONMEM.* Pharm Res, 1998. **15**(9): p. 1463-8.
102. Ravva, P., et al., *Population pharmacokinetic analysis of varenicline in adult smokers.* British journal of clinical pharmacology, 2009. **68**(5): p. 669-81.
103. Savic, R.M. and M.O. Karlsson, *Importance of shrinkage in empirical bayes estimates for diagnostics: problems and solutions.* Aaps J, 2009. **11**(3): p. 558-69.
104. Bergstrand, M., et al., *Prediction-Corrected Visual Predictive Checks for Diagnosing Nonlinear Mixed-Effects Models.* Aaps J, 2011. **13**(2): p. 143-51.
105. Cella, M., et al., *Dosing rationale for fixed-dose combinations in children: shooting from the hip?* Clinical pharmacology and therapeutics, 2012. **91**(4): p. 718-25.
106. Vong, C., et al., *Rapid sample size calculations for a defined likelihood ratio test-based power in mixed-effects models.* The AAPS journal, 2012. **14**(2): p. 176-86.
107. Karlsson, K.E., *Benefits of Pharmacometric Model-Based Design and Analysis of Clinical Trials*, 2010, Acta Universitatis Upsaliensis: Uppsala. p. 71.

108. Jamsen, K.M., et al., *Optimal designs for population pharmacokinetic studies of the partner drugs co-administered with artemisinin derivatives in patients with uncomplicated falciparum malaria.* Malaria journal, 2012. **11**(1): p. 143.
109. Abdelrahim, II, et al., *Pharmacokinetics of quinine and its metabolites in pregnant Sudanese women with uncomplicated Plasmodium falciparum malaria.* J Clin Pharm Ther, 2007. **32**(1): p. 15-9.
110. Phillips, R.E., et al., *Quinine pharmacokinetics and toxicity in pregnant and lactating women with falciparum malaria.* Br J Clin Pharmacol, 1986. **21**(6): p. 677-83.
111. White, N.J., et al., *Quinine pharmacokinetics and toxicity in cerebral and uncomplicated Falciparum malaria.* Am J Med, 1982. **73**(4): p. 564-72.
112. Paintaud, G., G. Alvan, and O. Ericsson, *The reproducibility of quinine bioavailability.* Br J Clin Pharmacol, 1993. **35**(3): p. 305-7.
113. Babalola, C.P., et al., *Absolute bioavailability of quinine formulations in Nigeria.* Afr J Med Med Sci, 2004. **33**(3): p. 185-9.
114. Dyer, J.R., et al., *The pharmacokinetics and pharmacodynamics of quinine in the diabetic and non-diabetic elderly.* British journal of clinical pharmacology, 1994. **38**(3): p. 205-12.
115. Wanwimolruk, S., et al., *Cigarette smoking enhances the elimination of quinine.* British journal of clinical pharmacology, 1993. **36**(6): p. 610-4.
116. Salako, L.A. and A. Sowunmi, *Disposition of quinine in plasma, red blood cells and saliva after oral and intravenous administration to healthy adult Africans.* Eur J Clin Pharmacol, 1992. **42**(2): p. 171-4.
117. Wanwimolruk, S. and S. Chalcroft, *Lack of relationship between debrisoquine oxidation phenotype and the pharmacokinetics of quinine.* British journal of clinical pharmacology, 1991. **32**(5): p. 617-20.
118. Wanwimolruk, S., et al., *Pharmacokinetics of quinine in young and elderly subjects.* Transactions of the Royal Society of Tropical Medicine and Hygiene, 1991. **85**(6): p. 714-7.
119. Wanwimolruk, S., et al., *Lack of effect of oral contraceptive use on the pharmacokinetics of quinine.* British journal of clinical pharmacology, 1991. **31**(2): p. 179-81.
120. Salako, L.A., A. Sowunmi, and F.O. Akinbami, *Pharmacokinetics of quinine in African children suffering from kwashiorkor.* Br J Clin Pharmacol, 1989. **28**(2): p. 197-201.
121. Jamaludin, A., et al., *Relative bioavailability of the hydrochloride, sulphate and ethyl carbonate salts of quinine.* British journal of clinical pharmacology, 1988. **25**(2): p. 261-3.
122. Wanwimolruk, S., et al., *Effects of cimetidine and ranitidine on the pharmacokinetics of quinine.* British journal of clinical pharmacology, 1986. **22**(3): p. 346-50.
123. Viriyayudhakorn, S., et al., *Pharmacokinetics of quinine in obesity.* Trans R Soc Trop Med Hyg, 2000. **94**(4): p. 425-8.
124. Supanaranond, W., et al., *Disposition of oral quinine in acute falciparum malaria.* Eur J Clin Pharmacol, 1991. **40**(1): p. 49-52.
125. Hendriksen, I.C., et al., *Population pharmacokinetic and pharmacodynamic properties of intramuscular quinine in Tanzanian children with severe Falciparum malaria.* Antimicrobial agents and chemotherapy, 2013. **57**(2): p. 775-83.
126. Krishna, S., et al., *Population pharmacokinetics of intramuscular quinine in children with severe malaria.* Antimicrob Agents Chemother, 2001. **45**(6): p. 1803-9.
127. Pukrittayakamee, S., et al., *A study of the factors affecting the metabolic clearance of quinine in malaria.* Eur J Clin Pharmacol, 1997. **52**(6): p. 487-93.

128. Newton, P., et al., *Pharmacokinetics of quinine and 3-hydroxyquinine in severe falciparum malaria with acute renal failure.* Transactions of the Royal Society of Tropical Medicine and Hygiene, 1999. **93**(1): p. 69-72.
129. Mansor, S.M., et al., *Effect of Plasmodium falciparum malaria infection on the plasma concentration of alpha 1-acid glycoprotein and the binding of quinine in Malawian children.* Br J Clin Pharmacol, 1991. **32**(3): p. 317-21.
130. Babalola, C.P., et al., *Pharmacokinetics of quinine in African patients with acute falciparum malaria.* Pharm World Sci, 1998. **20**(3): p. 118-22.
131. Krishna, S. and N.J. White, *Pharmacokinetics of quinine, chloroquine and amodiaquine. Clinical implications.* Clin Pharmacokinet, 1996. **30**(4): p. 263-99.
132. White, N.J., et al., *Severe hypoglycemia and hyperinsulinemia in falciparum malaria.* The New England journal of medicine, 1983. **309**(2): p. 61-6.
133. White, N.J., et al., *Hypoglycaemia in African children with severe malaria.* Lancet, 1987. **1**(8535): p. 708-11.
134. Claessen, F.A., et al., *Quinine pharmacokinetics: ototoxic and cardiotoxic effects in healthy Caucasian subjects and in patients with falciparum malaria.* Tropical medicine & international health : TM & IH, 1998. **3**(6): p. 482-9.
135. Le Jouan, M., et al., *Quinine pharmacokinetics and pharmacodynamics in children with malaria caused by Plasmodium falciparum.* Antimicrob Agents Chemother, 2005. **49**(9): p. 3658-62.
136. Silamut, K., et al., *Alpha 1-acid glycoprotein (orosomucoid) and plasma protein binding of quinine in falciparum malaria.* Br J Clin Pharmacol, 1991. **32**(3): p. 311-5.
137. Zhang, H., et al., *Evidence for involvement of human CYP3A in the 3-hydroxylation of quinine.* Br J Clin Pharmacol, 1997. **43**(3): p. 245-52.
138. Zhao, X.J., et al., *Identification of human cytochrome P450 isoforms involved in the 3-hydroxylation of quinine by human live microsomes and nine recombinant human cytochromes P450.* The Journal of pharmacology and experimental therapeutics, 1996. **279**(3): p. 1327-34.
139. Tracy, T.S., et al., *Temporal changes in drug metabolism (CYP1A2, CYP2D6 and CYP3A Activity) during pregnancy.* Am J Obstet Gynecol, 2005. **192**(2): p. 633-9.
140. Pavek, P., M. Ceckova, and F. Staud, *Variation of drug kinetics in pregnancy.* Curr Drug Metab, 2009. **10**(5): p. 520-9.
141. Tarning, J., et al., *Population pharmacokinetics of Artemether and dihydroartemisinin in pregnant women with uncomplicated Plasmodium falciparum malaria in Uganda.* Malaria journal, 2012. **11**(1): p. 293.
142. Teja-Isavadharm, P., et al., *Comparative pharmacokinetics and effect kinetics of orally administered artesunate in healthy volunteers and patients with uncomplicated falciparum malaria.* Am J Trop Med Hyg, 2001. **65**(6): p. 717-21.
143. Binh, T.Q., et al., *Oral bioavailability of dihydroartemisinin in Vietnamese volunteers and in patients with falciparum malaria.* Br J Clin Pharmacol, 2001. **51**(6): p. 541-6.
144. Newton, P., et al., *Antimalarial bioavailability and disposition of artesunate in acute falciparum malaria.* Antimicrob Agents Chemother, 2000. **44**(4): p. 972-7.
145. McGready, R., et al., *Artesunate/dihydroartemisinin pharmacokinetics in acute falciparum malaria in pregnancy: absorption, bioavailability, disposition and disease effects.* Br J Clin Pharmacol (submitted for publication: BJCP MP-00293-11-AS), 2011.
146. Onyamboko, M.A., et al., *Pharmacokinetics and pharmacodynamics of artesunate and dihydroartemisinin following oral treatment in pregnant women with asymptomatic Plasmodium falciparum infections in Kinshasa DRC.* Malar J, 2011. **10**: p. 49.

147. Morris, C.A., et al., *Population pharmacokinetics of artesunate and dihydroartemisinin in pregnant and non-pregnant women with malaria.* Malar J, 2011. **10**(1): p. 114.
148. Batty, K.T., et al., *A pharmacokinetic and pharmacodynamic study of artesunate for vivax malaria.* Am J Trop Med Hyg, 1998. **59**(5): p. 823-7.
149. Navaratnam, V., et al., *Tolerability and pharmacokinetics of non-fixed and fixed combinations of artesunate and amodiaquine in Malaysian healthy normal volunteers.* Eur J Clin Pharmacol, 2009. **65**(8): p. 809-21.
150. Diem Thuy, L.T., et al., *Absence of time-dependent artesunate pharmacokinetics in healthy subjects during 5-day oral administration.* Eur J Clin Pharmacol, 2008. **64**(10): p. 993-8.
151. Orrell, C., et al., *Pharmacokinetics and tolerability of artesunate and amodiaquine alone and in combination in healthy volunteers.* Eur J Clin Pharmacol, 2008. **64**(7): p. 683-90.
152. Batty, K.T., et al., *Relative bioavailability of artesunate and dihydroartemisinin: investigations in the isolated perfused rat liver and in healthy Caucasian volunteers.* Am J Trop Med Hyg, 2002. **66**(2): p. 130-6.
153. Na-Bangchang, K., et al., *Pharmacokinetic and bioequivalence evaluation of two generic formulations of oral artesunate.* Eur J Clin Pharmacol, 1998. **53**(5): p. 375-6.
154. Davis, T.M., et al., *Assessment of the effect of mefloquine on artesunate pharmacokinetics in healthy male volunteers.* Antimicrob Agents Chemother, 2007. **51**(3): p. 1099-101.
155. Navaratnam, V., et al., *Comparative pharmacokinetic study of oral and rectal formulations of artesunic acid in healthy volunteers.* Eur J Clin Pharmacol, 1998. **54**(5): p. 411-4.
156. Na-Bangchang, K., et al., *The pharmacokinetics of oral dihydroartemisinin and artesunate in healthy Thai volunteers.* Southeast Asian J Trop Med Public Health, 2004. **35**(3): p. 575-82.
157. Zhang, S.Q., et al., *Multiple dose study of interactions between artesunate and artemisinin in healthy volunteers.* Br J Clin Pharmacol, 2001. **52**(4): p. 377-85.
158. Awad, M.I., et al., *Pharmacokinetics of artesunate following oral and rectal administration in healthy Sudanese volunteers.* Trop Doct, 2004. **34**(3): p. 132-5.
159. Krudsood, S., et al., *New fixed-dose artesunate-mefloquine formulation against multidrug-resistant Plasmodium falciparum in adults: a comparative phase IIb safety and pharmacokinetic study with standard-dose nonfixed artesunate plus mefloquine.* Antimicrob Agents Chemother, 2010. **54**(9): p. 3730-7.
160. Mwesigwa, J., et al., *Pharmacokinetics of artemether-lumefantrine and artesunate-amodiaquine in children in Kampala, Uganda.* Antimicrob Agents Chemother, 2010. **54**(1): p. 52-9.
161. Miller, A.K., et al., *Pharmacokinetics of chlorproguanil, dapsone, artesunate and their major metabolites in patients during treatment of acute uncomplicated Plasmodium falciparum malaria.* Eur J Clin Pharmacol, 2009. **65**(10): p. 977-87.
162. Ramharter, M., et al., *Fixed-dose pyronaridine-artesunate combination for treatment of uncomplicated falciparum malaria in pediatric patients in Gabon.* J Infect Dis, 2008. **198**(6): p. 911-9.
163. Karbwang, J., et al., *Pharmacokinetics of oral artesunate in thai patients with uncomplicated falciparum malaria.* Clin Drug Investig, 1998. **15**(1): p. 37-43.
164. Sinou, V., et al., *Pharmacokinetics and pharmacodynamics of a new ACT formulation: Artesunate/Amodiaquine (TRIMALACT) following oral administration in African malaria patients.* Eur J Drug Metab Pharmacokinet, 2009. **34**(3-4): p. 133-42.

165. Batty, K.T., et al., *A pharmacokinetic and pharmacodynamic study of intravenous vs oral artesunate in uncomplicated falciparum malaria.* Br J Clin Pharmacol, 1998. **45**(2): p. 123-9.
166. Saunders, D., et al., *Pharmacokinetics and pharmacodynamics of oral artesunate monotherapy in patients with uncomplicated P. falciparum malaria in western Cambodia.* Antimicrobial agents and chemotherapy, 2012.
167. Tan, B., et al., *Population pharmacokinetics of artesunate and dihydroartemisinin following single- and multiple-dosing of oral artesunate in healthy subjects.* Malar J, 2009. **8**(1): p. 304.
168. Newton, P.N., et al., *The pharmacokinetics of intravenous artesunate in adults with severe falciparum malaria.* Eur J Clin Pharmacol, 2006. **62**(12): p. 1003-9.
169. Li, Q., et al., *Pharmacokinetic profiles of artesunate after single intravenous doses at 0.5, 1, 2, 4, and 8 mg/kg in healthy volunteers: a phase I study.* Am J Trop Med Hyg, 2009. **81**(4): p. 615-21.
170. Navaratnam, V., et al., *Pharmacokinetics of artemisinin-type compounds.* Clin Pharmacokinet, 2000. **39**(4): p. 255-70.
171. Li, X.Q., et al., *Identification of human cytochrome P(450)s that metabolise anti-parasitic drugs and predictions of in vivo drug hepatic clearance from in vitro data.* Eur J Clin Pharmacol, 2003. **59**(5-6): p. 429-42.
172. Hanpithakpong, W., et al., *A liquid chromatographic-tandem mass spectrometric method for determination of artesunate and its metabolite dihydroartemisinin in human plasma.* J Chromatogr B Analyt Technol Biomed Life Sci, 2008. **876**(1): p. 61-8.
173. Simpson, J.A., et al., *Population pharmacokinetics of artesunate and dihydroartemisinin following intra-rectal dosing of artesunate in malaria patients.* PLoS Med, 2006. **3**(11): p. e444.
174. Karunajeewa, H.A., et al., *Disposition of artesunate and dihydroartemisinin after administration of artesunate suppositories in children from Papua New Guinea with uncomplicated malaria.* Antimicrob Agents Chemother, 2004. **48**(8): p. 2966-72.
175. Oga, E.F., et al., *Potential P-glycoprotein-mediated drug-drug interactions of antimalarial agents in Caco-2 cells.* The American journal of tropical medicine and hygiene, 2012. **87**(1): p. 64-9.
176. Das, D., et al., *Effect of high-dose or split-dose artesunate on parasite clearance in artemisinin-resistant falciparum malaria.* Clinical infectious diseases : an official publication of the Infectious Diseases Society of America, 2013. **56**(5): p. e48-58.
177. Karbwang, J., et al., *Pharmacokinetics and bioavailability of oral and intramuscular artemether.* Eur J Clin Pharmacol, 1997. **52**(4): p. 307-10.
178. Teja-Isavadharm, P., et al., *Comparative bioavailability of oral, rectal, and intramuscular artemether in healthy subjects: use of simultaneous measurement by high performance liquid chromatography and bioassay.* Br J Clin Pharmacol, 1996. **42**(5): p. 599-604.
179. Abdulla, S., et al., *Early clinical development of artemether-lumefantrine dispersible tablet: palatability of three flavours and bioavailability in healthy subjects.* Malar J, 2010. **9**: p. 253.
180. Ali, S., et al., *Pharmacokinetics of artemether and dihydroartemisinin in healthy Pakistani male volunteers treated with artemether-lumefantrine.* Malar J, 2010. **9**: p. 275.
181. Lefevre, G., et al., *Pharmacokinetics and electrocardiographic pharmacodynamics of artemether-lumefantrine (Riamet) with concomitant administration of ketoconazole in healthy subjects.* Br J Clin Pharmacol, 2002. **54**(5): p. 485-92.

182. Na Bangchang, K., et al., *Pharmacokinetics of artemether after oral administration to healthy Thai males and patients with acute, uncomplicated falciparum malaria.* Br J Clin Pharmacol, 1994. **37**(3): p. 249-53.
183. Mordi, M.N., et al., *Single dose pharmacokinetics of oral artemether in healthy Malaysian volunteers.* Br J Clin Pharmacol, 1997. **43**(4): p. 363-5.
184. German, P., et al., *Lopinavir/ritonavir affects pharmacokinetic exposure of artemether/lumefantrine in HIV-uninfected healthy volunteers.* J Acquir Immune Defic Syndr, 2009. **51**(4): p. 424-9.
185. Lefevre, G., et al., *Pharmacokinetic interaction trial between co-artemether and mefloquine.* Eur J Pharm Sci, 2000. **10**(2): p. 141-51.
186. Lefevre, G., et al., *Interaction trial between artemether-lumefantrine (Riamet) and quinine in healthy subjects.* J Clin Pharmacol, 2002. **42**(10): p. 1147-58.
187. van Agtmael, M.A., et al., *The effect of grapefruit juice on the time-dependent decline of artemether plasma levels in healthy subjects.* Clin Pharmacol Ther, 1999. **66**(4): p. 408-14.
188. van Agtmael, M.A., et al., *Grapefruit juice increases the bioavailability of artemether.* Eur J Clin Pharmacol, 1999. **55**(5): p. 405-10.
189. van Agtmael, M.A., et al., *The contribution of the enzymes CYP2D6 and CYP2C19 in the demethylation of artemether in healthy subjects.* Eur J Drug Metab Pharmacokinet, 1998. **23**(3): p. 429-36.
190. Tan-ariya, P., et al., *Pharmacokinetic interactions of artemether and pyrimethamine in healthy male Thais.* Southeast Asian J Trop Med Public Health, 1998. **29**(1): p. 18-23.
191. van Agtmael, M.A., et al., *Multiple dose pharmacokinetics of artemether in Chinese patients with uncomplicated falciparum malaria.* Int J Antimicrob Agents, 1999. **12**(2): p. 151-8.
192. Lefevre, G., et al., *A clinical and pharmacokinetic trial of six doses of artemether-lumefantrine for multidrug-resistant Plasmodium falciparum malaria in Thailand.* Am J Trop Med Hyg, 2001. **64**(5-6): p. 247-56.
193. Karbwang, J., et al., *Pharmacokinetics of oral artemether in Thai patients with uncomplicated falciparum malaria.* Fundam Clin Pharmacol, 1998. **12**(2): p. 242-4.
194. Salman, S., et al., *Population pharmacokinetics of artemether, lumefantrine, and their respective metabolites in Papua New Guinean children with uncomplicated malaria.* Antimicrobial agents and chemotherapy, 2011. **55**(11): p. 5306-13.
195. Huang, L., et al., *Concomitant efavirenz reduces pharmacokinetic exposure to the antimalarial drug artemether-lumefantrine in healthy volunteers.* Journal of acquired immune deficiency syndromes, 2012.
196. Mithwani, S., et al., *Population pharmacokinetics of artemether and dihydroartemisinin following single intramuscular dosing of artemether in African children with severe falciparum malaria.* Br J Clin Pharmacol, 2004. **57**(2): p. 146-52.
197. Hietala, S.F., et al., *Population pharmacokinetics and pharmacodynamics of artemether and lumefantrine during combination treatment in children with uncomplicated falciparum malaria in Tanzania.* Antimicrob Agents Chemother, 2010. **54**(11): p. 4780-8.
198. Ashley, E.A., et al., *How much fat is necessary to optimize lumefantrine oral bioavailability?* Trop Med Int Health, 2007. **12**(2): p. 195-200.
199. Hanpithakpong, H., et al., *A liquid chromatographic–tandem mass spectrometric method for determination of artemether and its metabolite dihydroartemisinin in human plasma.* Bioanalysis, 2009. **1**(1): p. 37-46.

200. Ilett, K.F., et al., *Glucuronidation of dihydroartemisinin in vivo and by human liver microsomes and expressed UDP-glucuronosyltransferases.* Drug Metab Dispos, 2002. **30**(9): p. 1005-12.
201. Staehli Hodel, E.M., et al., *Effect of single nucleotide polymorphisms in cytochrome P450 isoenzyme and N-acetyltransferase 2 genes on the metabolism of artemisinin-based combination therapies in malaria patients from Cambodia and Tanzania.* Antimicrob Agents Chemother, 2013. **57**(2): p. 950-8.
202. Wahajuddin, et al., *Intravenous pharmacokinetics, oral bioavailability, dose proportionality and in situ permeability of anti-malarial lumefantrine in rats.* Malaria journal, 2011. **10**: p. 293.
203. Ezzet, F., R. Mull, and J. Karbwang, *Population pharmacokinetics and therapeutic response of CGP 56697 (artemether + benflumetol) in malaria patients.* Br J Clin Pharmacol, 1998. **46**(6): p. 553-61.
204. Ezzet, F., et al., *Pharmacokinetics and pharmacodynamics of lumefantrine (benflumetol) in acute falciparum malaria.* Antimicrob Agents Chemother, 2000. **44**(3): p. 697-704.
205. Na-Bangchang, K., et al., *Pharmacokinetics of benflumetol given as a fixed combination artemether-benflumetol (CGP 56697) in Thai patients with uncomplicated falciparum malaria.* Int J Clin Pharmacol Res, 1999. **19**(2): p. 41-6.
206. Ashley, E.A., et al., *Pharmacokinetic study of artemether-lumefantrine given once daily for the treatment of uncomplicated multidrug-resistant falciparum malaria.* Trop Med Int Health, 2007. **12**(2): p. 201-8.
207. Annerberg, A., et al., *High throughput assay for the determination of lumefantrine in plasma.* J Chromatogr B Analyt Technol Biomed Life Sci, 2005. **822**(1-2): p. 330-3.
208. van Vugt, M., et al., *The relationship between capillary and venous concentrations of the antimalarial drug lumefantrine (benflumetol).* Trans R Soc Trop Med Hyg, 1998. **92**(5): p. 564-5.
209. Tyner, S.D., et al., *Ex vivo drug sensitivity profiles of Plasmodium falciparum field isolates from Cambodia and Thailand, 2005 to 2010, determined by a histidine-rich protein-2 assay.* Malaria journal, 2012. **11**: p. 198.
210. Cheeseman, I.H., et al., *A major genome region underlying artemisinin resistance in malaria.* Science, 2012. **336**(6077): p. 79-82.
211. Wong, R.P., et al., *Desbutyl-lumefantrine is a metabolite of lumefantrine with potent in vitro antimalarial activity that may influence artemether-lumefantrine treatment outcome.* Antimicrobial agents and chemotherapy, 2011. **55**(3): p. 1194-8.
212. Noedl, H., et al., *Desbutyl-benflumetol, a novel antimalarial compound: in vitro activity in fresh isolates of Plasmodium falciparum from Thailand.* Antimicrob Agents Chemother, 2001. **45**(7): p. 2106-9.
213. Tarning, J., et al., *Population pharmacokinetic and pharmacodynamic modeling of amodiaquine and desethylamodiaquine in women with Plasmodium vivax malaria during and after pregnancy.* Submitted, 2012.
214. Kloprogge, F., et al., *Population Pharmacokinetics of Lumefantrine in Pregnant and Nonpregnant Women With Uncomplicated Plasmodium falciparum Malaria in Uganda.* CPT: Pharmacometrics & Systems Pharmacology, 2013 (in press).
215. Nosten, F., et al., *Malaria during pregnancy in an area of unstable endemicity.* Trans R Soc Trop Med Hyg, 1991. **85**(4): p. 424-9.
216. Lindegardh, N., et al., *Development and validation of a bioanalytical method using automated solid-phase extraction and LC-UV for the simultaneous determination of*

lumefantrine and its desbutyl metabolite in plasma. J Pharm Biomed Anal, 2005. **37**(5): p. 1081-8.
217. Bergtrand, M., *Modeling of the concentration-effect relationship for piperaquine in preventive treatment of malaria*, in *Oral presentation at PAGE-meeting*2013: Glasgow.
218. FDA, *Guidance for Industry Population Pharmacokinetics*, F.a.D.A. U.S. Department of Health and Human Services, Editor 1999.
219. Jamsen, K.M., et al., *Optimal designs for population pharmacokinetic studies of oral artesunate in patients with uncomplicated falciparum malaria.* Malaria journal, 2011. **10**: p. 181.